THE UNIVERSITY
of EDINBURGH

INVESTIGATING NUCLEATION CONTROL IN BATCH AND FLOW USING NON-PHOTOCHEMICAL LASER-INDUCED NUCLEATION

Alasdair Morgan Mackenzie

PhD in Chemistry

The University of Edinburgh

2017

Declaration

I declare that this thesis has been composed by me and the work is my own, unless clearly indicated.

I declare that this work has not been submitted for any other degree or professional qualification.

I declare that the publications included below are my own work except where indicated:
(No publications included).

Alasdair Morgan Mackenzie

Abstract

The practical application of non-photochemical laser-induced nucleation (NPLIN) to continuous flow was investigated. Supersaturated aqueous solutions were screened with a 5 ns pulsed laser (532 nm 44 MW cm^{-2}) for NPLIN activity. Upon irradiation succinic acid nucleated at S_{20} = 4.3 and adipic acid at S_{20} = 2.0 – 3.0. NPLIN activity is reported for the first time in nicotinic acid (S_{20} = 2.6 – 3.0). No overall pattern was observed of chemical structure on NPLIN activity.

From inorganic compounds similarly screened, ammonium chloride (S_{20} = 1.04 – 1.20) was identified as most suitable for further tests. It was shown to have an increase of NPLIN crystals with higher supersaturation from 13 at S = 1.038 to 252 at S = 1.135. A quadratic increase in number of crystals with increased laser power. The effects of NPLIN upon ammonium chloride are diminished upon filtration through a 0.2 μm poly (ether sulfone) filter, reducing the number of crystals from 350 to 10 per 70 mJ pulse (25 MW cm^{-2}).

The use of NPLIN in continuous flow was demonstrated from the first time. A S_{23} = 1.1 solution of aqueous ammonium chloride in flow produced crystals when irradiated by 10 pulses s^{-1} of a 1064 nm 6 ns laser. When the laser was stopped, crystals were no longer produced and the system returned to flowing supersaturated solution.

Lab scale apparatus for continuous NPLIN experiments was developed. A design involving a re-dissolution step and loop flow was constructed for both laminar and slug-flow regimes. Nucleation of ammonium chloride (S = 1.1) was demonstrated in both systems. Repeatable NPLIN experiments were hindered by spontaneous nucleation. Spontaneous nucleation in flow was observed around areas where supersaturated solution passed from one component to another. Spontaneous nucleation was also observed upon cooling (25 to 10 °C). Filtration was observed to both suppress NPLIN and spontaneous nucleation in flow.

Lay Summary

Pharmaceutical companies are always searching for ways of making medicines cheaper. One proposed way of doing this is to change the manufacturing methods from batches at a time to a production line of chemical processes continuously making medicine. A key steps in continuous chemistry is purification from unwanted by-products. A way to both purify a substance and make it easier to manufacture is through crystallisation.

Crystallisation, the transformation of liquid into an ordered solid, is a common process which can be observed in our freezers at home or on a cold winter's day. However, despite being performed all around us and in the laboratory, it is still not fully understood on a fundamental level. The first step of crystallisation, when there is only liquid present, is called homogeneous nucleation. Although there are some good ideas on what happens in the liquid, it is hard to study because homogeneous nucleation occurs in a random place throughout the solution and at unpredictable times.

In this thesis a technique called non-photochemical laser-induced nucleation (NPLIN) is used as a way to start crystallisation within a few billionths of a second and along an area of a few mm^2 of solution. Much like nucleation, the exact way NPLIN works on a molecular scale is not fully known. It forms crystals by passing a short pulse (ns) of laser beam unfocussed through a solution which is nearly ready to crystallise. The laser light appears not to be absorbed by the solution, but crystals can be seen forming exactly where the beam passed through the solution. It has been previously shown to be able to control certain desirable properties of the formed crystals by changing aspects of the laser pulse or of the solution it is passed through. The overall aim of this work is to see if NPLIN can be applied to control crystal properties in batch and flow.

As NPLIN does not work with every compound the first part of the work looks at what sort of chemicals NPLIN works with to see if there is a pattern, so that it can be shown to be applicable to medicines. There was no clear reason found for what

chemicals that worked and what did not. However these experiments revealed a new chemical which is NPLIN active: nicotinic acid, dissolved in ultrapure water (>18.2 MΩ cm) at 2.6 to 3.0 times its saturation concentration at 20 °C (the supersaturation, S_{20} = 2.6 – 3.0). The conditions for succinic acid NPLIN (S_{20} = 4.3) and adipic acid (S_{20} = 2.0 – 3.0) are also reported for the first time. Ammonium chloride in water was also found to undergo NPLIN at S = 1.045 – 1.2.

The second part of the work looks to examine the effect of changing laser power on crystal number produced per laser pulse in batch. Studies were performed with ammonium chloride in water. This chemical system was chosen because it grows visible crystals one second after the laser is fired. It was found that increasing the supersaturation increased the number of crystals produced per pulse from 13 crystals at S = 1.038 to 252 crystals at S = 1.135. Increasing the laser energy on S_{25} = *1.1* unfiltered solutions increased the number of crystals produced from 17 at 0.005 J to 350 at 0.07 J.

Previous studies on NPLIN have required a lot of identical solutions to be made and a lot of time required to perform experiments on them. The third part of this work then examines whether it is possible to perform NPLIN in a continuous flow environment, where solution is constantly moving through pipes. Because the properties of solution can be better controlled in flow, a section of pipe should have identical solution running through it. This may offer a way to better study the NPLIN technique. Being able to demonstrate crystal control in flow would also show its viability for continuous manufacturing. An apparatus was constructed demonstrating for the first time NPLIN in flow of ammonium chloride (S_{23} = 1.1) in ultrapure water. Development of the apparatus to enable longer and more repeatable experiments faced difficulties, which are highlighted within.

Acknowledgements

I would like to express my dearest thanks to both my supervisors Andy and Colin for guiding me through the ups and downs of this PhD experience. They are the smartest two people I have ever met in my life and I hope some of it will have rubbed off. For Colin I will always remember our discussions over whisky of blue sky ideas on how to tackle chemical problem and having such a positive outlook on people. For Andy I will always remember the secrets of the nanoscopic world open up in our conversations, your life advice on how to keep grounded in the real world, and the amazing feeling of having both these lessons delivered simultaneously in our epic meetings. You are both role models to me in different ways and I will carry your spirit with me into the future.

Jean and Gordon, you raised me to follow my curiosity and helped me grow hungry for knowledge. You gave me love and a healthy upbringing and supported me when I chose to run away to the windy East coast and were always on hand at my lowest to give practical and emotional support when I needed most. You even managed to put up with me in your house while I was writing my thesis, which I don't know how you stayed sane! There are no words to say how much I am grateful for you.

My thanks goes out to Martin for teaching me the ins and outs of everything and distilling his experiences with NPLIN. I won't tell anyone about the cheesy music we played in the lab. To Paris for hiding all the equipment and listening to my rubbish stories. To the Pulham group for sharing an office and welcoming someone who is obsessed with fancy coherent light that doesn't even explode. You managed to make Christmas fun all year round. To the fika mailing list and the Physical Chemistry journal club, your cakes are legend. To the hundreds of wonderful people I have met in the Chemistry department over the years, you helped me learn what it is to belong.

Lastly I would like to give a special thanks to Stuart Johnstone whose glass-blowing wizardry helped make the continuous experiments possible.

Table of Contents

List of tables

List of figures

List of abbreviations used.

2SN	Two-Step Nucleation Theory
AC	Ammonium chloride
CMAC	Engineering and Physical Sciences Research Council Centre for Innovative Manufacturing in Continuous Manufacturing and Crystallisation
COBC	Continuous oscillatory baffled reactor
$C_{SAT\#\#}$	Concentration of saturation (at T= ## °C) in g_{solute} per $g_{solvent}$
CSD	Crystal size distribution
DMP	Dimethyl phthalate
HC	Heater / chiller
ID	Internal diameter
IPT	Isotropic Polarizability Theory
k_B	Botzmann constant
MSZ	Metastable zone
MSZW	Metastable zone width
NPLIN	Non-photochemical laser-induced nucleation
OFR	Oscillatory Flow Reactor (used interchangeably with COBC)
PES	Poly (ether sulfone)
PPE	Personal protective equipment
PXRD	Powder X-Ray diffraction
ROI	Region of Interest
RPM	Revolutions per minute
$S_{\#\#}$	Supersaturation ratio (C / $C_{SAT\#\#}$) at T = ## °C
S&W	Soap and water
SCXRD	Single crystal X-ray Diffraction
TC	Thermocouple
T_{sat}	Temperature of saturation where S = 1

1 Background

1.1 Introduction and motivation

Continuous processing is simply a process which has constant inputs and outputs and operates continuously. Several industries have become continuous-based including fossil fuel processing, bulk chemical manufacturing and commercial food processing. The Engineering and Physical Sciences Research Council Centre for Innovative Manufacturing in Continuous Manufacturing and Crystallisation (CMAC) is a UK based centre comprising of 6 universities and industrial partners looking to explore the feasibility of switching the fine chemical industries (with a focus on the pharmaceutical industry) from batch to continuous processing. It has links with GSK, AstraZeneca and Novartis as well as The Massachusetts Institute of Technology continuous manufacturing centre and Nanyang Technological University in Singapore.

The main impact of continuous systems on chemical process is the control of heat flow. Batch reactors have a large thermal mass and small surface: volume ratio; tubes offer a higher surface: volume ratio allowing a much faster heat transfer rate and therefore enabling better thermodynamic control as well as the possibility of control of very fast heating and cooling cycles. This leads to better control of many stages of chemistry to give a more consistent product. Not only does this mean a safer, higher value product but also enables better supply chain management. Less wastage of "bad" batches, demand-led production with predictive marketing and lower inventories. A lower plant capital cost and footprint enables distributed production and saves on transport costs and time to market.

It is estimated by CMAC that 10 % of specific industrial processes definitely would be more efficient with continuous manufacturing, 20 % would definitely not be more efficient and around 70 % would be roughly the same. However, if these processes were continuous they would enable a continuous supply chain with the benefits outlined above.

The main difference between fine chemical industries and bulk chemicals is that fine chemicals tend to have processing steps involving solids. Many solids do not flow well and so pose a challenge to continuous processes, especially solid-specific ones. One important solid-specific process is crystallisation as it involves both formation of a solid and purification in one step. The formed solid then needs to be filtered out and processed until it resembles a particle with properties required in the next processing step or the final product. Solids can also undergo undesirable processes such as fouling from excessive growth, which blocks flow, or contain impurities due to poor growth control.

New expertise is therefore needed in dealing with solids in flow, with a focus on developing the steps involved in crystallisation.

One of the key issues with moving to a continuous flow crystallisation is an incomplete theoretical knowledge of the fundamental nucleation step. As such experiments into nucleation techniques are needed to build up an empirical base of knowledge to build from. Practical methods for inducing nucleation in flow can be very stochastic and can lack precise control over the location, time, solution conditions or final crystal properties. This also makes it hard to offer repeatable experiments to offer insight into nucleation mechanisms.

For almost 60 years lasers have offered a powerful tool for investigating physical and chemical processes. The discovery of non-photochemical laser-induced nucleation (NPLIN) in 1996 by Garetz *et al.* showed the ability to grow crystals using pulsed laser light without affecting the underlying chemistry. It has subsequently been show to offer control of nucleation within the space of the laser beam width and within the duration of the nanosecond pulse width as well as offer finer controls over some crystal properties. However studying the phenomena still requires a lot of repetitions and needing careful control over the solution variables can lead to very slow progress.

To our knowledge there has been no report in the literature to this date of implementing NPLIN in a continuous flow environment. To have a stable experimental setup which could easily control solution variables and offer many

repetitions of laser induced nucleation would be of benefit to both theoretical understanding of NPLIN and nucleation as well as benefiting practical applications of control over continuous flow crystallisation. The aim of this thesis is to construct a continuous flow NPLIN apparatus for control over nucleation and explore the challenges involved in doing so.

1.2 What is crystal nucleation?

1.2.1 Crystallisation

The IUCr defines a crystal as "A material [which] has **essentially** a sharp diffraction pattern" i.e. most of the diffraction pattern is in sharp Bragg peaks. Usually a crystal is a highly structured solid phase of molecules, atoms or ions arranged in a lattice of identical repeating units packed together form a crystal.[1]

Crystallisation is an essential process in many industrial sectors including: pharmaceuticals, explosives, dyes and fine chemicals. Crystallisation can be split into two processes: nucleation and crystal growth. Nucleation is the initial phase change of liquid to solid and growth is the addition of further molecular building blocks to pre-existing crystallites. These processes are discussed in detail below.

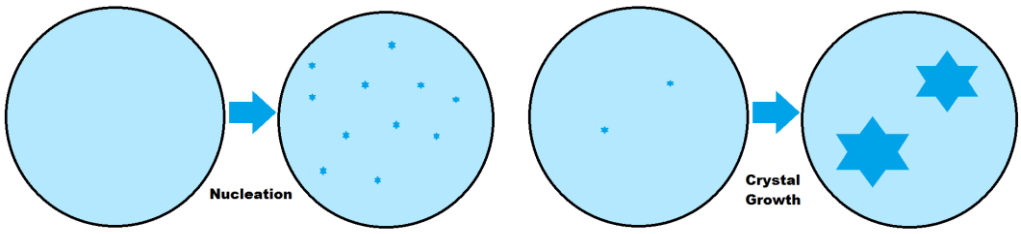

Figure 1-1 - (Left) Nucleation in a supersaturated solution. (Right) Critical nuclei in a supersaturated solution grow to stable crystals in a saturated solution.

Nucleation

Nucleation can be split into three categories: primary, homogeneous nucleation where crystals grow from pure solution spontaneously; primary, heterogeneous

nucleation with assistance from another surface (e.g. glass wall or dust); and secondary nucleation where new daughter crystals form from breakage of an original crystal.

Primary heterogeneous nucleation is similar to homogeneous nucleation but introduces a catalytic-like environment that stabilises an otherwise unfavoured intermediate. This can be modelled with a simple function:

$$\Delta G_{het} = f(\theta)\Delta G_{hom} \quad (1)$$

where ΔG_{hom} is the free energy change of homogeneous nucleation and the wetting function, f, is defined:

$$f(\theta) = \frac{1}{4}(2 + \cos\theta)(1 - \cos\theta)^2 \quad (2)$$

and θ is the contact angle between the cluster and the substrate ($f(\theta) \leq 1$).

Secondary nucleation is the appearance of new crystals only after introduction of an initial crystal. This can be explained by microscopic fragments of the introduced crystal breaking off and growing, often occurring for dendritic crystals or by collisions against the vessel wall or stirrer. This can be regarded as attrition and growth rather than creation of solid form liquid, but is called nucleation as it increases the final number of crystals (often with an unwanted increase in particle size dispersion).[2]

Homogeneous primary nucleation is the crucial step that precedes the others and is still not fully understood at a fundamental level.

The physical mechanism of nucleation is not entirely known as it is hard to measure. The initial formation of a crystal nucleus occurs at sizes smaller than the visible light diffraction limit; therefore cannot be observed through an optical microscope. The process from disorder to order is very fast, on the order of picoseconds; therefore good time-resolved techniques are needed to measure it. Nucleation happens in a disordered solution environment and so cannot be observed by high-resolution x-ray

techniques to observe the structure. It occurs in a complex environment with many different components involved, so is not amenable to study by NMR spectroscopy.

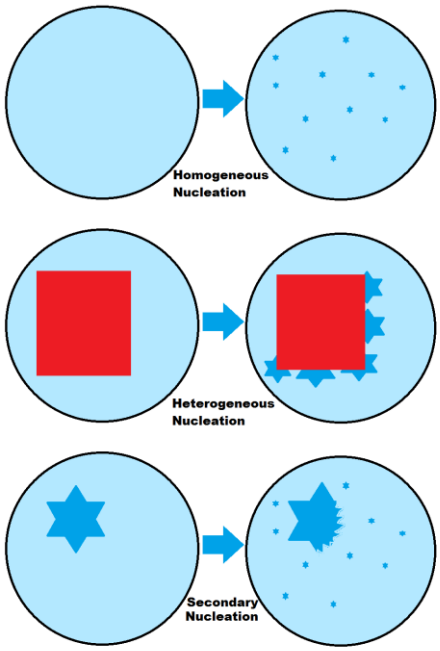

Figure 1-2 - The types of nucleation. (Top) Homogeneous nucleation from solution only. (Middle) Heterogeneous nucleation due to the lowering of energy barrier to nucleation at the surface of an introduced solid or a vessel wall. (Bottom) Secondary nucleation due to attrition of an existing crystal.

It is thus a challenge to describe, with studies so far looking at the growth effects and preceding solution conditions in order to model potential mechanisms.

Growth

Once a nucleus ($r > r_c$) is formed, crystal growth occurs: the nuclei favourably increase in size until supersaturation is depleted.

In *Crystallization*,[1] Mullin summarises the groups of proposed theories which describe crystal growth by their mechanism. The rate of growth is governed by several factors including temperature, supersaturation, size, shape and system mixing and can be probed by several methods including optical microscopy, light reflectance

techniques, acoustics and turbidity measurements amongst others. A simple measurement of growth is to add crystal seeds to a supersaturated solution, leave for a set time, and compare weight before and after.[1]

Meta-stable zone

The metastable zone (MSZ) is an area on the concentration/temperature chart where only growth and not nucleation takes place. The metastable zone width (MSZW) is the degree of supersaturation where this is true. For cooling crystallisation this is the degree of undercooling. In industrial manufacturing of chemicals MSZ is the desired region to crystallise as seed crystals can be added in of a fixed size distribution and the resulting crystals will grow to a tighter crystal size distribution than if primary nucleation had been allowed to take place. The size of the zone is not a fixed value, it is determined empirically for each chemical system and is different under different experimental conditions. The amount of undercooling allowed increases with increased rate of cooling, not seeding the solution, adding certain ppm levels of ionic impurities, longer time kept above saturation temperature, higher temperature of storage above saturation temperature and smaller volumes of solution.[1]

1.2.2 Nucleation theories

Classical Nucleation Theory (CNT) is the treatment of nucleation as a first-order phase transition from a supersaturated phase to an ordered solid. It was originally derived for the condensation of a vapour into a liquid and it was extended by analogy to explain solid formation .

CNT describes the process of ordered proto-crystals identical to a final crystal in a constant equilibrium of growing and dissolution. Because it is energetically favourable for a molecule or ion to be in the bulk solid and unfavourable to be at the solid/liquid interface, there are two competing contributions to the free energy of the crystal: the free energy change for transformation from liquid to solid (ΔG_{fus}) and the free energy change for formation of a surface (ΔG_s) which, in a spherical particle, are dependent on the radius proportional to $-r^3$ and r^2 respectively.[3] Hence there exists a

critical radius, r_c, above which the growing of the proto-crystal is thermodynamically favourable. A proto-crystal of this size is called the critical nucleus.

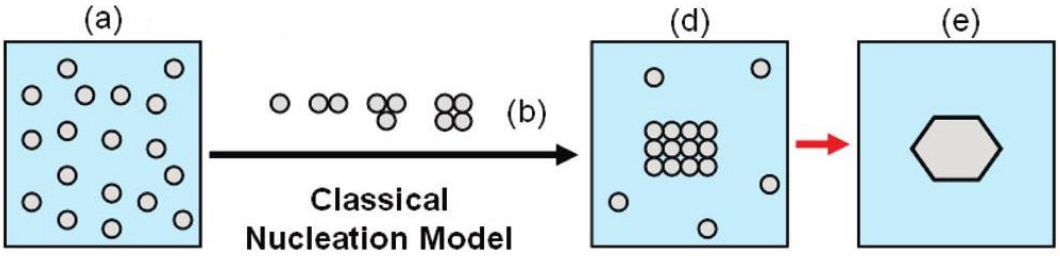

Figure 1-3 - The CNT nucleation model (adapted from Ref. 3). (A) Molecules in solution. (B) Growth of ordered nucleus one molecule at a time. (D) Ordered nucleus reaches critical size. (E) The resultant crystal.

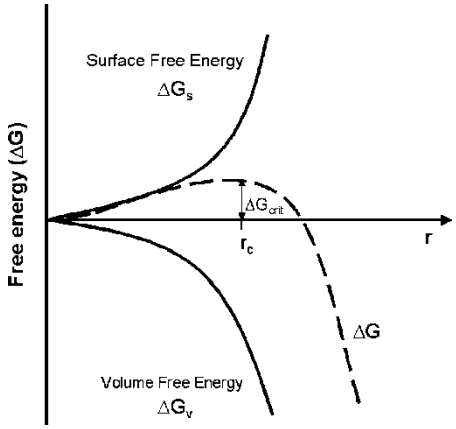

Figure 1-4 - Free energy of spherical nucleus as treated in CNT (reproduced from Ref. 3). The critical nucleus is defined as when the rate of change of volume free energy from forming a solid crystallite matches the rate of change in free energy from creating a solid-liquid interface.

The CNT model makes several assumptions:[3]

1) The clusters are spherical and the molecular arrangement is the same as for the large crystal.
2) The surface energy is temperature independent and independent of curvature and size.
3) Growth occurs one monomer at a time with clusters at rest and not in colliding.
4) The nucleation rate is time-independent and is perfectly distributed in space.
5) The formation of clusters does not change the vapour state and they are incompressible in ideal gas.

With these assumptions, the steady-state rate of nucleation, J, is governed by the Arrhenius expression:[1]

$$J = A\,exp\left(\frac{-\Delta G_{crit}}{k_B T}\right) \tag{3}$$

Where A is the pre-exponential factor, k_B is the Boltzmann constant, T is the thermodynamic temperature and ΔG_{crit} is the free energy change of the formation of a critical nucleus from solution. For crystals growing from solution this can be rearranged in terms of the supersaturation, S:[4]

$$J = A\,exp\left(\frac{-16\,\pi\gamma^3 v^2}{3\,k_B^3 T^3 (ln\,S)^2}\right) \tag{4}$$

Where γ is the interface tension of the critical nucleus and v is the molecular volume.

These predictions have enabled CNT to become the main theory that describes crystal nucleation for many years and a lot of good research has been built upon it. CNT is still very useful as it presents a reasonably low calculation cost for computational simulations of crystallisation. However there has been experimental evidence building which is beyond the capability of CNT to describe. In their review, Erdemir *et al.* listed the limitations faced when trying to apply CNT.

These are:[3]

1) CNT predicts nucleation rates 1-2 orders of magnitude higher than the rates inferred from expansion cloud chamber experiments.
2) Temperature dependent corrections are required.
3) CNT assumes uniform composition and so therefore fails for binary systems with concentration gradients.
4) The steady state perfect distribution fails.
5) One cannot predict the pre-exponential factor A. This is related to molecular mobility and can account for tens of orders of magnitude difference of rate in solution.
6) CNT cannot deal with small nuclei.
7) The properties of nuclei differ dramatically from that of the final crystal.
8) CNT does not provide any information about the structure of aggregates or pathways leading from the solution to the solid crystal. Only size determines whether or not the nucleus grows to a crystal.
9) CNT cannot account for molecular self-assembly of non-monomers and cannot predict which polymorph is produced.

These limitations have led researchers to develop new theories to replace CNT as the dominant model for nucleation.

2 step nucleation theory

Over the last 20 years two-step nucleation theory (2SN) has been developed from empirical evidence. The main difference compared to CNT is that instead of a nucleus being built up molecule by molecule in the exact shape of the final crystal lattice, molecules in solution cluster together with solvent forming regions of higher density approaching that of a crystal, yet are highly disordered. These clusters can lie in local energy minima or can even be thermodynamically favoured compared with the perfectly dilute solution. The clusters then overcome a smaller energy barrier than predicted in CNT to form a more ordered solid of comparable density, which will become a crystal. There is evidence to suggest that this solid may still be partially amorphous and has to undergo a further phase transition into a stable crystal.[5]

Prior theories involve infinitely diffuse solute in solvent, where each molecule of solute has a perfect solvent shell around it. The real environment is not like that and involves molecular interactions that bring solute molecules together in a dense liquid-

like cluster which is stabilised by the solvent. As solute increases in concentration a wide distribution of sizes of these clusters is obtained. A cluster needs to overcome an energy barrier to organisation required to form a lattice and, if it is of high enough density, form a stable nucleus. Much like in CNT, if the candidate nucleus is too small the crystallite will dissolve back into solution.[6]

Pan *et al*. presented a numerical model to two-step nucleation in their 2005 paper based on crystallisation of proteins *via* a dense liquid intermediate.[7] It presumes that cluster formation occurs on a much faster timescale than crystal formation within the cluster, giving the overall crystal formation rate as:

$$J = \frac{k_2 C_1 T \, exp\left(-\frac{\Delta G_2^*}{k_B T}\right)}{\eta(C_1,T)\left[1+\frac{U_1}{U_0} exp\left(\frac{\Delta G_C^0}{k_B T}\right)\right]} \tag{5}$$

Where k_2 scales the nucleation rate of crystal inside the clusters, C_1 is the protein concentration inside the clusters (estimated ~300 mg mL^{-1}), ΔG_2^* is the barrier for nucleation of crystal inside the clusters, η is the viscosity inside the clusters, U_1 and U_0 are the effective rates of decay and formation of clusters at temp T, and ΔG_C^0 is the standard free energy of a protein molecule inside the clusters in excess to that in the solution, depicted schematically in (Fig. 5c). Recent experimental determinations indicated that this is on the order of 10 $k_B T$.[8]

The disadvantage of this model is that, aside from temperature, it does not feature direct external control of parameters and will therefore require many *in-situ* measurements of localised parameters rather than bulk parameters in order to validate it. It also is much more intensive to model computationally, therefore in dynamic simulations CNT is still the preferred theoretical framework.

With no strong method of reliably predicting crystal forming behaviour, then empirical work is necessary to develop understanding and control.

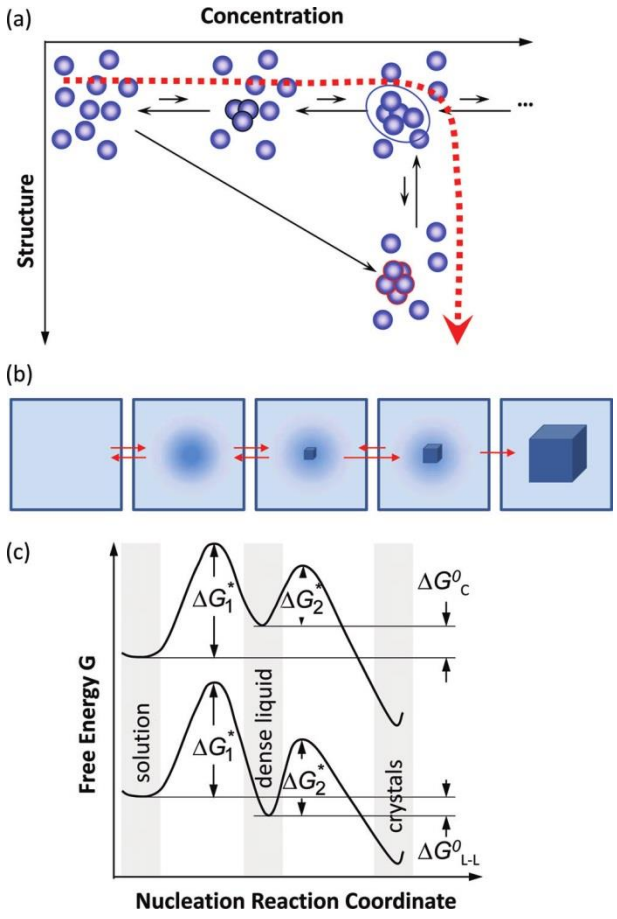

Figure 1-5 - The two-step nucleation model (reproduced from Ref. 61). (A) Disorganised clusters form and grow in size and density. These clusters then organise and, if above the critical nucleus size, go on to form a crystal. (B) A mesoscopic view of cluster formation and crystal growth from within it. (C) The 2SN free energy diagram showing the dense clusters either more or less favoured than that of a diffuse solution, but in a stable local minima with barriers to crystallisation and dissolution.

1.2.3 The need for nucleation control

Nucleation versus growth control

Nucleation control determines when crystals will first appear, their initial polymorph, the total number of crystals and where they will form (in bulk solution or on an interface etc). Growth control determines the crystal habit, the survival of

competing polymorphs and the crystal size distribution (CSD). Since nucleation is the initial process it can affect crystal growth control significantly. If there is only one polymorph formed then there is no competition. If there is ten times as many crystals formed, they should be equally ten times as small. Therefore true control of crystallisation needs nucleation control.

Industrial uses of nucleation control

For many chemists who synthesise new molecules, they need a large single crystal to perform single crystal X-ray diffraction and verify their structure. However nucleating with unknown physical properties can be very hard. Often a crystallographer can be waiting weeks to see if one forms spontaneously. This is especially important in protein crystallisation where a crystal structure is the only way to verify the structure and function of the molecule. It can take months of waiting before any crystal is made and that might not even be of high enough quality to diffract! These are nucleation control problems looking for solutions.

Polymorphism

Polymorphism is the ability for the same molecule to crystallise in different three-dimensional packing arrangements. Each form has different thermodynamic and crystalline properties. According to Ostwald's rule of stages the form which initially appears is the least thermodynamically stable and, therefore, dependent on the environment. Further polymorphs may form from solution after it, or through transformation.

Elusive polymorphs are polymorphs that initially appear but are unable to be experimentally reproduced once a more stable form appears. Since crystal growth is easier than primary nucleation and a thermodynamically favoured polymorphic crystal has the lowest solubility, once it forms it will grow at the expense of the less favoured form by solution-mediated transformation. Since it can be hard to purge this from a system, growing the original polymorph again may prove extremely

impractical: eliminating contamination of new polymorph and finding correct conditions that favour the original one, although this has been shown to be possible.[9]

Since different polymorphs have different crystal properties, they are considered different materials in pharmaceutical regulation and patent law. To be unable to recreate a polymorph can therefore have disastrous effects on drug manufacturing, whereby regulatory approval and trials are needed for the new polymorph, a very expensive and risky process. Ritonovir, an anti-retroviral drug, was temporarily removed from the market when a new polymorph was discovered.[10]

Thus there is a need to be able to control and select the formation of polymorphs preferably in a sealed environment to mitigate against seeds or contaminants that promote the formation of the other polymorph. Each polymorph has a different thermodynamic energy and a different kinetic selection factor therefore there are two factors to base a selection strategy upon.

With nucleation control being needed, what are the current methods for achieving this?

1.3 Nucleation control in batch

1.3.1 Non-laser techniques

Seeding

Seeding involves placing controlled amounts of the desired crystal into the mother liquor to grow larger. This avoids homogenous nucleation, and, if the crystals undergo secondary nucleation, can be self-sustaining: generating new seed crystals for the next batch. Measurement methods (involving for example a spectroscopic probe) can be combined with computer control of an experimental variable (for instance jacket temperature) to tailor the growth conditions for desired crystal properties (such as fines removal).[11,12] This is the preferred industrial method, although it does offer the possibility of contamination when the seeds are introduced.

Solution conditions: Temperature, supersaturation, impurities, solvent

The solution conditions for nucleation: concentration, temperature (and supersaturation), level of impurities and choice of solvent can all have an impact on nucleation, and changing them can offer some degree of control. However this means running a process at conditions set by stochastic thermodynamic parameters. If a lower temperature is desired (for instance for safety reasons), then the other parameters need to be changed to accommodate that. To get more parameters into desired industrial ranges then a different control method is needed.

Role of solvent

Although different solvent environments affect the thermodynamic solubility of solutes, it was seen by Davey *et al.* that the solvent can have a strong effect of directing which polymorph is kinetically favoured as well.[4]

Antisolvent

Introduction of a liquid miscible with the solvent but unfavourable to the solute can very quickly reduce the solubility of the solution. Solution which is completely outside the metastable zone crystallisation will be instantly induced and so this can be a reliable nucleation method.

Ultrasound

Using ultrasound to induce nucleation (sonocrystallisation) can give a tight CSD similar to seeding.[13,14] It works by creating cavitation of solvent to gas in solution which induces nucleation upon the collapse of the cavity. The proposed nucleation method is via a large increase in concentration as the solution rushes to fill the collapsing cavity. It has also been suggested a collapsing cavity is the cause for the old trick of scraping a spatula along the inside of the crystalliser to induce nucleation.

Shock

By sending a shockwave through solution it is possible to induce nucleation. It is suggested this is due to a shockwave passing through the solution increasing density

as it passes. This is used in commercial hand warmers to induce nucleation of sodium acetate trihydrate.

1.3.2 Laser techniques

NPLIN

The use of a collimated, nanosecond pulsed laser to induce nucleation is described below (Section 1.5).

There are other techniques which also induce nucleation using a laser. Each have a different mechanism of nucleation which have advantages and disadvantages compared with NPLIN.

Laser-induced cavity formation nucleation

Laser induced cavity formation nucleation is a technique which uses high intensity, focused beams to rapidly heat up solvent to form a bubble during a laser pulse and, when the bubble collapses, cause a localised increase of solution density and therefore supersaturation and collisions and form nuclei.[15] It is a useful way of spatio-temporal control over nucleation as it has potential to work with many systems. However it does not have control over local supersaturation, the number of nuclei or the amount of damage caused to the system.

Continuous wave optical pressure

One paper showed control of nucleation at a surface using an optical trap-like setup.[16] Using photon pressure created a concentration gradient at the surface and nuclei began to form.

This technique would not work in flow because it takes time to build up a sufficient concentration gradient and with reasonable mixing or moving fluid this would not occur.

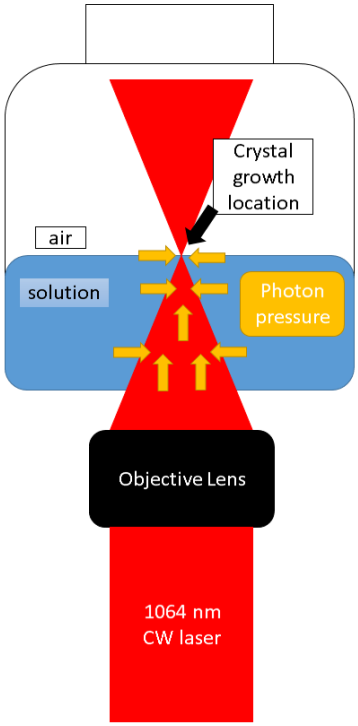

Figure 1-6 – Principle of continuous wave optical pressure nucleation. A CW 1064 nm beam is focused onto an air-solution interface causing photon pressure (orange arrows) to push the solution towards the air interface where it is trapped. At this location the concentration of the solute will increase and a crystal will form (after tens of seconds).

Photochemical Nucleation

Some of the first light-induced nucleation studies used photochemical degradation of the solute to form a compound which is insoluble in the solvent and crystallises out.[17] Using a high-intensity laser it is possible to do this at a small focussed point. This then creates a localised heterogeneous nucleation point upon which the desired product will find it easier to grow. Although this creates spatio-temporal nucleation control, it leaves all the crystals with contaminants in them which may completely change the

properties or characterisation of a substance and may also be banned by regulatory bodies. It is therefore something to be aware of and avoid when using LIN techniques.

With the exception of seeding none of these methods can offer single crystal nucleation possibilities. Most of the non-laser techniques can't offer precise spatial and temporal control, operating on bulk solution.

1.4 Nucleation control in flow

CMAC is dedicated to understanding and developing continuous flow technologies. Currently the apparatus of choice is a continuous flow baffled crystalliser (COBC or OFR). They are based on the principle of using oscillations to create turbulent mixing through restrictions in the pipes. They have water jackets to allow good heat transfer in combination with the mixing. This means their growth phase is very homogenous and reliable. However they would benefit from a very reliable source of nucleation.

Seeding

By pre-preparing a seed suspension of controlled size, growth can be studied in continuous environments eliminating the need for a nucleation method. This is fine for limited laboratory tests but limits the ability to function continuously or in very large volumes. This seems to be the method favoured by many papers on COBC crystallisation.[18]

Cooling

By cooling the solution supersaturation can be generated and when a critical supersaturation is reached the solution will nucleate.[19,20] This works well for generating nucleation reliably, but also has the downsides of fouling on the walls and being limited in thermodynamic conditions.[18] By mixing hot and cold solutions the cooling can be achieved much faster and altered depending on mixing regime.[21]

Mechanical

It was seen that scraping the sides of a crystalliser with a moving baffle rather than moving fluid setup could induce nucleation, whereas having a gap between the

baffles and sides would not induce nucleation.[22] This principle was used with a wet milling machine to achieve nucleation before an MSMPR.[23]

Antisolvent

The use of an anti-solvent generated supersaturation has advantages over cooling nucleation as different temperatures can be chosen and different antisolvents can be chosen which affect growth rate and polymorph. By adjusting the rate on antisolvent addition different parameters are affected such as crystal size distribution.

This can be achieved by simply mixing the two liquids, firing a jet of antisolvent in or using ultrasound to disperse the anti-solvent in the solvent or vice versa.[24]

Ultrasound

Ultrasound can be used to induce nucleation, it was proposed that this is due to reducing induction time via increased micromixing as well as increased concentration during cavity collapse.[24–26] It is also useful for discouraging fouling on the walls and can help dissolving smaller crystals to decrease the CSD width. By changing the intensity of the ultrasound the number of crystals produced per second can be altered.[26]

Laser

To the author's knowledge there is no laser-based technique which has been reported in the literature to nucleate in a continuous flow environment.

1.5 NPLIN

1.5.1 What is NPLIN

Non-photochemical laser-induced nucleation (NPLIN) was first discovered by Garetz *et al.* in 1996 while trying to observe second harmonic generation of light in supersaturated urea solutions.[27] Urea was added to water in test tubes and then sealed to create solutions of different concentrations. By heating to 45 °C the solid was dissolved and, upon cooling to 25 °C, supersaturated solutions were formed which

were stable against spontaneous nucleation for several weeks. The polarization of 20 ns pulsed 1064 nm laser light was selected using a zero-order quarter lambda waveplate and a portion of the annular shaped beam was selected using an aperture to create a spot of even intensity. The supersaturated solutions were then subjected to this irradiation at a rate of 10 pulses per second with an intensity of 250 MW cm^{-2} and nucleation occurred within 20 s to form a needle-shaped crystal observed to be orientated with the polarization.

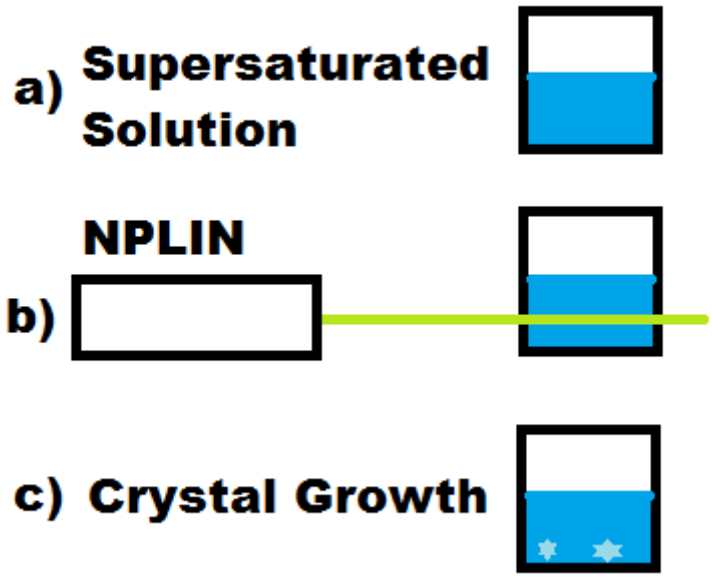

Figure 1-7 - Diagram of NPLIN process. (A) Prepare a solution above the NPLIN supersaturation threshold which is stable with respect to spontaneous nucleation over the crystal growth time. (B) Initiate laser induced nucleation with the required number of pulses above the intensity threshold. (C) Allow crystals to grow in a temperature controlled environment.

NPLIN uses light of a wavelength that does not induce photochemical degradation, and with an intensity and pulsewidth that does not induce absorption, cavitation or prolonged photon pressure.

As the study of NPLIN developed, other nucleation techniques were discovered which use a similar apparatus setup, but have a distinctive mechanism. These are discussed above.

To initiate NPLIN a nano-second pulsed laser is fired at a sufficiently supersaturated solution. The wavelength is selected so that absorption is negligible even at high intensities.

1.5.2 Empirical evidence

Experiments have been undertaken to show evidence for a supersaturation threshold, an intensity threshold,[27,28] and a minor wavelength dependence for each solute/solvent system.[29] If the solution absorbs a wavelength at any more than a very small degree, heating can detract significantly from the NPLIN effect. Some experiments required several days at the supersaturated temperature (ageing),[30] while others did not.[28] The number of nuclei formed was proportional to the intensity of the laser.[31] Ultrapure samples were harder to nucleate and unfiltered samples were easier to nucleate to some degree.[28] There was a dependence on pulsewidth,[32] ps pulses being very poor, ns pulses being optimum and μs pulses not tested. There was a dependence on temperature for solutions at the same supersaturation.[29]

1.5.3 NPLIN uses

NPLIN is an exciting area for study because it enables control of nucleation in time and space. Spatio-temporal control allows deterministic rather than stochastic nucleation, enabling study of nucleation events under a microscope, predicting crystal growth size and number, and a way to determine the correct conditions for selection of a polymorph. It offers a non-invasive way to initiate nucleation in a controlled manner, helping to minimise contamination and primary nucleation-related fouling. Further, because it is a form of nucleation, study of NPLIN will help develop the experimental underpinning of nucleation theories.

1.5.4 Environments / chemicals

NPLIN has been demonstrated in a variety of chemicals as seen in Table 1-1. Initially it was mostly small organic model compounds: glycine, urea, histidine. More recently

NPLIN of pharmaceuticals and proteins has been shown in solvents other than water as a good precursor to industrial use.[33,34] The work on inorganic aqueous solutions demonstrates the much lower intensities needed for these ionic compounds which may offer wider study possibilities.

Table 1-1 - List of compounds in literature that undergo NPLIN from an unfocused laser.

Compound	Solvent	Year	Supersaturation	Laser	Intensity	Duration	Reference (First author only)
Organic Crystals					**(MW cm^{-2})**		
Urea	Water	1996	1.15 – 1.24	20 ns 1064 nm	250 MW cm^{-2}	10-20 s 10 Hz	Garetz[27]
	Water	2002	1.24	9 ns 1064 nm	>40 MW cm^{-2}	60s 10 Hz	Garetz[35]
	Water	2005	1.23	7 / 9 ns 532 / 1064 nm	>60 MW cm^{-2}	60 s 10 Hz	Matic[36]
Glycine	Water	2001	1.38 – 1.45	9 ns 1064 nm	700	mins 10 Hz	Zaccaro[30]
	Water	2002	1.38 – 1.45	9 ns 1064 nm	700	60 s 10 Hz	Garetz[35]
	Water	2006	1.19 – 2.00	9 ns 1064 nm, 7 ns 532 nm	460, 240	60 s 10 Hz	Sun[37]
	Water	2014	1.34	7 ns 532 nm	> 83	60 s 10 Hz	Clair [38]
L-Histidine	Water	2008	1.40 – 1.80	7 ns 532 nm	240	60 s 10 Hz	Sun[39]
Acetic Acid	(melt)	2011	25.6 °C supercooling	7 ns 1064 nm	> 9.0	10 s 10 Hz	Ward[40]

Compound	**Solvent**	**Year**	**Supersaturation**	**Laser**	**Intensity / (MW cm^{-2})**	**Duration**	**Reference**
Carbemazepine	Acetonitrile	2014	1.1 – 1.5	7 ns 532 nm	> 150	60 s 10 Hz	Ikni[33]
	Methanol	2014	1.1 – 1.5	7 ns 532 nm	> 150	60 s 10 Hz	Ikni[33]
Sulfathiazole	H_2O / etOH	2016	1.1 – 1.7	7 ns 532 nm	130 - 300	1 – 60 s	Li[41]
Inorganic Crystals							
KCl	Water	2009	1.053 – 1.102	7 ns 1064 nm	> 6.4	1 pulse	Alexander[28]
	Agarose gel	2009	1.06	6 ns 1064 nm	> 7	1 pulse	Duffus[31]
	Water	2009	1.066 - 1.076	6 ns 1064 nm 202 ns	2.14 – 2.30	10 s 10 Hz	Ward[32]
	Water	2012	1.060	5.3 ns 532 nm 6.3 ns 1064 nm	> 5.6	1 pulse	Ward[29]
	Water	2015	1.08	5.3 ns 532 nm	>17	10 pulses	Ward[42]
KBr	Water	2012	1.060	5.3 ns 532 nm 6.3 ns 1064 nm	> 2.8	1 pulse	Ward[29]

Compound	**Solvent**	**Year**	**Supersaturation**	**Laser**	**Intensity / (MW cm^{-2})**	**Duration**	**Reference**
$NaClO_3$	(Melt)	2011	<14 °C supercool	7 ns 1064 nm	> 161	4 – 20 pulses	Ward[43]
Others							
Hen Egg White Lysosyme	0.1 M Acetate aqueous buffer + 3 % NaCl	2008	n/a	100 ps, 4 ns 532 nm	250, 10 - 26	10 s 30Hz, 10 s 20 Hz	Lee[44]
Bovine Pancreas Trypsin	CaCl/ H_2O / benzamide HCl/ Hepes	2008	n/a	5 ns 1064 nm	156	20 pulses	Lee[44]
4′-*n*-pentyl-4-cyanobiphenyl	(melt)	2009	(~1 °C supercool)	45 ps 532 nm	3.9	10 Hz continuous	Sun[45]

1.6 How does NPLIN work?

The exact mechanisms for nucleation using NPLIN have not been elucidated. In the context of two-step nucleation it is suggested that NPLIN provides a way to overcome the barrier from dense cluster to organised crystal nucleus, *i*.e. it alters the potential energy landscape to reduce the barrier for organisation of ions and molecules into a crystalline lattice.[36]

1.6.1 Optical Kerr Effect

The optical Kerr effect (OKE) is where the oscillating electric field of light induces a temporary dipole in electron distribution around an atom or molecule. The degree to which the orbital then deforms to match this dipole is called the polarizability. If a molecule has a coordinate that is more polarizable than the rest, this is called anisotropic polarizability and the molecule will feel a force to align itself to arrange this coordinate to the electric field vector of the photon.

The NPLIN mechanism of rotationally orientating molecules using OKE was first proposed by Garetz *et al.* in 1996 because NPLIN was more likely to involve induced dipoles *via* polarizability rather than a possible alignment of permanent dipoles. This was on the basis that the ~10^{14} Hz oscillating frequency of the light is several orders of magnitude faster than molecular rotation, resulting in a zero net electric field effect experienced by permanent dipoles.[27,30] However, they did not claim to rule out other mechanisms.

In their first experiments it was noted that the urea solutions required ageing for several days, as did glycine and l-histidine in later experiments.[30,39] They proposed this as evidence for NPLIN affecting the organisational step of 2SN. Although they did not suggest a reason for why aging is required, it could be to give enough time for the solution to have the correct distribution of cluster sizes required to have a critical cluster undergo organisation when the laser strikes. In the OKE model the energy barrier to nucleation is lowered by:

$$\Delta W(E) = -{}^{1}/_{2}\,(\Delta\alpha)E^{2} \qquad (6)$$

where $\Delta\alpha$ is polarizability anisotropy (the difference between the largest and smallest parts of the molecular polarizability tensor), E is the electric field vector.

Zaccaro *et al*. showed that the OKE mechanism predicts a lowering of the activation energy within the oscillating field of ~10^{-5} k_BT for most systems, much lower than that required by CNT kinetic predictions (~10^{1} k_BT). They suggested that the interactions of many molecules can work in a concerted manner to further lower the barrier, but that this was still only ~10^{-3} k_BT. This was confirmed by computational studies by Knott *et al*. which show that these cooperative interaction contribute little to lowering the activation energy.[46]

A very persuasive argument for the OKE mechanism was based on the observation that the resultant polymorph of NPLIN of glycine was dependent on eccentricity of polarization.[35] It was suggested this is matching of the shape of polarization to the shape of clusters which favour one polymorph or the other. However, this operates in a very limited supersaturation space; therefore polarization could mask other underlying reasons. Di Profio *et al.* suggested differing permittivity of the polymorph crystals lead to stronger interactions with the electric field and therefore will be more sensitive to variations in polarization.[47] It is also noted that later experiments strongly suggested glycine only forms dimer clusters of one shape that can form both polymorphs.[48]

1.6.2 Isotropic Polarisability

Alexander and Camp demonstrated NPLIN on KCl solutions in 2009.[28] Both K^+ and Cl^- have closed electron shell configurations and the KCl crystal unit cell is cubic. There is no anisotropy to the polarizability and therefore optical Kerr effects should not arise in this system. Instead they proposed a theory that the laser light affects the isotropic polarizability of the ions. However, they do not rule out the OKE as the mechanism operating in the organic systems previously studied.

The isotropic polarizability theory (IPT) of NPLIN assumes that the polarizability of a particle is equal in all directions (*i.e.* isotropic) and they examined it using the CNT model. Classical nucleation treats the energy of a growing particle in solution (and therefore a growing crystal) in the absence of an electric field as:

$$\Delta G(0) = A_P\gamma - V_P\, A\, ln\, S \tag{7}$$

where A_P is the surface area of the particle, γ is the solution-crystal interfacial tension, V_p is the volume of the particle, S is the supersaturation and the coefficient A is defined:

$$A = \frac{\rho RT}{M} \tag{8}$$

where ρ is density, M is molar mass of solid, R is the molar gas constant. The energy reduction, $\Delta W(E)$, for a dielectric particle residing in a static electric field is given as:

$$\Delta W(E) = -aV_pE^2 \tag{9}$$

where V_p and E are as defined above and a is the isotropic polarizability

$$a = \frac{3}{2}\varepsilon_0\varepsilon_s \left(\frac{\varepsilon_p - \varepsilon_s}{\varepsilon_p + 2\varepsilon_s}\right) \tag{10}$$

where ε_0 is the vacuum dielectric permittivity and ε is the relative permittivity for a particle or solution. Therefore the free energy in an electric field becomes:

$$\begin{aligned}\Delta G(E) &= A_P\gamma - V_P\, A \ln S - aV_PE^2 \\ &= A_P\gamma - V_P(A\, ln\, S - aE^2)\end{aligned} \tag{11}$$

and for a spherical particle:

$$\Delta G(r,E) = 4\pi r^2\gamma - {}^4/_3\,\pi r^3(A\, ln\, S - aE^2) \tag{12}$$

where r is the radius of the particle. Therefore CNT describes a critical radius $r = r_c$ where it is favourable for crystals above this size to grow, at the stationary point of the free energy change (when $\frac{d\Delta G}{dr} = 0$):

$$r_c(E) = \frac{2\gamma}{A \ln S - aE^2} \quad (13)$$

Thus there are terms that reflect supersaturation dependence (S), electric field dependence (E), solute dependence (a), crystal dependence (A) and solvent dependence (γ) on the critical nucleus size. This, however, suggests that the mechanism for NPLIN is that the electric field of the laser enables a smaller size of ordered nuclei to grow to stable crystals, rather than helping clusters to form ordered nuclei.

The IPT adequately models the slope of nucleation events vs. intensity just above the threshold for certain values of solution-particle interfacial tension; yet it does not predict the existence of a threshold. It also suggests a good reason for slight wavelength variation: the relative permittivity of dielectric particle is dependent on wavelength.

IPT predicts $\Delta W(E)$ to be between 10^{-4} and 10^{0} $k_B T$, depending on interfacial tension. Yet this is still below the CNT barrier of around 10^{1} $k_B T$.

1.6.3 Other Theories

The OKE mechanism suggests an orientational bias of molecules in the laser field, and the isotropic polarizability model suggests a lowering of their dielectric resistance. Although both theories assume transition of a dense cluster to an ordered nucleus, they rely on CNT which predicts an energy barrier much higher than that observed. Therefore, a physical description of the ordering step in two-step nucleation theory would be beneficial to understanding of NPLIN and which could be then modelled to test the influence of the laser upon ordering.

Other possible mechanisms might involve localised, instantaneous heating of the dense cluster such that it retains its density but decreases the viscosity of the molecules within thereby enabling rearrangement, ordering and nucleation.

Knott *et al.* point out that given the intensity of the lasers used, even if water transmits 99.98 % of light, 10^{12} - 10^{14} photons are not transmitted and so could be interacting with the solution in some way.[46]

2 Common Methods

In this thesis there are some methods which are used repeatedly and are written out here for brevity.

2.1 Laser Setup

Pulsed Nanosecond Lasers

Two nanosecond pulsed lasers were each used to induce NPLIN. A Surelite II (Coherent, USA) 532 nm frequency doubled Nd:YAG laser (max average power at 10 Hz: 1.1 W) and a Brilliant (Quantum, France) 1064 nm Nd:YAG laser (max. average power at 10 Hz: 2.1 W).

Q-switch power selection

The power output of the lasers could be adjusted by changing the Q-switch delay on the pulse. This altered the power output but also affected the nanosecond pulse-width and, at very low settings, beam quality. Average power at 10 pulses per second was measured using a power meter (Nova, Ophir, USA). The laser beam was cleaned up using an iris of a recorded size (typically 6 mm). With these parameters, pulse energy, peak pulse power, average intensity and peak pulse intensity can be calculated.

Polarizing beam cube power selection

For experiments where altering the average power but not the pulse width then a fixed Q-switch setting was used and intensity was attenuated by rotating a Glan-laser polarizing beam-splitter cube (Thor) with an anti-reflective coating at the laser wavelength used.

Telescope

If increased intensity or smaller beamwidth of the same intensity is needed then the laser beam can be passed through a pair of lenses in a telescope configuration.

High reflection mirrors (> 99 % at wavelength used, Eksma) were used to align the beam and deliver it to the NPLIN target.

2.2 Imaging

Images of lab equipment were taken with a mobile phone camera (Galaxy III, Samsung ; Moto G4, Motorola). For crystal images of vials, digital cameras (Powershot, S95, Canon) on optical mounts were used. For flow experiments or fast nucleation capture a laboratory camera with global shutter was used (acA2040-90uc, Basler, Germany) and a c-mount macro lens (MLH-10X, Computar, USA).

Filters were placed in front of the cameras when imaging laser strikes to prevent damage to the sensors from the intense laser light. A 716 nm short pass (KG1, Comar) was used with the 1064 nm laser. A 570 nm long pass (OG570, Comar) was used with the 532 nm laser.

2.3 Solution preparation

Ultrapure water

Ultrapure deionised water (>18.2 MΩ cm) was obtained from a water purification system (Arium Comfort I, Sartorius).

Weighing direct into vial

The fastest way of preparing a solution is to weigh dry solute into a pre-weighed vial and then weigh solvent into the vial. Due to the limited precision of the scale this makes the concentration of the solution less precise compared with the stock solution preparation method below and therefore was only used for preliminary experiments where exact concentration is not needed.

Stock solution

To make several samples of identical concentration a larger "stock" solution is first made as follows:

A borosilicate bottle (Duran) and lid are cleaned by submerging in water with detergent and scrubbing inside and out with a pipe cleaning brush. The bottle and lid are then rinsed in hot water 3 times, cold water 3 times and ultrapure deionised water 3 times. They are then placed in an oven at > 50 °C for 16 hours to dry and allowed to cool to room temperature with the lid partially on to minimise dust entry.

The solute is then weighed into the pre-weighed bottle using a pre-cleaned funnel to avoid losses to the top of the bottle. The solvent is then weighed into the bottle and the concentration is calculated. The stock solution is then ready to be dissolved in one of several ways outlined below.

Dissolving

The method of dissolution did not seem to affect the nucleation so long as no decomposition occurred. Therefore the preferred method was in a hot water bath with ultrasound irradiation for speed or in an oven overnight for convenience. Once visibly clear the solution was held at the high temperature for at least an hour to make sure smaller crystals were dissolved. Having the solution held at undersaturated temperatures should help extend the MSZW enabling larger supersaturations achievable in experiments.

Once dissolved it can be used as is or filtered into another pre cleaned bottle for continuous experiments. Otherwise it can be portioned into smaller containers as outlined below.

2.4 Sample preparation

7 ml squat vial

The squat vials could be used straight from the manufacturer "without cleaning" or with "soap and water cleaning". Soap and water cleaning involves submerging the

vials and lids in a hot water bath, scrubbing the inside and screw lip of the vial with a pipe brush in the soap water then rinsing off the lids and vials 3 times in warm water, 3 times in cold water and 3 times with ultrapure deionised water. They are then placed in a 55 °C oven on a clean piece of aluminium foil to dry for 16 hours.

2 ml vials

2 ml vials can be "soap and water cleaned" as above, but without the scrubbing step as they are too narrow to allow entry. They are usually used "without cleaning". When syringing stock solution into 2 ml vials, they require a vial box to stop them from falling on their side and a needle at the end of the syringe to allow precise entry into the vial.

Vial filling

The stock solution was taken into a syringe and passed through a syringe filter of choice and, if using 2 ml vials, a needle for precision. The solution is portioned out into each vial and the caps immediately placed to preserve absolute concentration. The caps are then fully tightened to seal and the vials labelled and placed back into the oven or to cool at room temperature as desired.

The typical filters for H_2O, etOH, meOH, *i*-prOH, were poly (ether sulfone) (PES) syringe filters (0.22 μm, Millex-GP) and for MeCN PTFE syringe filters (0.2 μm, MillexGP) unless stated otherwise. If unfiltered solution then the solution was portioned out using only the syringe or syringe and needle.

For most experiments an exact volume was not needed, only that the NPLIN irradiation volume did not touch the sides or meniscus of the solution in the vial. Unless otherwise stated, the volumes used were approximately 5 ml for 7 ml vials, 3 ml for cuvettes and 1.8 ml for 2 ml vials.

3 Screening of Chemical Systems

The overall aim of this thesis is to discover practical uses for non-photochemical laser-induced nucleation of crystals from supersaturated solution, in particular for pharmaceutical compounds. Theories on the mechanism of NPLIN have been shown to fail to predict what systems would and would not work, and the number of combinations of solute and solvents is almost infinite. Therefore having some selection criteria for studies and applications of NPLIN was considered to be important.

The three approaches taken were: firstly look at any pattern in previous systems confirmed to work in literature to seek a testable hypothesis. Secondly, if there is an infinite palette, then choose compounds on desirable properties to determine useful delimiters. Finally, an unknown parameter may display itself through repeated experiment and a new hypothesis could be built around this.

3.1 Solvents and supersaturation

The choice of chemical system for NPLIN studies is important as a limited number of compounds have been studied to date, with no indication of what selection criteria is necessary. An attempt is made here to outline the physical constraints on the chemical system as well as selection choices for desirable systems used within this range. As previously mentioned in Chapter 1 for NPLIN to occur the solution must be transparent to the laser wavelength and have a supersaturated solution that is metastable at the experiment temperature for a period longer than the experimental time of setup and irradiation. Finally the solution must be labile to laser nucleation, an unknown variable to be determined by the screening experiments.

When deciding what is the best solute and solvent combination to use for NPLIN the availability of a region of metastability is a key consideration.

Supersaturation can be defined in many ways depending on the expression of solution composition.[1] The supersaturation used here is the ratio of C ($g_{substance}$ per $g_{solvent}$ dissolved) to $C_{sat(T)}$ the theoretical saturation concentration at T where T is the

experimental temperature, which in the present work is normally near to room temperature and pressure.

In systems where C_{sat} increases with temperature, the absolute maximum supersaturation obtainable would be limited by the boiling (T_b) and melting (T_m) points of the solution. As a rough guide these will be near to T_m and T_b of the solvent, e.g., within 1 to 99 °C for water.

A minimum supersaturation is needed: the threshold below which NPLIN does not occur. This generally needs to be determined empirically, but is always greater than saturation ($S > 1.0$). Other perturbation techniques have nucleated at below bulk saturation, but these create a locally concentrated area of high supersaturation by depleting other local areas, e.g., focussed LIN and optical trap LIN.[49,50]

In practice the lower temperature for most batch experiments was determined by the ambient room temperature and C low enough to dissolve using standard laboratory techniques, e.g., in an oven at T < 90 °C. For the present work, the ambient T is usually between 18 – 24 °C depending on the day of year. To ensure stability, a heated water bath would hold the vials at a steady temperature, and they would undergo laser irradiation quickly after removal and drying as to limit the effects of surface evaporation and heat conduction.

The choice of supersaturation is therefore above the threshold supersaturation for NPLIN while still being metastable with respect to spontaneous nucleation: these conditions must be determined empirically for each system. Previous work in the group had indicated a rule of thumb for simple systems, to dissolve a maximal amount of solute at 40 °C and to cool to supersaturation at 25 °C. Therefore untested systems were made up at C_{sat40} and tested at 25 °C. Further solutions were made at concentrations adjusted higher or lower if no nucleation or spontaneous nucleation occurred (respectively).

In some cases the solution supersaturation was limited by reactions that the solutions undergo. Maleic acid was initially found to be resistant to dissolution at oven

temperatures high above the literature solubility values (65 °C for C_{sat} = 40 °C) until it was realised that it was undergoing water-catalysed conversion into fumaric acid, which has a much lower solubility limit, thereby depositing crystals (Figure 3-1).

Paracetamol solutions were seen to undergo a dark orange colouration (Figure 3-2) when heated in a terminal protic solvent, e.g., H_2O, MeOH, EtOH but not i-PrOH. The coloured solution would absorb the laser light and so bely the non-photochemical premise of the experiment. Vials of this coloured solution which were subject to irradiation did not nucleate. The discolouration is thought to be due to formation of para-aminophenol.[51]

Within the constraints above a range of supersaturation can be achieved by having a fixed concentration solution and varying temperature, or by using differing concentrations held at the same temperature. This enables the versatility of the technique to be adapted to different requirements of each unique chemical system or for efficient use of energy.

Figure 3-1 - Crystals of fumaric acid formed upon heating an aqueous maleic acid solution. Fumaric acid has much lower solubility which means the crystals form at high temperatures even when maleic acid is undersaturated. Bottle diameter 100 mm.

Figure 3-2 - 20 mm diameter vial containing a solution of paracetamol in ethanol (S_{20} = 2). This vial has been kept at elevated temperature for a prolonged time and turned from colourless to a dark orange colour. On cooling a colourless paracetamol crystal formed spontaneously, as can be seen at the meniscus. A coloured solution suggests the paracetamol has reacted to form an impurity which would absorb the laser light. Both coloured and clear paracetamol solutions irradiated with nanosecond pulses showed no crystal growth within the experimental timeframe.

3.2 Choice of chemical system

3.2.1 Investigating chemical systems

NPLIN has been observed to work for some systems and not others. It would be useful to have some guidelines for choosing chemical systems that are good candidates. For experiments on the nature of the NPLIN method itself, it is worth having a system which will behave in a predictable and desirable way. In literature only a small number of compounds have been reported as NPLIN active (see Section 1.5.4, above).

For the purpose of the present work, three different types of chemical system were tested, as follows:

- NPLIN model compounds

Key objectives of the present work are to study the physical principles underlying NPLIN and how NPLIN behaves in flow. For these purposes a compound is required which exhibits reliable NPLIN activity, is low cost, benign and produces repeatable results. An easy way of telling whether crystal nucleation was from the laser irradiation or not would also be desirable.

- Solvent effects

There has been shown evidence that NPLIN works in many solvents with some compounds showing activity in one and not another.[33] However, most previous experiments have been performed in water. Investigating if solvents have an effect on NPLIN activity was a high priority. It would be desirable to study systems where solubility data is available for a range of solvents.

- Compounds similar to current pharmaceutical ingredients

One of the aims of developing NPLIN would be to see it used as a reliable nucleation technique for industrial production of pharmaceuticals and fine chemicals. Having a test system which already resembles the macroscopic crystal properties of pharmaceutically active compounds would ease the transition into commercial use by demonstrating viability.

3.2.2 Choice of solvent system

We discuss the potential effects of solvent using a particularly relevant example. Paracetamol is a pharmaceutical which has been widely studied in the literature making it a useful model compound. Initial attempts to induce nucleation in aqueous solutions with the laser were unsuccessful. One reason for this may be the low solubility (~13 g kg^{-1}) in water.

Since paracetamol solubility changes significantly with solvent (Figure 3-3), the effects of different solvents on paracetamol NPLIN activity were tested. Stock solutions of the appropriate concentration (Table 3-1) were dissolved in an oven at 55 °C and syringed through a 0.2 μm PES or PTFE filter into sets of 10 glass vials

(7 ml). On cooling to 20 °C, half were subject to 532 nm irradiation and half kept as a control. The vials were examined for crystals 1 minute after irradiation and none were found. In some vials (both control and irradiated) crystals appeared spontaneously after about 15 minutes and grew to their maximum size within an hour. Any vials which had not nucleated were again irradiated, but did not produce any crystals within an hour. Thus the crystallisation was determined to be spontaneous only.

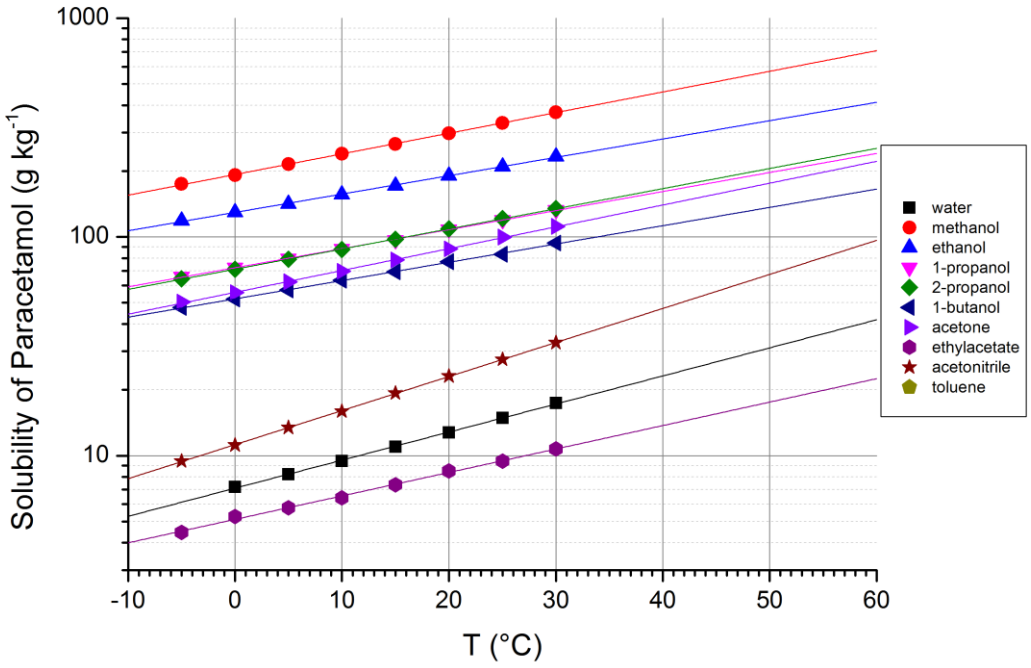

Figure 3-3 - Solubility of paracetamol in solvents adapted from (Reference 52).

Table 3-1 - Results of laser induced nucleation of paracetamol solutions

Solute	Solvent	C_{sat20} (g kg^{-1})	Max tested C (g kg^{-1})	S_{20} at max C	Laser nucleation
paracetamol	Water	12.78	25.86	2.0	No
paracetamol	ethanol	191	380	2.0	No
paracetamol	methanol	298	596	2.0	No
paracetamol	propan-2-ol	109	293	2.7	No
paracetamol	acetonitrile	23.10	100.4	4.4	No

Although no laser-induced nucleation of paracetamol was discovered in these experiments, they did highlight some useful insights into the solubility of chemicals in their solvent: the paracetamol crystals in the solvents at higher solubility were much easier to screen by eye as the crystals within grew large enough to observe reasonably quickly.

Since the different solvents did not seem to have much effect on promoting NPLIN in this case the solvent for future screening was chosen to be water, since solubility data of compounds in water is abundant, a better selection of solutes which have reasonably high solubility can be chosen. This also keeps the safety aspects of future experiments simpler.

3.2.3 Choice of Solute

The general criteria to meet for desired compounds were:

- Inclusion in CMAC target compound list / pharmaceutical-like properties. The target-compound list was devised by CMAC for investigating continuous crystallisation processes through the many stages in the supply chain. By experimenting on the same compounds, the centre can achieve better progress to real-world applications.
- Carboxylic (–COOH) functional group. Carboxylic acids were of high interest, as it seemed a common structural motif across the previous literature of organic molecules which are NPLIN active.
- Water as a solvent. Water was chosen as a solvent due to ultrapure 18.2 MΩ cm deionised water being available and its safety and cost being very reasonable.
- Solubility in water at 20 °C of between 5 and 300 g kg_{water}^{-1}. The solubility levels were chosen due to crystals forming lower than 5 g kg_{H2O}^{-1} were very hard to detect (see Figure 3-4) and solutions above 300 g kg_{H2O}^{-1} were hard to dissolve and nucleate, assumed to be due to high viscosity.

- Low toxicity. The safety and costs of the material were chosen so as to be able to get high purity compounds which would be easy to handle in large amounts.
- Low cost of material.

.

Figure 3-4 - Image of sulfamerazine crystals in acetonitrile fully matured to their maximum size. These crystals could not be detected for 2 days after growth, and even at maximum size were hard to detect by eye. For this example, S_{20} = 2, giving 0.7 g excess SMZ per 120 g MeCN; per vial pictured is ~7 mg crystals formed. Vial width is 12 mm.

3.2.4 Methods for nucleation detection

A method of nucleation detection is important to determine if a crystal was nucleated by laser irradiation or spontaneously. The simplest method is if crystals in the vial can be seen forming along the laser path by eye. This works best if the crystal is fast growing: observed, ideally, within seconds of nucleation. Therefore the time of nucleation can easily be attributed to the laser and any pre-nucleated vials should be obvious before selection of a vial for irradiation. For accuracy and recording, video cameras were placed facing vials perpendicular to the beam to capture fast-growing crystals.

If it is assumed that the crystals grow at a steady, measurable rate it is possible to trace back their growth to the point of nucleation. To be able to see growing crystals

as early as possible, and thus gain the most accurate extrapolation, a high resolution image is required at close intervals. To use this as a screening tool then it needs to be able to image several vials at once.

3.2.5 Polymorphism

From the literature there is evidence of NPLIN being able to influence polymorphism through polarisation of the laser light or control of nucleation supersaturation.[36,39] All crystals observed or measured after laser irradiation were of the thermodynamic form in all the systems studied in this work, tested with PXRD, SCXRD, polarized microscopy and Raman spectroscopy where appropriate.

However during the course of experiments it was noted that the metastable, orthorhombic form 2 of paracetamol and the metastable tetragonal form of malonamide were spontaneously nucleated (before any laser irradiation) upon cooling to room temperature in several vials over several experiments. There was no obvious difference between the vials that nucleated each form in a batch and no obvious difference from the experiments which formed each batch with or without the metastable forms. It is possible that there is a precise combination of cooling rate and concentration which could easily form these otherwise hard to get polymorphs which may be eludicated through a series of screening experiments. However the appearance during the current set of experiments was purely stochastic and no obvious experimental variable controlled was responsible. Fine tuning of the process could be performed in the future to try and achieve repeatable metastable polymorph formation through cooling of these systems.

3.3 Selected compounds and Results

3.3.1 Organic compounds

Compounds were prepared by dissolving a stock solution of each concentration in an oven at 75 °C. Solutions were hot filtered through a 0.22 um PES filter using a syringe and needle into 2-ml autosampler vials. Vials were then placed into a 25 °C oven to

cool down slowly. In general, 10 vials were prepared at each concentration. Un-nucleated vials were tested by irradiation (532 nm, 44 MW cm^{-2}) of several, single pulses. If NPLIN was not observed the vial was subjected to 10 pulses per second for 10 s (100 pulses). The vials were monitored immediately after irradiation for each single pulse, and one hour later and subsequently one day later after the train of pulses. Single pulse nucleation is preferred for initial observations, but trains of pulses increase the chance of discovering whether the solution is NPLIN-labile or not. For each solution system that did not nucleate it is possible that they are still labile but not under easily accessible laboratory conditions: investigation more extensive than the screening described here would be required to verify.

Specific systems and comments are detailed below. The results are summarised in Figure 3-5. It can be seen that there is a window between stable, unnucleated supersaturations and unstable supersaturations of spontaneous nucleation where the metastable systems can be NPLIN active. There is no universal trend across different systems as to which absolute concentration or supersaturation could be expected to be NPLIN active or not. For systems that show no NPLIN activity it is proposed that their NPLIN supersaturation threshold is below their upper limit of metastability under the conditions used. Further work using different conditions (e.g., containerless droplets) would be required to verify NPLIN inactivity.

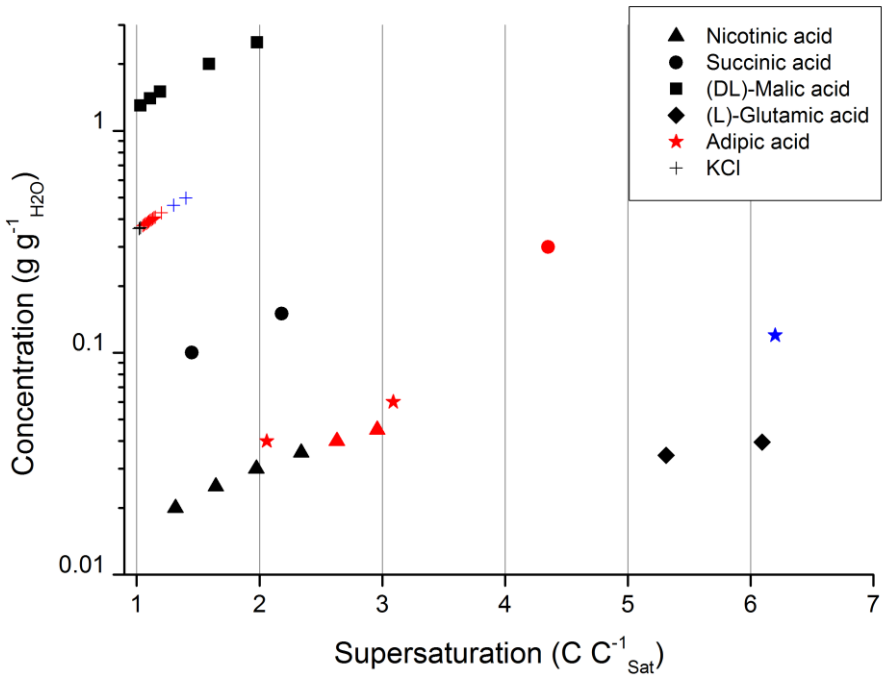

Figure 3-5 - Concentration supersaturation patterns in NPLIN of organic acids and KCl. Each shape represents a chemical system and each colour represents a supersaturation which was either stable (black), labile to NPLIN (red) or unstable to spontaneous nucleation (blue). A trend for each system can see an increase of supersaturation with concentration as is expected, but there is no absolute region of *C* or *S* where NPLIN lability can be predicted. As supersaturation increases either the solutions go from stable to laser labile to unstable or they are unstable before laser lability is observed.

Adipic Acid / H_2O

Adipic acid (99%, Sigma) was previously mentioned as being NPLIN active by Garetz *et al*.[35] It has two polymorphs at ambient conditions (one monoclinic and one triclinic) and one stable below 136 K (monoclinic). A range of concentrations were tested: (Table 3-2). At the higher concentrations, spontaneous nucleation was observed predominantly. Upon laser induced nucleation the vials only produced 1 or 2 crystals. Upon agitation the 40 kg_{H2O}^{-1} solution produced numerous crystals.

Table 3-2 - Results of laser-induced nucleation testing of solutions of adipic acid in water.

S_{20}	Concentration / g kg_{H2O}^{-1}	Spontaneously nucleated vials	Laser-induced nucleation vials	Unreactive vials	Other
6.0	120.0	10/10	n/a	n/a	
3.0	60.0	7/10	3/3 (1 pulse)	0/3	
2.0	40.0	1/10	1/1 (pulse train)	8/9	1/10 agitation nucleation
1.5	30.0	6/10	0/2	2/2	

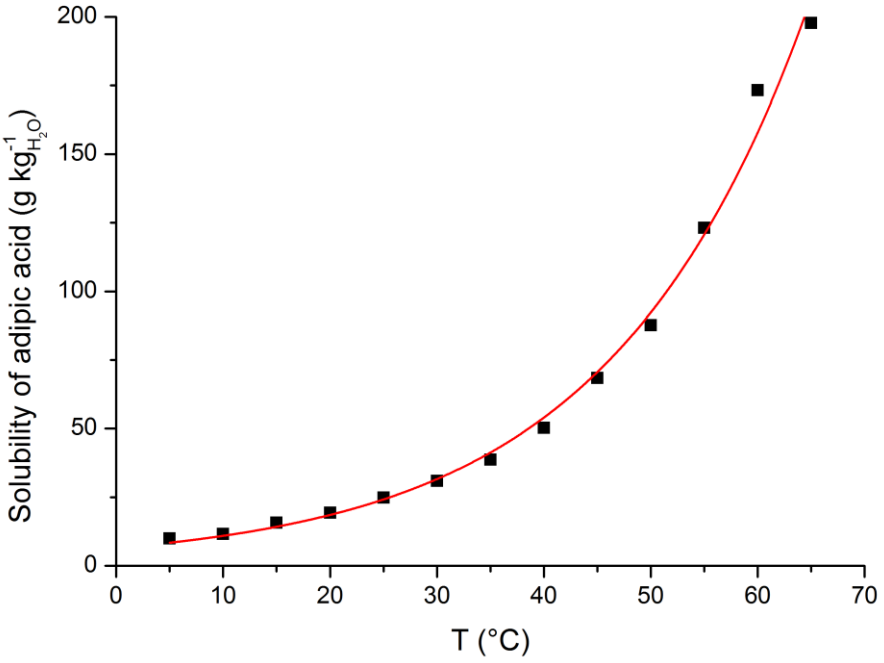

Figure 3-6 - Solubility of adipic acid in water adapted from Reference 53.

DL -Malic Acid / H_2O

DL-Malic acid (99%, Sigma) has high solubility in water, and was tested to see if related high solubility compounds such as sugars would be interesting to follow up.

Only solutions of 1800 g kg_{H2O}^{-1} and below could be dissolved in water, but did not nucleate upon laser irradiation.

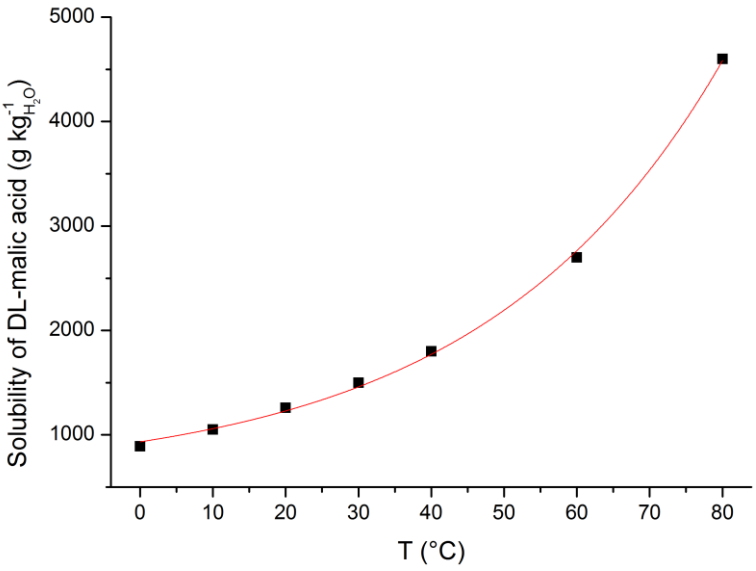

Figure 3-7 - Solubility of DL-malic acid in water adapted from Reference 53.

Nicotinic Acid / H_2O

Nicotinic acid (99.5 %, Acros Organics) was chosen due to its similarity to nicotinamide.

Table 3-3 - Results of laser irradiation of aqueous nicotinic acid solutions

S_{20}	Concentration / g kg_{H2O}^{-1}	Spontaneously nucleated vials	Laser-induced nucleation vials	Unreactive vials	Other
3.0	45.0	4/10	2/5 (1 pulse)	3/6	Crystals observed in <5 minutes
2.67	40.0	1/10	3/5 (1 pulse)	6/9	
2.33	35.0	1/10	(not irradiated)	9/9	

Nicotinic acid produced slow, radially growing needle crystals.

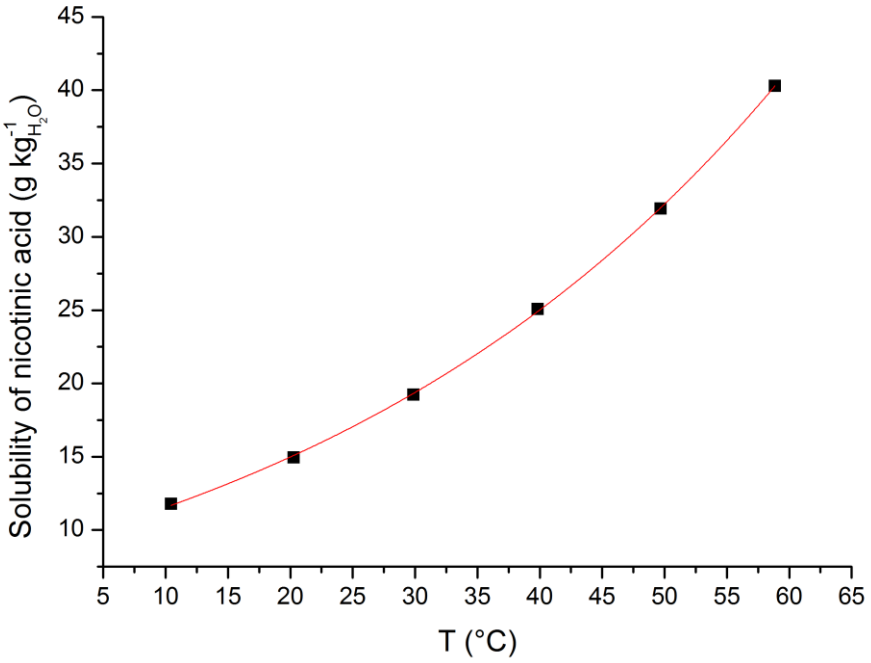

Figure 3-8 - Solubility of nicotinic acid in water from Reference 54.

Malonamide / H_2O

Malonamide was chosen due to its polymorphic activity at ambient conditions and, although not a carboxylic acid, had a desirable aqueous solubility. Three polymorphs have been identified in the literature: monoclinic, orthorhombic and tetragonal (from most stable to least).[55] The malonamide concentration tested was 240 g kg_{H2O}^{-1}, corresponding to $S \approx 2$ at $T = 20$. The beam diameter was 2 mm. A range of laser powers (60 - 100 mJ $pulse^{-1}$, 341 – 512 MW cm^{-2}) with up to 500 pulses were tried. Crystals were occasionally observed, but only over time periods where some control vials had also nucleated. No clear indication of NPLIN was observed.

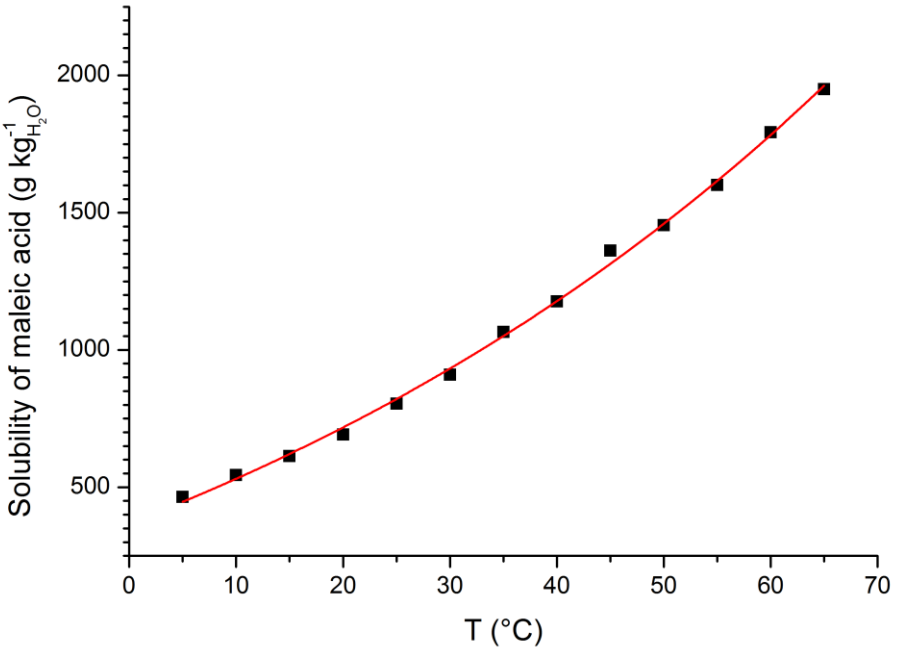

Figure 3-9 - Solubility of maleic acid in water from Reference 53.

Maleic acid / H_2O

Maleic acid was chosen due to its polymorphic activity. It has 2 known polymorphs, both monoclinic. The most thermodynamically stable has space group Pc and has a plate habit, the least thermodynamically stable has space group P2z/c and a rod habit.

Supersaturation could not be generated by the standard heating–cooling process due to decomposition to fumaric acid at elevated temperatures, as described in Section 3.1. Maleic acid may be suitable for study by cooling an undersaturated solution from room temperature: however, this was not attempted due to time constraints.

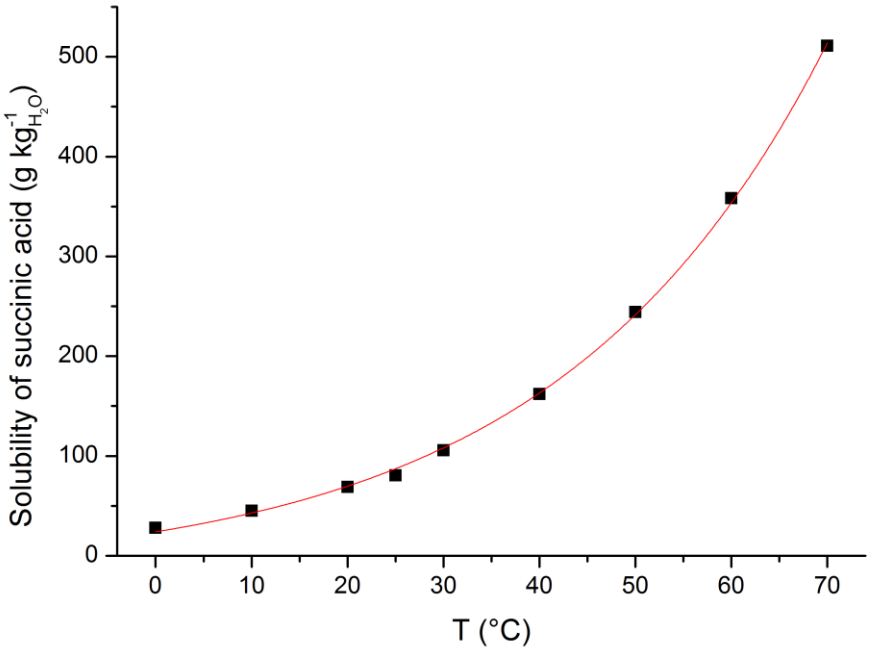

Figure 3-10 - Solubility of succinic acid in water adapted from Reference 53.

Succinic acid / H_2O

Table 3-4 - NPLIN irradiation of vials of succinic acid solutions in water

S_{20}	Concentration / g kg_{H2O}^{-1}	Spontaneously nucleated	Laser-induced nucleation	Unreactive	Other
4.3	300	1/10	3/3 (1 pulse)	5/10	Agitation of one vial also causes fast nucleation of many crystals
2.2	150	0/10	0/1 (60 s 10 Hz)	10/10	

Succinic acid was chosen due to its polymorphism and was previously mentioned as NPLIN active.[35] Succinic acid has 2 known polymorphs at STP: triclinic and monoclinic. Concentrations of 300, 150, 100 g kg_{H2O}^{-1} at T = 20 °C were tested.

300 g kg_{H2O}^{-1} succinic acid undergoes laser irradiation (0.8 W, 51 MW cm^{-2}) from a single pulse and produces very fast growth of needles radiating spherically from the point of nucleation.

L-Glutamic acid (LGA) / H_2O

LGA was chosen due to its polymorphism and was briefly mentioned as NPLIN active in literature.[35] l-glutamic acid has two polymorphs at STP: thermodynamically stable beta and metastable alpha, both with space goup $P2_12_12_1$.

No NPLIN was observed at 27 g kg_{H2O}^{-1} or below under this experimental regime.

It can be seen that not all organic compounds tested could be nucleated under these easy-to-obtain conditions, including compounds previously reported to be NPLIN active. Succinic acid showed the most promise as a future system, however at 300 g kg_{H2O}^{-1}, low numbers of large crystals were produced so may not be ideal for further studies on the NPLIN process. Adipic acid produced such small crystals that it may be good for developing studies on that particular system, but not studying the NPLIN mechanism or developing NPLIN flow systems. This is also the first time NPLIN activity has been found in nicotinic acid.

In conclusion, NPLIN may only be practical for certain organic compounds.

3.3.2 Inorganic systems

Previous work on KCl / water system in our group showed the ease of NPLIN (at $S_{23} = 1.06$) and that it produced discrete, countable crystals. However, the ability to nucleate an isotropic cubic crystal did not fit into the OKE model for NPLIN, proposed by Garetz, based on anisotropic polarizability. Systems which are similar but have a slightly different property were chosen to be studied to hopefully reveal a pattern in NPLIN activity which can improve our understanding on the phenomena.

From the screening of organic compounds crystals only adipic, nicotinic and succinic acids were found to be NPLIN active. However, the growth of these crystals was

slow, and the crystals often needle-shaped and difficult to count. In general inorganic systems, such as KCl and KBr, showed much faster NPLIN action and higher absolute concentration compared to the organic systems. The product crystals also tended to be more blocky and easier to identify. If a reliable stream of crystals is needed to test a flow system, this could be a good way of generating them. Previous work in the group had not screened broadly over a range of inorganic systems, and therefore several aqueous salt systems were tested under a similar regime for NPLIN lability.

The general methods outlined above (Section 3.3.1) were followed. The solutions were made at $C = C_{sat40}$ and cooled to 20 °C to generate supersaturation.

$Ca(NO_3)_2 \bullet 4(H_2O)$

Calcium nitrate tetrahydrate was chosen because it is a salt-hydrate system, with a divalent cation. Due to the one component nature of solubility in its own water of crystallisation, supersaturation was generated by melting and undercooling a pure crystal rather than changing concentration. After melting (to 50 °C) and cooling (back to a metastable liquid at 21 °C), no NPLIN activity was observed under conditions tested.

K_2SO_4 / H_2O

Potassium sulphate was chosen due to its high solubility in water, relation to potassium chloride and divalent anion. A vial (S_{20} = 1.28) was prepared via heating to 50 °C and cooled to 21 °C before laser irradiation (44 MW cm^{-2}). Within 15 s after the laser pulse small crystals < 0.1 mm were observed in the beampath. These were too small and grew too slowly to be of use for counting experiments, however it does demonstrate that systems with divalent anions can undergo NPLIN.

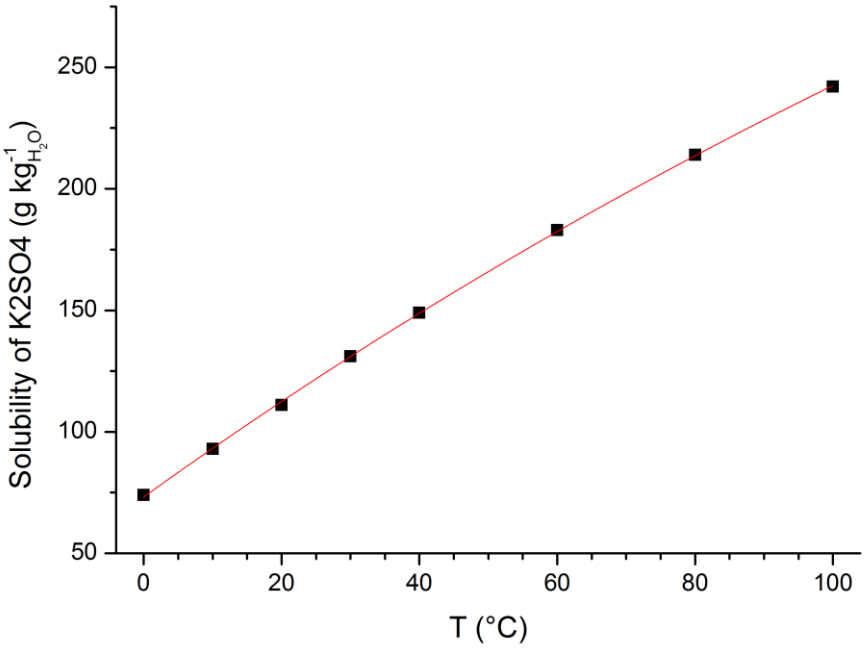

Figure 3-11 - Solubility of K_2SO_4 in water as reported in Reference 1.

$NaNO_3$ / H_2O

Sodium nitrate was chosen due to its cubic crystals. Vials (S_{20} = 1.14) were prepared via heating to 50 °C and cooled to 21 °C before laser irradiation (44 MW cm^{-2}). Cubic crystals were noticed forming along the laser beam path. Occasionally a rectangular prism was observed growing; however this was shown to be the same crystal polymorph using SC-XRD and polarized microscopy. Changing the concentration of the system (S_{20} = 1.05 – 1.20) showed crystal numbers varying with laser power, however the solutions were very unstable, often nucleating spontaneously. Upon filtration for the purpose of eliminating any stray particles a very curious detail was observed: the NPLIN activity nearly completely vanished in otherwise identical solutions. This observation was to be further investigated later (see Section 4.2.3).

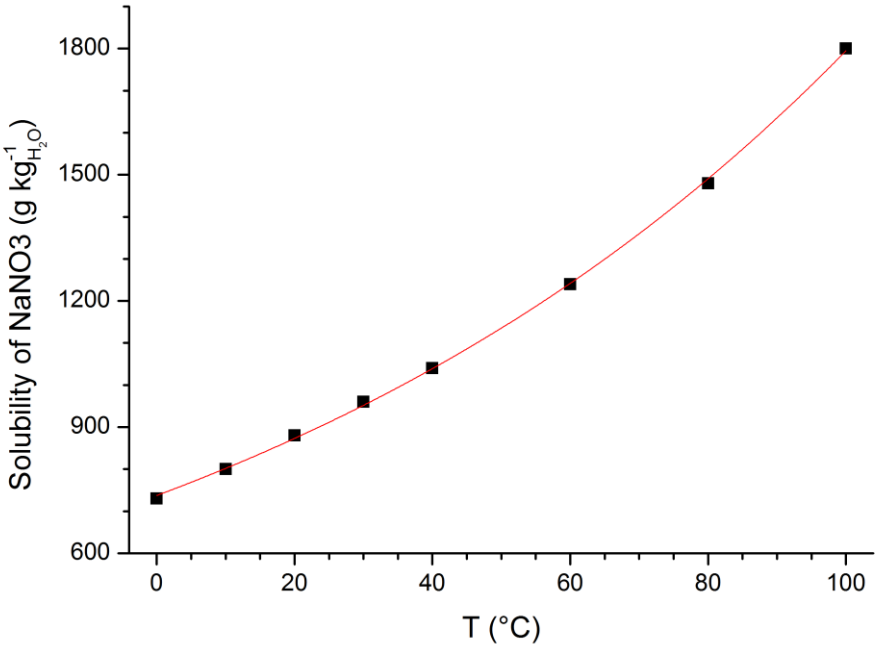

Figure 3-12 - Solubility of $NaNO_3$ in water as reported in Reference 1.

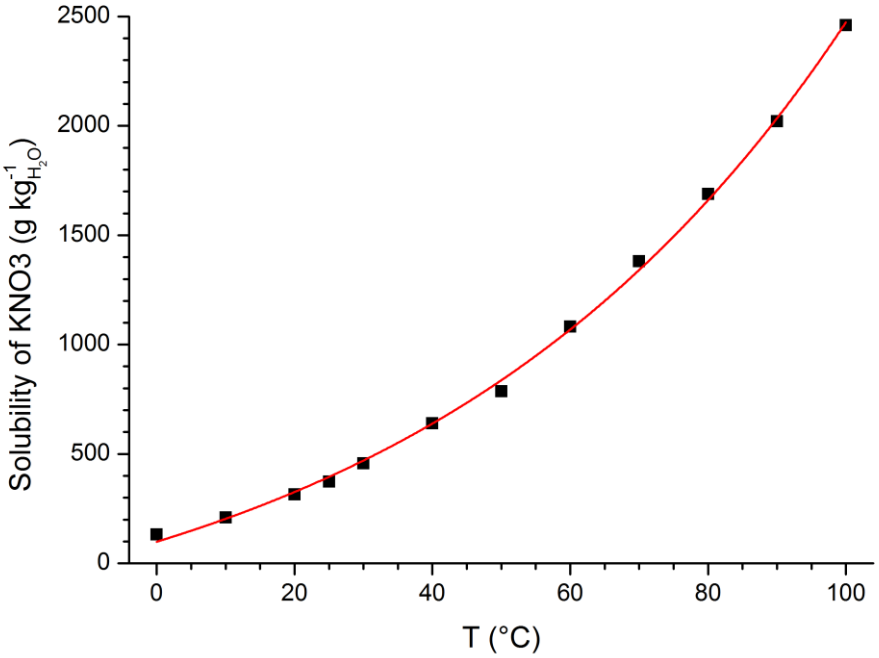

Figure 3-13 - Solubility of KNO_3 in water as reported in Reference 56.

KNO_3 / H_2O

Potassium nitrate was chosen due to its aqueous solubility and relation to KCl and $NaNO_3$. A vial (S_{20} = 1.20) was prepared via heating to 50 °C and cooled to 21 °C before laser irradiation (44 MW cm^{-2}). KNO_3 did not show any signs of crystals soon after irradiation but, an hour later, large crystals had formed in the container. The growth was deemed too slow and the final crystals would be too large to work with for further studies of crystal properties.

NH_4NO_3 / H_2O

Ammonium nitrate was chosen due to its relation to ammonium chloride and sodium nitrate. A vial (S_{20} = 1.48) was prepared via heating to 50 °C and cooled to 21 °C before laser irradiation (44 MW cm^{-2}). Upon irradiation, a crystal formed on the front and rear of the vial, within a second the two crystals had grown throughout the whole solution forming a solid. This would not be a good compound to use in continuous flow as it would cause a blockage! However it is very useful as a binary indicator of the timeframe of laser-induced nucleation.

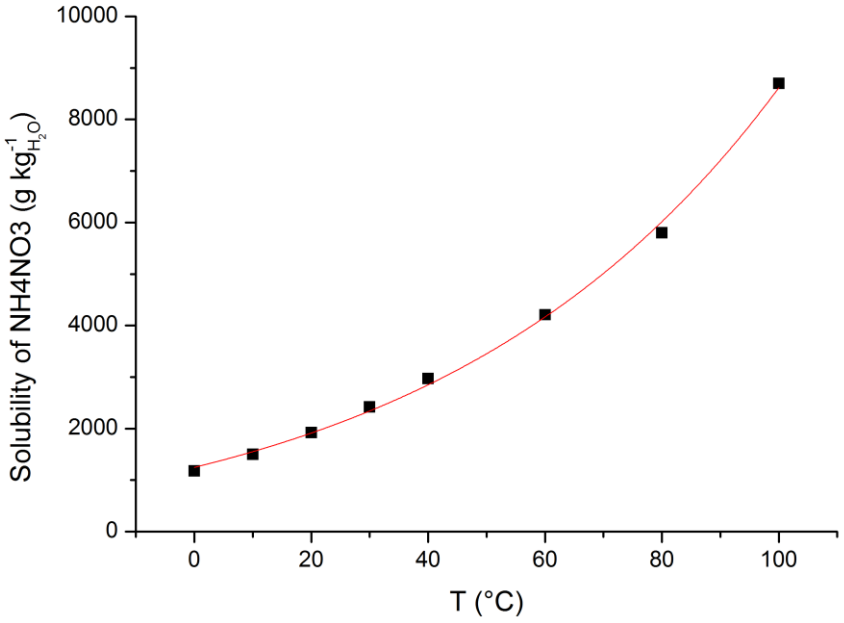

Figure 3-14 - Solubility of ammonium nitrate in water from Reference 1.

NH_4Cl / H_2O

Ammonium chloride (AC) was chosen for its relation to KCl and its molecular cation. A vial (S_{20} = 1.23) was prepared via heating to 50 °C and cooled to 21 °C before laser irradiation (44 MW cm^{-2}). AC was observed to easily undergo laser-induced nucleation, forming a very high number of crystals in the beam path at S_{20} = 1.23 within a second after irradiation.

Further tests showed AC is labile to the laser at supersaturations 1.045 and above. It was observed to always grow dendritically in 6 directions along the face-normals of a cube, filling into a rectangular prism shape through Ostwald ripening gradually over 3 days at 20 °C. Due to this dendritic nature it was also observed to readily form secondary nuclei several seconds after initial nucleation.

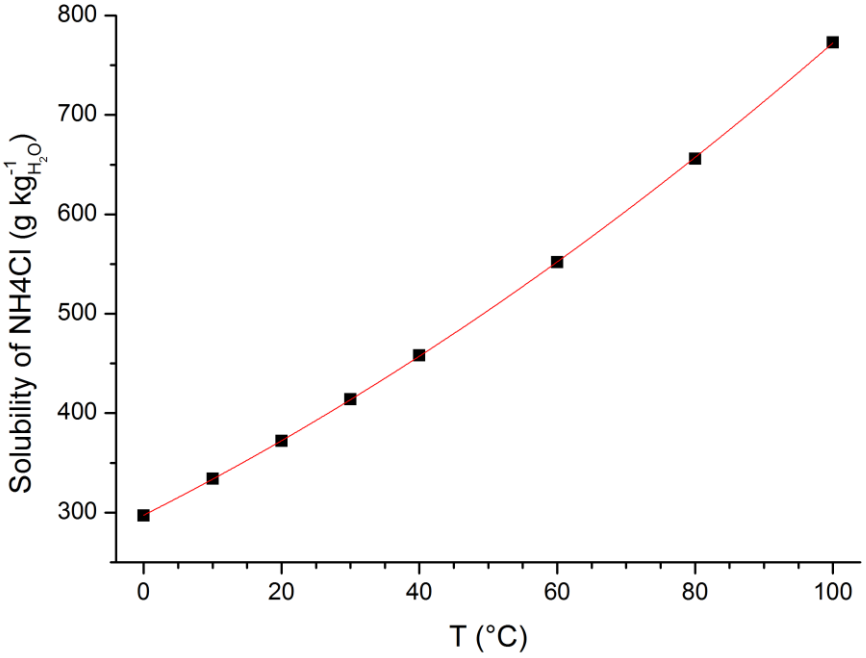

Figure 3-15 - Solubility of ammonium chloride in water from Reference 1.

KCl / H_2O

KCl was well-studied in the group prior to this project and was included for reference to compare against other systems. Vials were prepared via heating to 50 °C and

cooled to 21 °C before laser irradiation (44 MW cm^{-2}). KCl shows NPLIN activity from S_{20} = 1.03 – 1.20 in vials. At high supersaturations S > 1.08, crystals are produced and grow dendrites rapidly, often but not always leading to secondary nuclei. Eventually, after ~ 1 min, they grow into a familiar cubic habit with the occasional rectangular prism. The different morphologies were confirmed to be the same crystal polymorph by SCXRD.

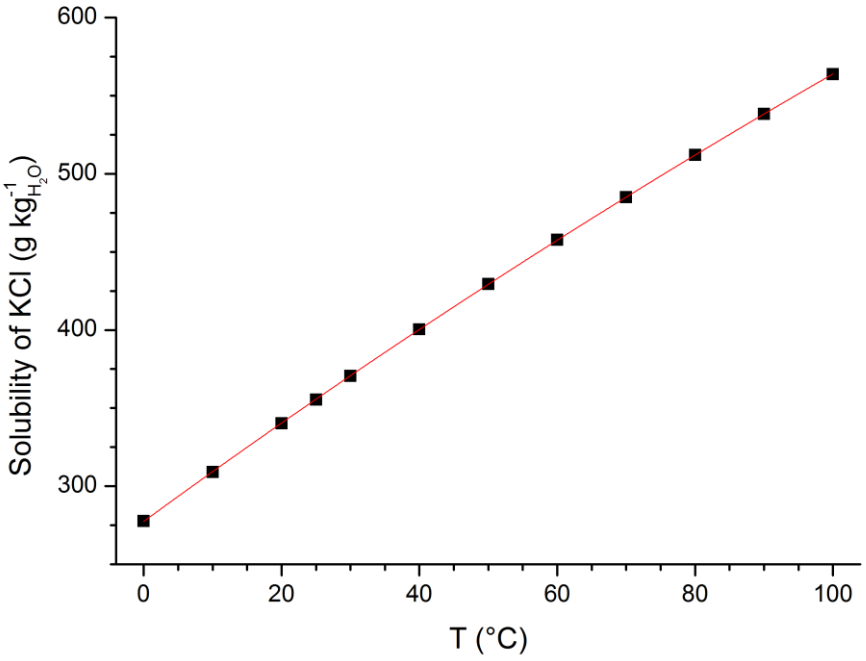

Figure 3-16 - Solubility of potassium chloride in water from Reference 57.

3.4 Choice of system for further studies

The only three systems in water to show fast-growing countable crystals were KCl, NH_4Cl and $NaNO_3$. $NaNO_3$ was ruled out of further studies due to complete suppression of activity after filtering through a PES membrane, a critical step in the screening process. However this system could be reconsidered for future unfiltered experiments in the future.

Ammonium chloride (AC) in water was picked as first choice due to its similarities with KCl: room temperature solubilities in water ~ 300 g kg_{H2O}^{-1}, both having cubic crystal space groups. They also both have highly symmetrical crystal habits enabling easy discrimination between individual nuclei. The supersaturation range for NPLIN activity was found to be similar and they both can be purchased off the shelf with reasonably high purity. NH_4Cl is also relatively low cost and benign (it is a minor eye irritant: mitigated by safety glasses) which enables a lot of it to be used with a low-risk protocol. Both chloride salts have very low absorbance at the laser wavelengths and in solution appear colourless and transparent to the eye. Both systems show reduced NPLIN lability and number of nuclei with filtering.

Despite their similarities, NH_4Cl is different from KCl in some significant ways. The most useful difference is the speed of crystal growth is much higher in AC than KCl. This means that growing AC crystals can be detected sooner, making it easier to count or confirm NPLIN. Because of the initial dendritic morphology, AC is much more prone to secondary nucleation compared to KCl. These two factors mean that when a solution has spontaneously nucleated, it is much more obvious that nucleation has not happened by NPLIN, which would avoid false positive results. Lastly, while both can undergo shock nucleation, AC tends to nucleate quickly at numerous points throughout the whole solution, but KCl is not as obvious: again, this is a good indication to identify spontaneous versus laser-induced nucleation.

4 Characterisation of NPLIN

Having selected a suitable system, aqueous ammonium chloride, for studying, this chapter looks at non-photochemical laser-induced nucleation (NPLIN) in more detail. What considerations are needed to perform an NPLIN experiment? What variables can be controlled to affect the nucleation or crystallisation outputs? Can NPLIN be easily incorporated into a continuous flow environment? The chapter discusses ammonium chloride studies in batch to directly translate to flow experiments; but other systems are used when necessary.

4.1 NPLIN experimental considerations

NPLIN is a relatively new and unstudied phenomenon, therefore considerations need to be taken into the experimental design to ensure that what is observed is truly laser-induced and not some other nucleation event. This section examines conditions which, through foresight or experience, were needed to learn enough about the phenomenon to take the method to a continuous-flow regime.

4.1.1 Container

The first constraint on NPLIN experiments is what container is the experiment going to be performed in and how does that affect it? In a batch experiment the container is where the NPLIN experiment takes place, and so it determines certain experimental parameters. Firstly the container must be able to permit the laser to pass through. This means having the whole container or at least a window made of material which transmits and does not absorb the laser light. If the laser is absorbed it will lead to damage and loss of containment. For physical experiments there needs to be a way to measure an experimental variable. If this is to do with observable crystal properties then having the container transparent to visible light also allows for imaging and illumination. The container also affects the uniformity and rate of heat transfer into or out from the solution.

The containers have to be cost effective verses the number required. If doing a parallel study on 1000 samples at once, it is prudent to have many cheap containers. Alternatively if using a window for a flow experiment that will be repeatedly

irradiated, having a much tougher material that can withstand laser irradiation for longer—even if initially more costly—may be worth it. The containers should have resistance to chemical interaction, both being influenced by the solution (e.g. corrosion) and influencing the solution (i.e. seeding or diluting the solution).

For experiments where supersaturation is generated by heating and cooling the containers need to have good seals which can resist any pressure increase without losing solvent to evaporation. Given the container material will have a different refractive index from air and from the solution, loss of laser intensity due to reflection can occur and, with curved surfaces, focusing within the solution can cause varying intensity through the solution. Having a large beam diameter relative to the container will cause only a fraction of the power to be used; having a small beam will leave large volumes of solution not irradiated. Finally, the size and shape of the container determines the volume of solution that can be irradiated, as well as the relative cost of the solution. A long narrow container will have poorer mixing, but enable a larger volume of solution to be irradiated compared to a similar volume spherical container.

Figure 4-1 - (left) Standard borosilicate glass vials: 7 ml, 20 mm diameter . (Right) the same vial showing screw neck and lid with aluminium inset.

Having a larger container of the same shape will allow more solution to be irradiated per pulse, but will also require longer heating and cooling times, and the contents will cost more.

The material of the container used for NPLIN experiments is important. It needs to be able to allow the laser to pass through unaffected while also having little effect on the nucleation environment.

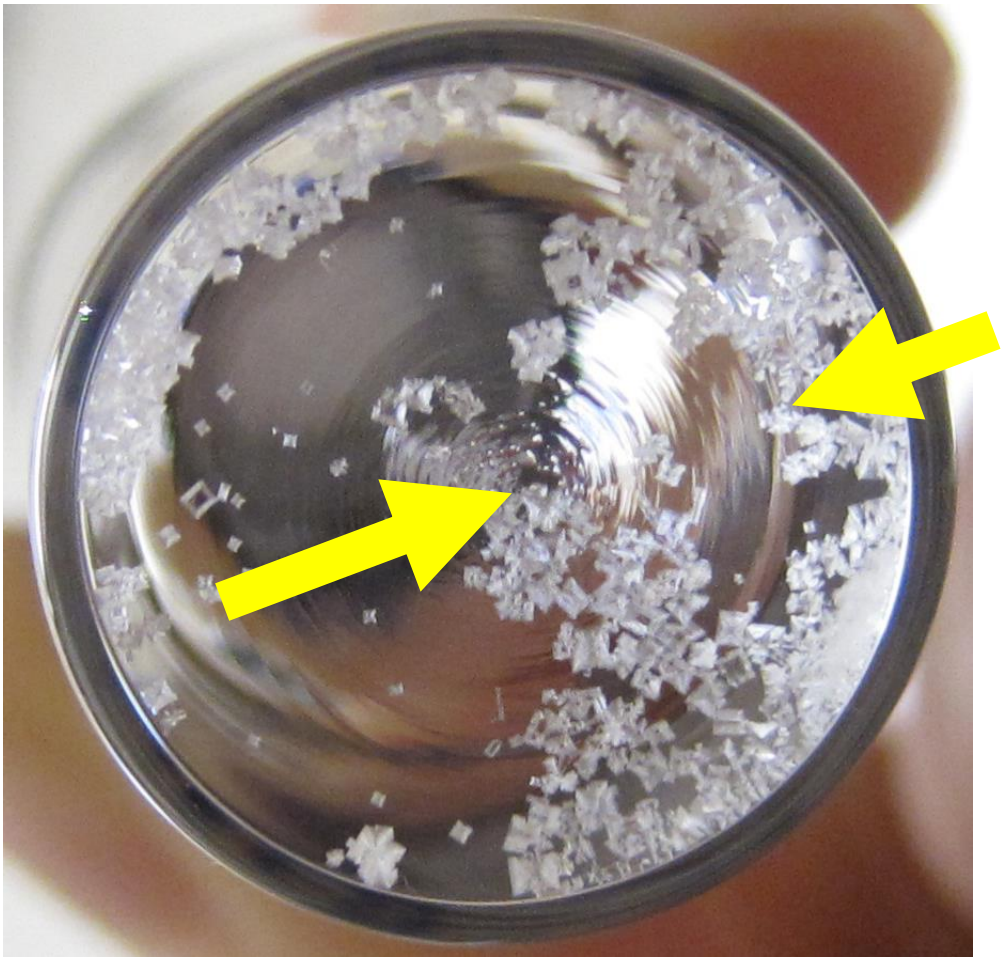

Figure 4-2 - Image of a 20 mm diameter squat vial from underneath containing a nucleated solution of KCl (S_{25} = 1.1) crystallised showing the change in focus due to the indented bottom. The yellow arrows highlight a distortion in the height of the bottom of the vial showing "rings" around the centre.

The laser wavelengths most commonly used for NPLIN are 532 nm and 1064 nm. Borosilicate glass gives good transmission of the laser wavelengths and is compatible

with a wide range of chemical environments. 7 ml glass squat vials (Fisherbrand, Fisher) with a (polypropylene) screw lid and an internal insert made of plastic-aluminium-coated cardboard glued in to it were initially used due to cost and availability (Figure 4-1). They have an external diameter of 20 mm with a relatively smooth cylindrical surface allowing for easy observation of the internal contents. On the underside there is a slight spherical cavity which is made of glass with a smooth internal but irregular external surface. This offered difficulty imaging these vials from underneath as seen in Figure 4-2.

To obtain clear imaging and enable laser irradiation from all sides, an ideal environment would be a fluorescence-type 4-sided cuvette, with the bottom polished for imaging and a clear lid on top. The price for one of these in either fused silica or optical glass is about £ 40 (Thorlabs) roughly the same as 250 squat vials making them prohibitively expensive for the high numbers of repetitions needed for statistical analysis of the NPLIN experiments.

Using cuvettes made of plastic would incur an acceptable cost £ 40 per 100 (Kartell 1960, Fisher). The most widely available material for cuvettes is polystyrene, which is susceptible to absorption of both laser wavelengths used, and has a very low tolerance to most non-aqueous solvents. The other common cuvette material, poly-methyl methacrylate (PMMA), will absorb 1064 nm light, but has minimal absorption at 532 nm. Repeated irradiation > 10 pulses shows slight darkening of the transparent plastic, which suggests some interaction; however the PMMA seems to be barely affected by a single pulse, therefore it could be used for experiments which only require single pulses and high optical clarity. PMMA is good for optical clarity and flatness, although not as good as optical glass and is much more reactive with solvents. Finally, the cuvettes have corners, which if not cleaned properly could harbour seed crystals, so are really single-use only.

The 7 ml glass squat vials were used for initial experiments demonstrating NPLIN. With a slow-growing system like paracetamol in IPA, it was found that crystals could form on the lid where solution droplets evaporate. Upon disturbances, such as

moving from storage location to target area, these crystals would drop into solution, initiating growth. This obscured observation of whether NPLIN had occurred or not. With a faster growing system, like ammonium chloride, the lid crystals would initiate spontaneous crystals quite clearly before irradiation.

The cause of these lid crystals was considered to have been due to (i) glue in the lid inset dissolving in the solvent; (ii) the area of the lid offering enough space to retain a droplet; and (iii) the material of the inset being attractive to droplets.

To mitigate effects from the lids, smaller 2 ml autosampler vials with PTFE septa were introduced. The septa curved inwards when the lid was tightened, allowing any droplets to run off the hydrophobic PTFE back into solution. The main advantages of these vials were they used smaller volumes and took up less area, so more vials could be made from the same stock solution and stored in a smaller footprint. The outside diameter of the vials was 12 mm, so the laser was more focussed by the vial, and passed through a smaller volume of solution. The vials had a taller profile so were more prone to being accidentally knocked over unless they were stored in a box. The 2 ml vials had poorer tolerances for lid tightening: they could lose their seal if tightened too hard, and took longer to fill and seal because of this. Since ammonium chloride was fast growing it self-indicates pre-nucleation and 7 ml squat vials could be used for most experiments. The 2 ml vials were not further used.

4.1.2 Cleaning

When using glass, the surface can be cleaned or coated to alter surface properties. Although received clean from the manufacturer, the vials possibly could have dust or detergent residues on them. Being able to clean down to the glass layer reduces the risk of a heterogeneous nucleation agent, or a solution contaminant interfering with the experiment. This was performed as outlined in the cleaning section in methodology.

Applying a commercial silane coating (Rain-X) decreases the surface tension of the aqueous solution on the glass and should prevent polarised nuclei being attracted to the surface. However, no studies in vials were performed on this, and may yet be of interest for the future.

4.1.3 Handling

Ease of handling is how practical the experiment is to perform. The first handling consideration should be safety. When filling open vials on the bench from a stock solution: if the solute or solvent is harmful then filling should be performed in a fume hood. Increased evaporation by the air flow requires filling being performed quickly. Solvent that gets trapped under a vial will cause it to start moving around on a polished surface. Ammonium chloride is an eye irritant, but while in aqueous solution, is stable enough to require only basic PPE precautions. Any spills quickly dry to reveal white crystals allowing clean up shortly after. Upon later implementation of vial racks, spillage was much reduced due to easier handling. So long as a good seal is kept on the container, evaporation at room temperature is negligible.

If the container was not sealed properly when placed in the oven overnight, a decrease in volume compared to the other vials can be observed. On the first fill the likely cause of this is not being tightened properly. On repeated dissolving of the same vials, occasionally a vial will show evaporation if left for periods of 3 weeks. Since it did not show decreased volume on first fill, it is possible the aluminium insert had degraded.

When filling up vials from hot stock solution, the 5 -10 minutes it takes to fill and seal the vials while exposed to lab temperature can cause significant cooling; sometimes enough to nucleate. For ammonium chloride this is not much of an issue due to the levels of undersaturation available at the concentrations and temperatures used: typically 60 °C hot and S_{20} of 1.1 (0.4132 g kg^{-1}, which is the value of C_{sat30}). During the time to fill 20 vials (7 ml squat) a vial of water was measured to drop from 60 °C to 30 °C. For other systems it was observed that cooling was rapid enough to cause

nucleation before putting the vials back into the hot oven. This rapid cooling could be a factor for the spontaneous forming of unusual polymorphs observed in paracetamol and malonamide samples.

As discussed above, spontaneous nucleation can occur due to splashed droplets inside the vial or inside the lid, which can evaporate over time to create a micro-environment of high supersaturation. Because such spontaneous crystals are out of the main solution, they do not dissolve upon heating, but also do not initiate nucleation if undisturbed. If disturbed, for instance by moving the vial or tapping the lid, these crystals can fall into the solution initiating secondary nucleation. Inverting the vials so that the base is at the top showed no crystal growth on the base. However since the lids were on the bottom it lead to more degradation of the aluminium insets and an inability to observe produced crystals in experiments. It was decided inverting the vials was not worth it.

In many cases, shocking the solution with something like a tap or finger flick seems to induce nucleation when there are apparently no crystals previous. Although it is possible that this could be due to microcrystals dropping into solution, it is possible there is some particular shock-induced nucleation mechanism as well. Certainly it has been shown that ultrasound can cause nucleation in a pipe completely filled with flowing solution (and therefore without dropping crystals) by creating extremely high local levels of supersaturation after cavitation events in the solution.[26]

The placement of vials in laser path is important. Initially the vials were placed by eye onto a traced laser path. They were then placed onto a traced vial outline which could be imaged by a camera. Improvements were made by using microscope slides as stops to hold the vial in a fixed position. Finally this was improved upon by using a 3D printed holder which could be anchored as an optical table component.

It was assumed that positioning would not make too much of a difference so long as the laser traced a path roughly through the centre of the vial, with striking slightly off-centre having little effect. However, tests on NPLIN in aqueous CsCl showed a laser pulse, slightly askew on a cylindrical vial, reflecting off the inside to cause

further nucleation outside the initial irradiated volume (Figure 4-3). This suggests that reflection of the beam could cause additional nucleation events.

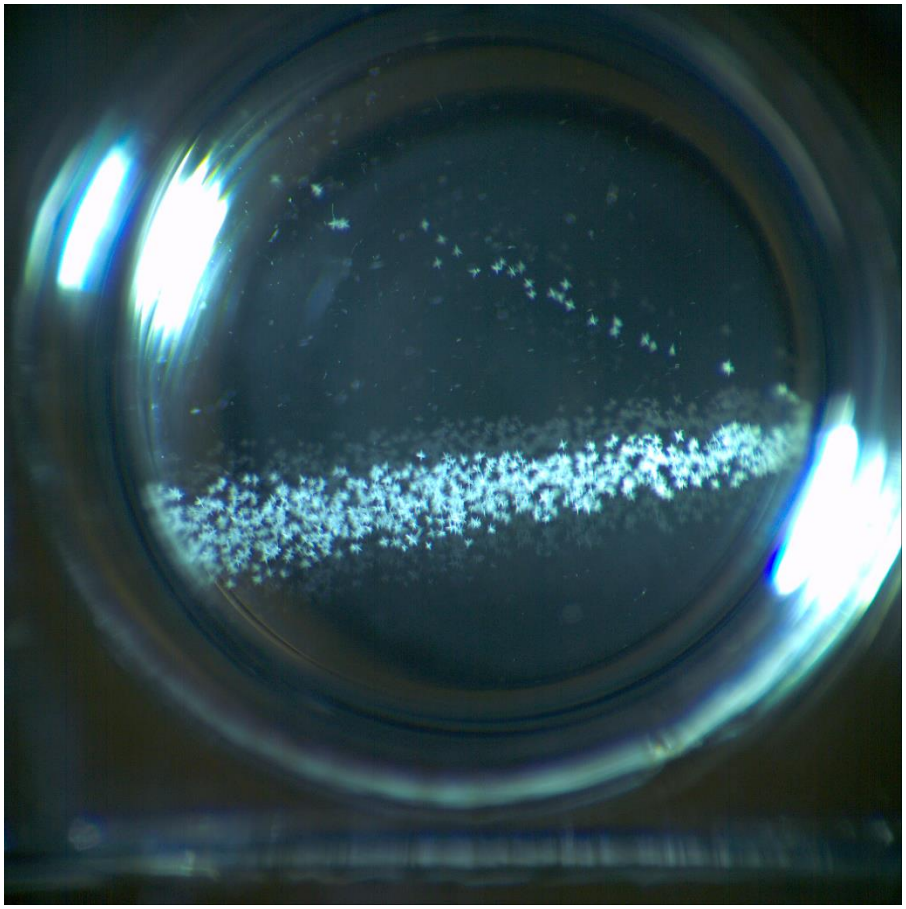

Figure 4-3 - Image from underneath a 20 mm vial showing NPLIN of aqueous CsCl off-centre. The forming crystals show part of the laser reflecting back into solution causing more nucleation.

4.1.4 Growth speed observations

For trial experiments we want very fast growth because it can show when nucleation occurs. Growth to visible < 1 s after nucleation can show clearly the beampath of the laser nucleating crystals. This means it can be used as an "indicator" for NPLIN: clear growth in a laser path and none outside it indicate the nuclei were generated only in areas where the laser passed. It is an added bonus that if the crystals grow fast they tend to be dendritic, giving the ability to quickly redissolve them upon heating to perform multiple experiments with the same solutions.

- Very fast growth at high absolute concentration can be problematic. For instance, aqueous ammonium nitrate at S_{20} = 1.5 grows so fast and so large that it occupies the entire volume of the solution, sometimes jutting out above the surface of the solution. If this system were used in flow it would instantly cause a blockage. However these systems can be great for studying dynamics of nucleation and growth as they will not travel far with fluid motion before they are observed.
- Fast speed growth systems (visible within 1 s – 1 min) don't work that well as NPLIN indicators, but can still be easily investigated using a camera to image nucleation.
- Medium speed growth systems (1 – 15 min) systems are harder to work with because it takes longer to get a measurement per sample, with fewer samples per day. Such systems have to be recorded or require a different sampling technique such as timelapse imaging.
- Medium-slow speed growth (15 mins – 2 hours) requires longer time-frame recordings, usually with multiple vials at a time. This is where a monitoring webcam offers a cheap solution. It can be set up in parallel with a thermometer to monitor changes in environmental conditions.
- Slow speed growth (2 hours – 2 weeks) really needs temperature control, non-irradiated control vials, time-lapse imaging of multiple containers and large sample sizes to determine evidence for NPLIN.
- Very slow speed growth (2 weeks +) would need statistical analysis as well as the above imaging and control techniques to determine whether NPLIN occurred.

Although aqueous ammonium chloride was chosen as the preferred system, if there were ways of detecting nucleation in the other systems then transferring this work to the other systems would be much easier.

4.2 Control of NPLIN variables

NPLIN offers a way of inducing nucleation events in a specific time and space. This in itself is an incredibly useful tool. However it also offers the possibility to control crystal number, morphology and size. This section examines what happens in batch when experimental conditions, laser and solution parameters, are controlled and adjusted.

4.2.1 Supersaturation

Supersaturation is the ratio of concentration over saturated concentration of a liquid solution at a specific temperature. In this thesis the mass of solute per mass of solvent is used as the concentration as it can be easily controlled when preparing solutions. Supersaturation is generated by dissolving the solute at a higher temperature where the saturation concentration is higher and then allowing to cool.

In the literature, control of supersaturation has been shown to affect the polymorph of resultant crystals.[58] In monomorphic systems (e.g., urea) supersaturation is still an important variable as it affects both spontaneous nucleation probability and growth speed. The effect of changing supersaturation on number of nuclei obtained through NPLIN was examined under batch conditions. The two systems studied were aqueous ammonium chloride and aqueous potassium chloride.

Ammonium chloride

A set of 10 pre-weighed 7 ml squat vials had between 1.56 – 1.80 g of ammonium chloride added to them. 4.00 g of water was then weighed into the vial to make up 10 vials of concentrations ranging from 0.3906 – 0.4501 g g_{H2O}^{-1} which gives S_{20} = 1.05 – 1.21.

The mixtures were then immersed in a water bath at 40 °C and also subject to ultrasound to dissolve. Once dissolved the samples were left for 1 h to equilibrate at 40 °C, before being allowed to cool to room temperature (22.8 °C).

The 1064 nm laser with 2.5x telescope and polarizer was used. The average power was measured as 0.460 W and the beam was reduced to 3 mm (102 MW cm^{-2}). Into

round 7 ml squat vials was shot a single pulse. The number of crystals formed was estimated by counting by eye. A revised figure for 0.4264 and 0.4352 g g_{H2O}^{-1} was made by counting crystals from video footage.

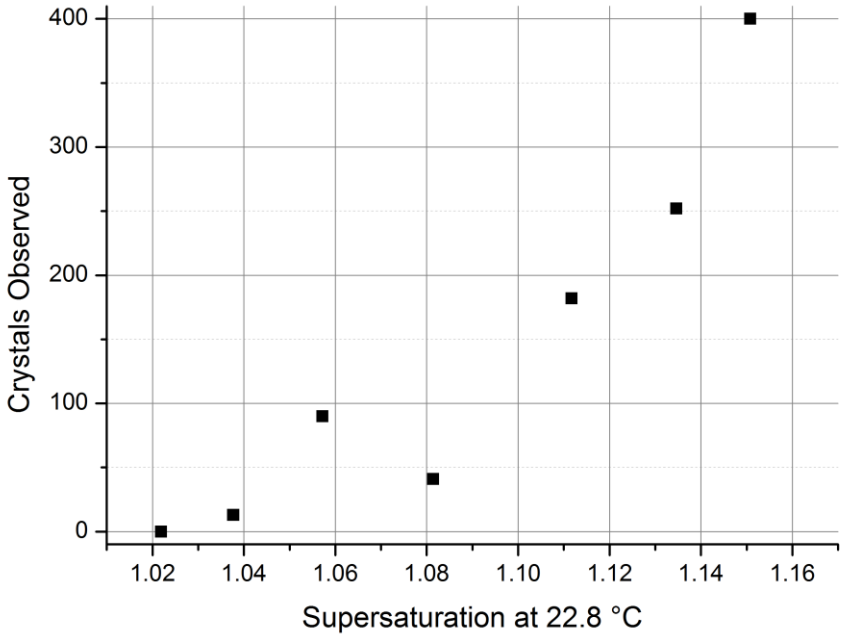

Figure 4-4 - Number of crystals produced after irradiation with single pulses of 0.0418 J (102 MW cm 2) 1064 nm laser light at different supersaturations of aqueous ammonium chloride. For S ≤ 1.1 crystal were estimated by eye, S = 1.11 and 1.138 were

For S = 1.15 (0.4414 g g_{H2O}^{-1}) it was only observed to be significantly higher than *S* = 1.135 (0.4352 g g_{H2O}^{-1}) and since it was impossible to count by eye data was recorded as "hundreds". Therefore 400 was selected as an approximation. *S* = 1.167 (0.4478 g g_{H2O}^{-1}) spontaneously nucleated on cooling and 0.39196 g g_{H2O}^{-1} did not respond to the laser.

In Figure 4-4 it can be seen that there is an increase in number of crystals produced per pulse as the supersaturation increases. Since only one sample vial was shot per supersaturation this curve is simply a useful guide for future experiments. Improvements to this experiment could be made by increasing the number of samples

per supersaturation, and using video recording to improve the accuracy and precision of crystals counted.

Potassium chloride

Into 7 ml vials were carefully weighed small amounts of KCl and 5 g of ultrapure water to make up a range of concentrations representing S_{25} of 1.02 – 1.20 . The solutions were dissolved in an oven at 50 °C and then cooled in a water bath to 25 °C. Each vial was irradiated with a single 0.052 J pulse of 532 nm laser light with 6 mm beam diameter, then checked for nucleation over a period of 60 s. Un-nucleated vials were shot again for 3 more attempts and then set aside (declared as 0 crystals). Once nucleated, the crystals were allowed to grow for 60 s before being counted by eye using a jeweller's loupe. For crystals < 100, each crystal was counted individually. For 100 – 500 the crystals were counted in estimated groups of 20. For > 500 crystals the crystals were estimated in groups of 50. These estimates were supplemented with a camera recording perpendicular to the laser path and a camera recording viewing from underneath the vial.

In Figure 4-5 a plot of crystal number versus supersaturation ratio at 25 °C is shown. No crystallisation was observed below a threshold (S ≈ 1.05) and then a gradual increase is observed before a rapid increase in nuclei number is observed. There is no indication of an upper limit of activity in the range tested.

This means that so long as the supersaturation is in the NPLIN labile zone then supersaturation is a convenient means to control the number of crystals produced.

The experiment could be improved in several ways. Creating more samples per supersaturation, using stock solutions, would give better statistics to reveal the underlying trend.

Regarding the imaging: the vials are not ideal for imaging, and so the crystals had to be counted manually. The video recorded from underneath showed crystals forming, but they were much too small on the image to get accurate numbers. Focus was also

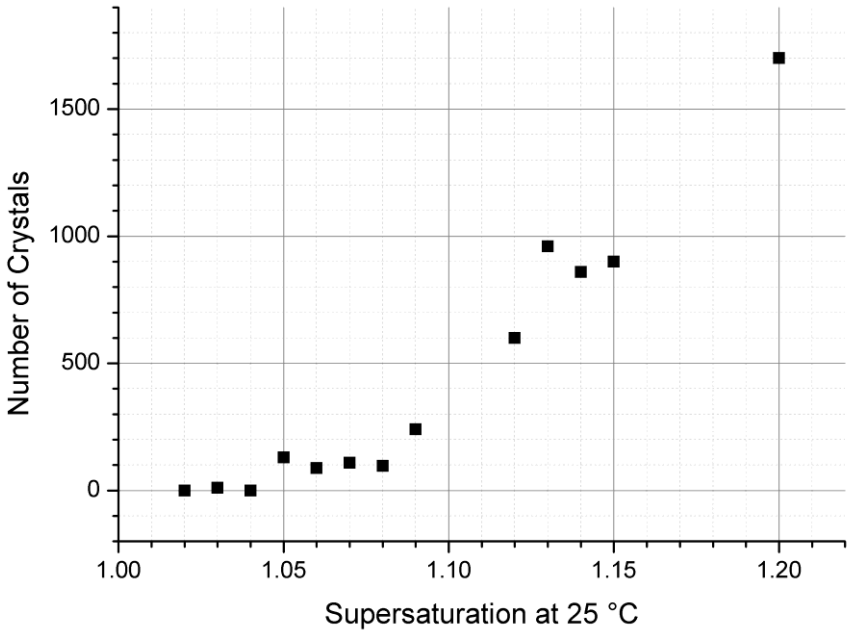

Figure 4-5 - The number of KCl crystals produced in a vial containing 5 g of water after a single pulse from a 532 nm laser at 0.052 J per pulse (6 mm beamwidth). An upwards trend can be seen as the supersaturation increases up to the metastable limit and a threshold between 1.04 and 1.05 is observed.

an issue: crystals forming mid-level in solution and sinking came in and out of focus as they fell. It is harder to measure from below than from the side where the laser path is in the focal plane. The video taken from the side was not illuminated strongly enough to observe all the crystals. KCl does not grow as quickly as ammonium chloride, and the crystals are transparent, providing a significantly harder challenge to video recording. If better recorded images could be produced then a more accurate crystal number per sample could be obtained.

4.2.2 Power & Power density

The average power of the laser can be varied easily two ways: The first is to change the microsecond Q-switch delay of the Pockels cell in the laser cavity. This varies the power with an easy setting on the laser, but also changes the temporal pulse width: undesirable if peak power is to be calculated from measured average power. The

second is to use some form of attenuation filter (at a constant Q-switch delay) that reduces the average power externally on the optics table. The solution used throughout these experiments is to pass the beam through a Glan laser polarizer, which can be rotated relative to the linear polarization exiting the laser.

Intensity is power over area illuminated, and peak intensity is the energy on one pulse over the time of that pulse per area the pulse travels through. Peak intensity is what our group believes to be one of the most crucial factors in deciding likelihood of nucleation. Therefore the peak power (volume) density of an experiment can be used as a crude comparison across experiments for absolute likelihood of nucleation.

For experiments where a simple yes/no to laser-induced nucleation is required, having maximum power in a large excitation volume would increase the chances of seeing rare NPLIN events, and therefore rule out whether or not nucleation occurred.

When trying laser-induced nucleation, if there is a low chance that a single pulse will cause nucleation, more pulses should increase the likelihood of any nucleation event happening. The laser can also be put into a multiple shot mode of 1 – 20 pulses per second. In the present work, only 10 pps or "10 Hz" mode was used in addition to single-pulse mode. There should, in principle, be no difference between 10 single pulses and 1 second of 10 Hz mode. However, it was noticed that the 10 Hz mode could often cause nucleation when a greater number of single pulses could not. One difference that explains this is that the same volume is irradiated in quick succession. It is unknown why this may increase the likelihood of nucleation.

The likelihood of nucleation can be increased by increasing the peak surface power density to the solution. [28,29,36] An experiment was performed to test whether increasing the peak power through a fixed volume can increase the number of crystals produced. Controlling the number of crystals produced within a fixed volume enables controlling of the final size of those crystals due to competition for the supersaturated solution. A supersaturation of $S_{25} = 1.1$ was chosen as it produced a countable number of crystals in the cuvettes used at an easily accessible temperature.

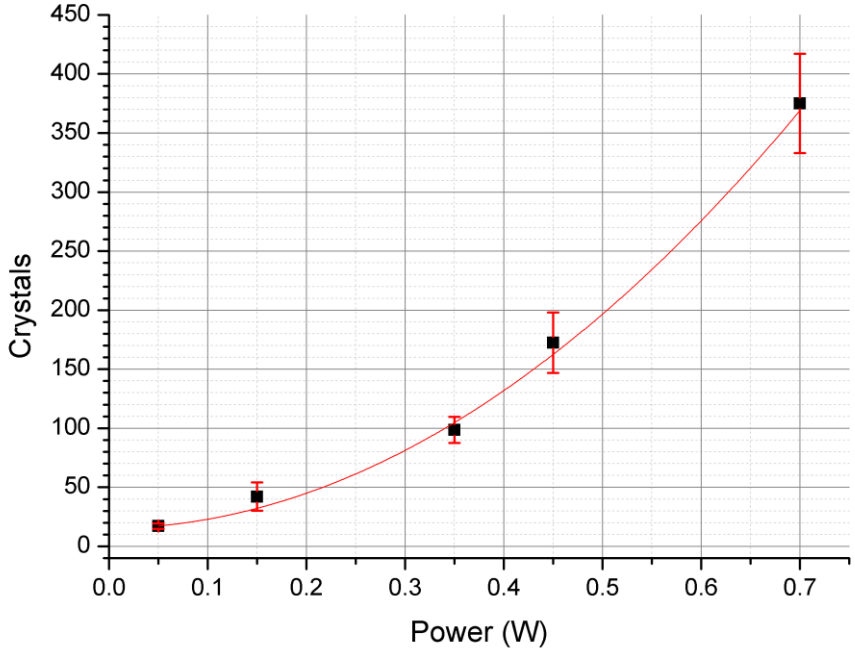

Figure 4-6 - Number of ammonium chloride crystals produced in a cuvette from a single pulse of 532 nm laser light. Unfiltered solutions (S_{25} = 1.1) were kept at and 25.0 °C. A quadratic line from the first observed power was fitted with a good fit R^2 = 0.9854.

Method summary:

Stock solution was prepared with ultrapure water and ammonium chloride at S_{25} = 1.1, which was then dissolved on hotplate and left in 60 °C oven for 1 hour to ensure complete dissolution. Solution syringed into 5 sets of 12 PMMA cuvettes (UP rinsed, oven dried) which were placed back into oven for at least an hour to make sure they were dissolved. Cuvettes were transferred into 25 °C waterbath, held in place with 3D printed holder to stop loss to WB currents. Any vials unnucleated were irradiated with a single pulse at a specific power 0.05 – 0.7 W with 8 mm beamwidth 532 nm laser. If no nucleation was observed the vial was irradiated again up to 5 times and declared inert if no nucleation after this (0 crystals). Nucleation was imaged from the side, as seen in Figure 4-7, using the Basler camera with LED illumination from above and crystals were counted from a selected video frame 1.0 s after first crystal appearance using ImageJ (ver. 1.50i) "find maxima" tool and manual refinement of the multi-point selection.

Results

The results shown in Figure 4.6 demonstrate a quadratic relation between laser intensity and the number of crystals produced. No attempt was made to find the minimum threshold intensity for this experiment. The points were fitted with a quadratic curve: $Y = 15(4) + 6\,(73)\,P + 710(150)\,P^2$ with an adjusted R^2 value of 0.9854, where Y is number of crystals and P is average power (W).

There is quite a bit of difference in the number of crystals observed at each repeat of a specific power, as can be seen from the single standard deviations shown in Figure 4-6. The most likely explanation for this is shot-to-shot variations in pulse power from the laser, as is expected for an (optically) unseeded Q-switched YAG laser of this generation (20 years old).

The square cuvettes would not increase the volume irradiated as much as a vial due to the 3D printed cuvette holder keeping the surface and angle irradiated by the laser to be mostly consistent.

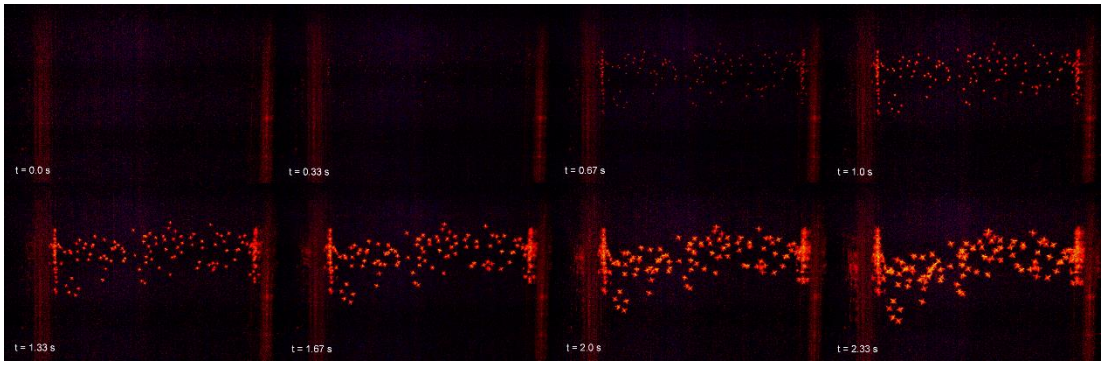

Figure 4-7 - Timelapse of a 10 mm diameter cuvette with ammonium chloride aqueous solution (S_{20} = 1.1) irradiated with a 0.45 W nanosecond pulse. The time from the pulse is shown where crystals can clearly be seen growing before 1 second and starting to move in the internal currents by 1.33 s. Image has been cropped to ROI and contrast enhanced.

The ability to control numbers of crystals nucleated has been demonstrated. In a continuous manufacturing environment this is advantageous because controlling the number of nuclei will affect the number and final size of the crystals. It should be noted that ammonium chloride readily generates secondary nuclei. To demonstrate

the control effect properly it would be beneficial to test with another system which is less prone to secondary nucleation.

4.2.3 Filtration

Choosing to filter the hot solution before further use was seen to have an effect on the NPLIN process. Filtration was initially performed to remove dust and other unwanted contaminants from the solution, which were thought to increase the chance of spontaneous heterogeneous nucleation in the solution. However a preliminary experiment on aqueous sodium nitrate found that the number of crystals produced by the laser was dramatically decreased on filtering through a 0.22 μm PES filter.

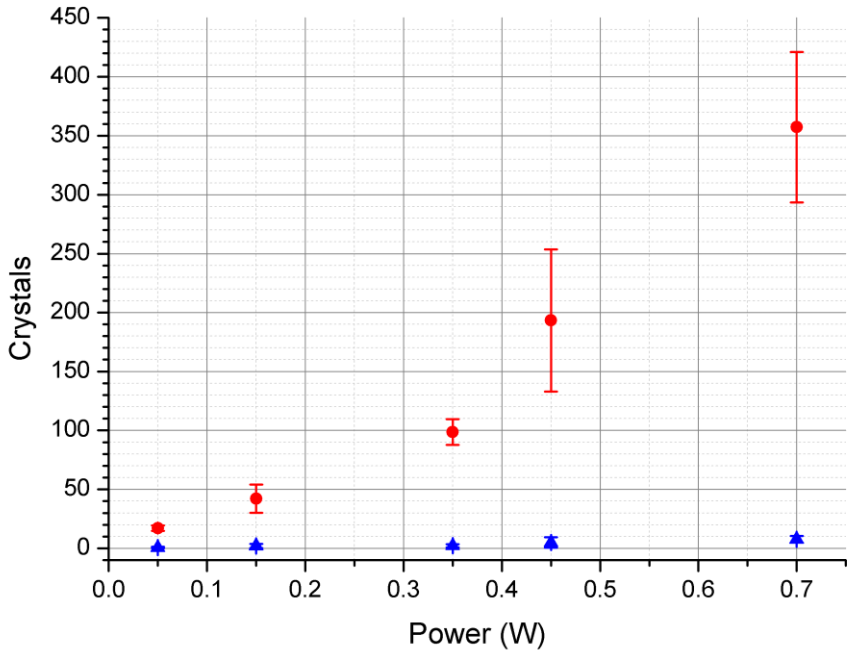

Figure 4-8 - Ammonium chloride crystals produced in a cuvette per single pulse of 532 nm light at different powers. The effect of filtered (blue tringles) vs. unfiltered (red circles) $S_{25} = 1.1$ supersaturated solution shows a dramatic decrease in NPLIN activity on filtered solutions.

The crystal counting experiment on ammonium chloride (Section 4.2.2) was repeated under the same conditions, but with solutions syringed while warm through a 0.22 μm PES filter into the cuvettes. The results in Figure 4-8 show an extremely large

difference in crystal number between the two regimes. Even at the highest laser powers, filtered solutions nucleate less than 10 crystals per pulse, compared with over a hundred for unfiltered samples.

4.2.4 Temperature

Temperature was the main way of generating supersaturation through cooling. It was mostly assumed that if relative supersaturation was kept the same at different temperatures, NPLIN would work independently and identically. This assumption has not been tested but is needed to be in the future.

The limits of temperature imposed by the solvent are the freezing and boiling points, for water this is 0 and 100 °C but it will be modified by the addition of solute. As seen previously in Chapter 3 maleic acid undergoes decomposition in solution at elevated temperatures. Ammonium chloride does not decompose easily and so can withstand heating and cooling within this range. A heated solution can evaporate: if there is not a good seal, it can deposit crystals around the rim of the flasks when heated for prolonged period. To counter this, kitchen film can be wrapped around the edge of the lids to help seal them from air, and prolonged heating should be avoided.

4.3 Testing NPLIN in flow conditions

Now that the main constraints on the NPLIN process have been considered and variables tested, verification that it is possible to nucleate crystals with the laser in a flow environment is needed. Since this has never been performed before, a prototype flow nucleation system was designed using basic available lab equipment. This would demonstrate if NPLIN in flow is possible and reveal what new challenges and constraints it presents.

Design:

In going from batch to continuous systems, it was important to keep things as simple as possible and use as much knowledge learned from batch experiments. The first experiment was to demonstrate if it is possible to induce nucleation in flow with a laser.

The experiment design outline was:

1) Have un-nucleated, flowing supersaturated solution.
2) Induce nucleation in that solution with a laser.
3) Detect any crystals produced.

It was assumed (2) would be possible so long as there was a high laser intensity, and high supersaturation. To increase the chance of (3) a camera was trained on a flow segment after the locus of nucleation, illuminated by both room light and a red diode laser to show up any crystallites.

It was assumed for condition (1) that the solution would be stable so long as supersaturation was kept in the regions of previously measured NPLIN activity (above minimum threshold and below spontaneous limit).

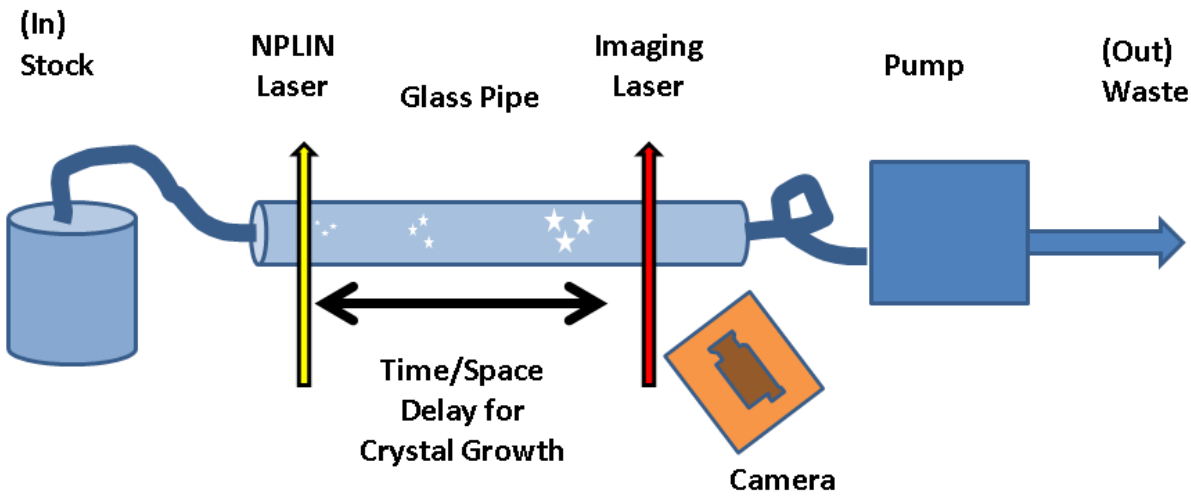

Figure 4-9 - Design of Prototype NPLIN in flow apparatus.

A prototype apparatus was designed around the above considerations, as illustrated in Figure 4-9. Basic flow of the target solution through a glass pipe was enacted by a pump which then sends it to waste. The glass pipe was where the flowing solution was nucleated by the pulsed laser. The crystals were given some time to grow during transit through the pipe before being illuminated and imaged by a camera.

The apparatus was constructed and used to nucleate ammonium chloride in a simple experiment as follows:

Summary Method:

Equipment: beaker, silicone tubing, platinum resistance thermometer (Traceable, Fisher), glass pipe with hose attachment, gear pump, Swagelok hose adapters, waste collection beaker. 1064 nm pulsed nanosecond laser (Quantel *Brilliant*) controller power setting 6 (6 mm iris, 58.5 mJ $pulse^{-1}$, ~14 ns pulse width), red 650 nm diode laser pen (generic) (2 mm iris), optics and optomechanics.

The equipment was set up as outlined in Figure 4-10.

Priming phase:

Ammonium chloride solution was taken out of a storage oven at 50 °C and cooled to laboratory temperature. When the room temperature, measured by a platinum resistance thermometer, reached 23 °C the system was primed to remove air by pumping the solution quickly (>300 $cm^3\,min^{-1}$) and then the pump speed was reduced to the target experimental speed (see below).

Experiment phase:

The stock solution was pumped through the system slowly ($30 < v < 300$ $cm^3\,min^{-1}$) so that the temperature at the pipe entrance measured 23 °C, and where the camera verified there were no crystals in solution at the pipe exit. The laser then irradiated the solution with laser pulses at 10 Hz. The camera recorded any resulting nucleation. The laser was then blocked, and the clear solution was then allowed to flow, entering flushing phase if necessary.

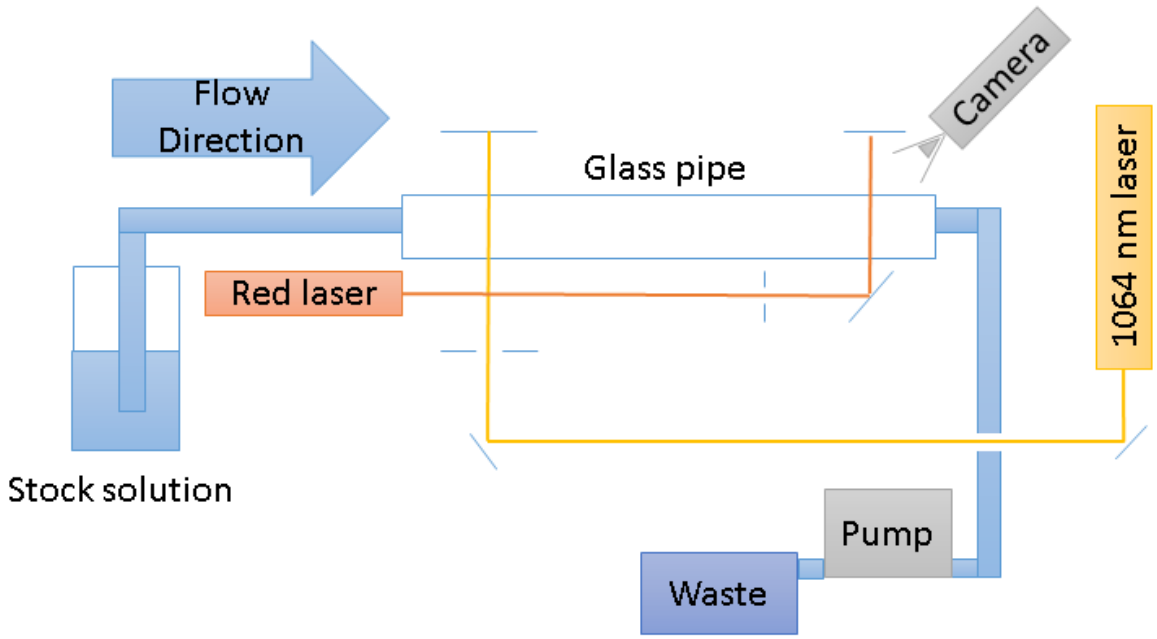

Figure 4-10 - Setup of prototype flow equipment. The supersaturated aqueous ammonium chloride stock solution flows through silicone tubing into a glass pipe where it can be nucleated by a 1064 nm pulsed ns laser. This induced crystal growth which can then be imaged using a digital camera and illuminated using a red 650 nm diode laser. The nucleated solution is then pumped through a gear pump out to a waste beaker. Irises, mirrors and beamstops are show for the two laser paths.

Flushing phase:

If there were any crystals in solution not clearing (due to attachment at walls causing secondary nucleation) the pump speed was increased (> 300 cm^3 min^{-1}) until clear and the flow was allowed to re-equilibrate to temperature at experimental speed.

End phase:

To end the experiment the tubing was removed from the stock solution and air allowed to fill the apparatus at high speed. The apparatus was then flushed with deionised water to prevent AC crystal build up.

Results:

The first experiment was performed with solution at supersaturation S_{23} = 1.20, but this spontaneously nucleated upon insertion of the silicone tubing.

The second experimental run was performed with solution at S_{23} = 1.10, and this was much more successful.

Table 4-1 - Observations of crystals observed in or outside the illumination laser path and the relative time in comparison to laser irradiation with pulses at 10 Hz in flowing ammonium chloride solution (S_{23} = 1.10). All delays and durations are given in seconds.

Irradiation	Duration of clear solution flow before irradiation	Delay after irradiation before small crystals illuminated	Delay after irradiation before large crystals observed	Delay after cessation before smaller crystals disappear	Delay after cessation before large crystals disappear
1st	11	3	6	8	17
2nd	4	2	5	3	11
3rd	4	2	3	1	11

Irradiation	Total irradiation time	Illuminated small crystal time	Observed large crystal time	Note
1st	9	14	20	flushed
2nd	6	7	12	
3rd	8	7	16	

Discussion:

To make sure that crystals observed were nucleated as a result of the laser irradiation and not spontaneously, the solution was allowed to flow for a few seconds observing no crystals. After initiating the laser pulses it took 2 – 3 s before small, fast moving crystals were illuminated by the scattered red laser light. Crystals which were observable by eye took longer to appear, 3 – 6 s before being recorded. This is likely because crystals growing in the fast-moving centre of a laminar flow will have less time to grow before being imaged whereas crystals in the slower moving edges of

flow have more time to reach a macroscopic size before they are imaged. This was reflected in the time it took after ceasing irradiation for the observations of the crystals at different sizes to disappear (flow out). The smaller, faster moving crystals disappeared in flow before the larger crystals did. It was visually quite clear that the 1064 nm laser beam was the source of the crystals, due to NPLIN.

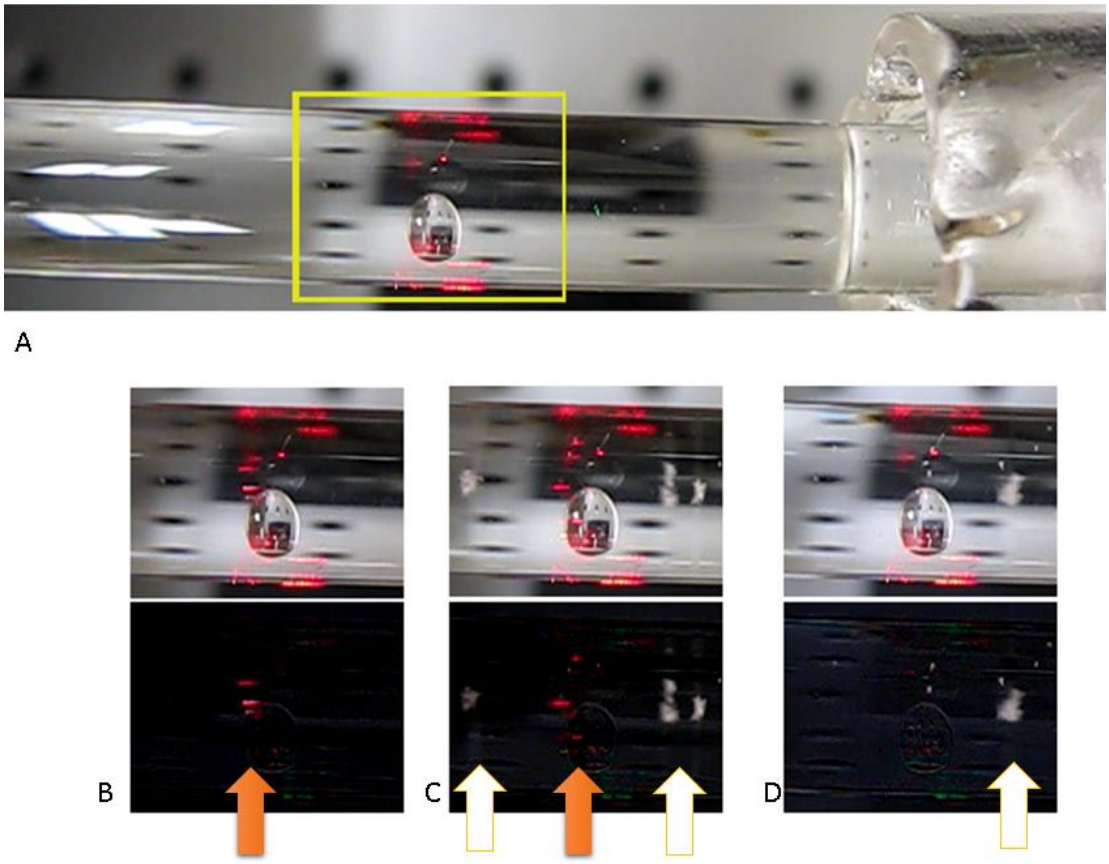

Figure 4-11 - Images taken of the flowing solution (A) before laser irradiation, showing un-nucleated flowing solution. (B) 2 s after irradiation showing small, fast moving crystals illuminated by the red laser. (C) 6 s after irradiation showing small crystals in red and large slow moving crystals visible under room light (white). (D) 10 s after cessation of irradiation showing only large crystals. (B - D lower) Using ImageJ difference images relative to (A) were created with arrows highlighting crystals.

The results in Table 4-1 and Figure 4-11 detail the first demonstration of NPLIN in continuous flowing supersaturated solution.

In comparison to static samples, it can be harder to obtain metastable solution in flow at the supersaturations needed for NPLIN due to spontaneous nucleation. Yet it was manageable for ammonium chloride solutions. The technique for recording images of crystals used was rudimentary and could be improved as part of an improved setup for observing the NPLIN under flow. The main problem with this experiment was the limited time afforded for measurements per experiment due to limited volume of sample. A larger volume of stock solution would enable longer experiments, but would also make them much more inconvenient and expensive for laboratory tests. In principle, if the stock solution were not contaminated by exposure to the inside of a gear pump, or diluted by the priming procedure, then the crystals could be re-dissolved and the solution used again.

To create a reproducible experimental setup, a new design was needed, and this will be discussed in the following chapter.

5 Development of Flow NPLIN

With proof of principle of NPLIN in flow, it is possible to have applications close to industry. However the features of systems wanted for industrial use and for testing the principles of such applications are different. In industrial use, a well-predicted, continuous process staying within parameters is required to minimize the chance of something going wrong. For testing the principles, a flexible system which can be easily modified to enable testing different conditions is more often desired. Further desired is a test system that can help identify when and where something goes wrong and not hide latent design flaws for later discovery.

Ammonium chloride in water is a good crystal system for testing because it grows quickly, identifying where nucleation has occurred and it spawns secondary nuclei to show flow rates. These properties are not ideal for a predictable, steady-state system but for the purposes of diagnosing problems in apparatus they are well suited. Ammonium chloride has been studied in batch by our group for many years and so is useful for identifying unusual behaviour.

The aim of this chapter is to know if it is possible to have a modular set of apparatus for continuous flow NPLIN experiments that is inexpensive and with parts easily available to the laboratory chemist which could lead easily into industrial scale continuous flow processes.

5.1 Loop Flow apparatus

5.1.1 Loop flow 1st design

Having demonstrated the following unit process (Figure 5-1):

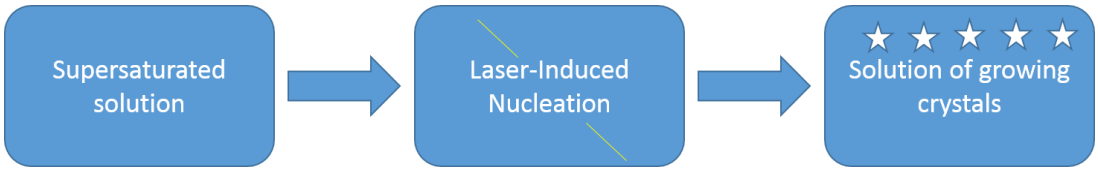

Figure 5-1 Scheme of NPLIN process.

as a working flow system in the previous chapter, it was found that a lot of solution was used per each 5-minute experiment. Using a gear pump that contacts the solution meant that the output may have been contaminated with grease or other particles and was treated as waste. By changing from a gear pump to a peristaltic pump the target solution is only in contact with the inside of tubing and the apparatus can be sealed giving the output as a (nucleated) clean solution. By then re-dissolving the output system, assuming only non-photochemical crystallisation effects have occurred, we have warm starting solution which can be cooled and reused for another NPLIN experiment.

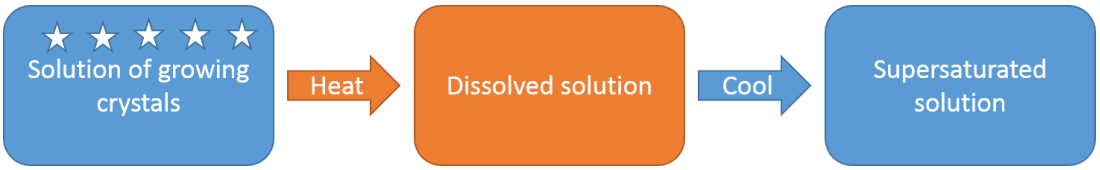

Figure 5-2 Scheme of regenerating supersaturation

By combining dissolution and nucleation systems we can make a loop flow system which, for a 500 ml solution, instead of lasting 5 minutes, can in principle be operated indefinitely.

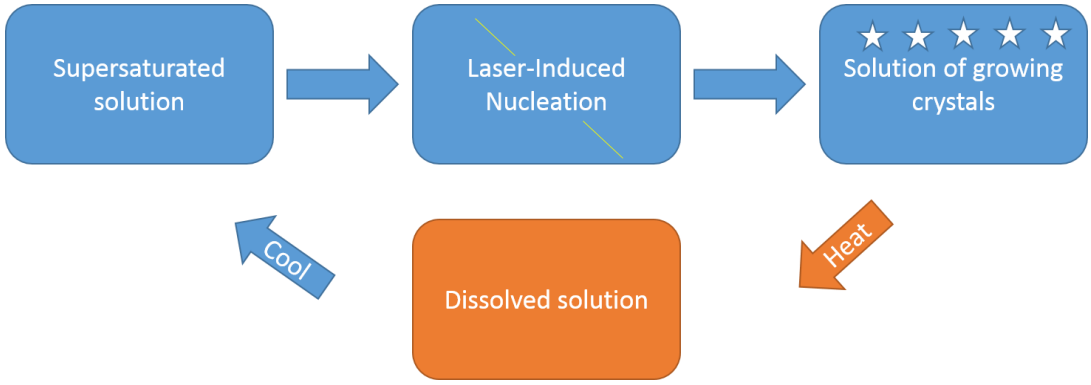

Figure 5-3 - Scheme of continuous flow NPLIN

Design

The principles for desinging this system were:

Use simple laboratory equipment available; flow solution in a loop with a hot volume where the solution is undersaturated causing the crystals to quickly dissolve and a colder volume where the supersaturation will be generated. Given that the same internal diameter (ID) of 6.5 mm silicone tubing (Saint-Gobain, Fisher) was used throughout, the volume is directly proportional to length and, assuming it is approximately a plug flow regime, length is directly proportional to residence time. Silicone tubing was chosen because it is easily availible, flexible enough to use with a peristaltic pump, and can easily slide over the glass pipe to form a fast connection.

Once cooled, the solution will reach desired supersaturation inside a 4.5 ID glass tube, and irradation with a laser should start crystal growth. After growth and imaging, the crystals can then be warmed through a hot volume to dissolve before flowing back into the hot resevoir to start the next loop of the experiment. By measuring the temperature before laser irradiation, exact supersaturation conditions can be known, and adjusting the water bath temperature can enable control of this.

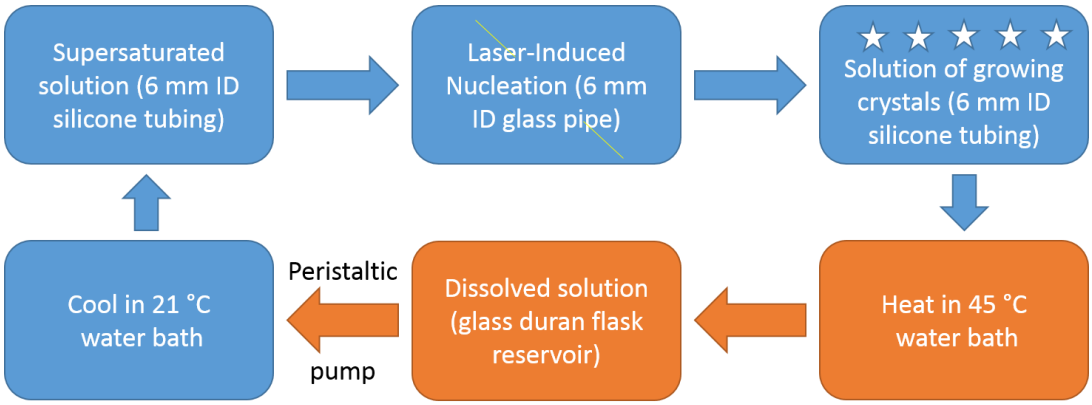

Figure 5-4 - Schematic of the initial loop-flow NPLIN apparatus design, showing the unit steps required to have a continuous crystallisation process with a limited volume of stock solution.

Experiment

The apparatus was assembled as shown in Figure 5-5 and ultrapure water was run through the system to test for leaks before being emptied and allowed to dry.

188.18 g of ammonium chloride was dissolved in 450.05 g of ultrapure (18.2 MΩ cm) water (S = 1.1 at 23 °C, C = 0.418 g g_{H2O}^{-1}) overnight in an oven at 75 °C. It was then placed in a heated water bath at 45 °C and connected to the apparatus. The silicone tube was ID 6.5 mm and the glass pipe was ID 4.55 mm. The laboratory temperature was 22.5 °C, below the target temperature of 23.0 °C. The cooling water bath was set to 23.7 °C, slightly higher than desired but obtainable with the lab temperature. A type-K thermocouple temperature probe was pressed onto the side of the silicone tube near the entrance to the nucleation pipe to enable good contact with bulk solution temperature but without risking the metal catalysing the crystallisation. Two cameras recorded the experiment, one imaging the output section of the nucleation pipe from close above with LED illumination, and one imaging the whole pipe from the side through an IR-blocking filter (KG5, Comar). The laser was aligned to strike the pipe 25 mm from its entrance through a 6 mm diameter iris.

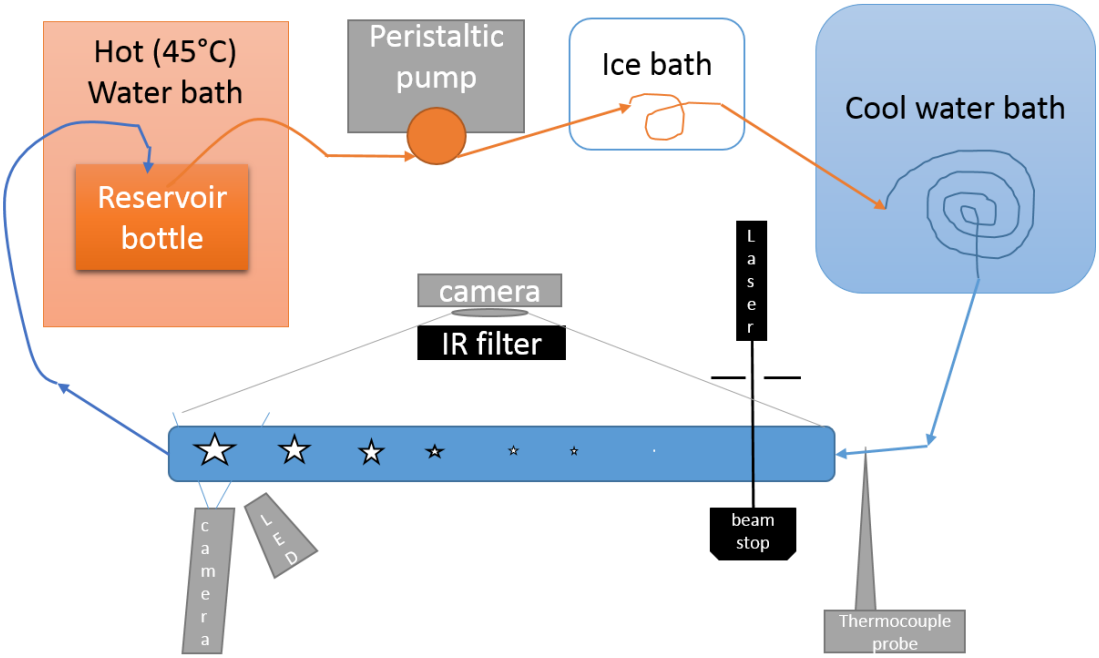

Figure 5-5 - Schematic of the initial loop flow experiment showing the laser equipment in black, measurement equipment and pump in grey and the solution when hot (orange) or when cool (blue). Arrows show the flow direction. The hot solution from the reservoir was pumped through silicone tubing using a peristaltic pump, precooled in a 30 cm ice tray and then run though a cool water bath for ~1 m. The cool solution was then flowed into a glass tube where it was irradiated by a nanosecond pulsed laser initiating crystal growth. The solution was imaged using cameras before flowing back into the hot reservoir to dissolve.

The hot solution was pumped at the maximum rate of 100 rpm (270 ml min^{-1}) through the apparatus to warm the pipes. A few turns of silicone tubing were then placed in the cool water bath at 19.4 °C and the temperature of the nucleation pipe was measured at 31.3 °C. On reducing the flow rate to 70 rpm (189 ml min^{-1}) the pipe temperature dropped to 28.8 °C. On further reducing the flow rate to 30 rpm (81 ml min^{-1}) the pipe temperature dropped to 25.3 °C before nucleation occurred in the pipes during the transit of the cool bath. Increasing the pump speed to 70 rpm (189 ml min^{-1}) allowed the crystals to be pumped round the system and dissolve in the reservoir. The cool bath temperature was raised to 20 °C and on dropping to 20 rpm (54 ml min^{-1}) nucleation occurred again (T = 24.12 °C). Raising the

cool bath temperature to 21 °C and the speed to 20 rpm (54 ml min^{-1}) a stable temperature of T = 24.0 °C was reached, giving a supersaturation at the pipe entrance of S_{24} = 1.076. Irradiation with a laser resulted in crystals produced.

Results and discussion

The experiment has demonstrated that it was possible to send the solution round in a closed loop. Under certain conditions it was also possible to perform looped continuous laser-induced nucleation. With an ice bath "precooling stage" before the cool water bath, the pump at 20 rpm and water bath set to 21 °C the inlet temperature gradually dropped to 23.96 °C where, on irradiation of 1 W (63 MW cm^{-2}), crystals were produced. This shows that it is possible to use a loop-flow system to take a small amount of solution and circulate it to allow large flexibility in time with which to get temperature and other experimental variables to the right condition to allow NPLIN experiments to take place.

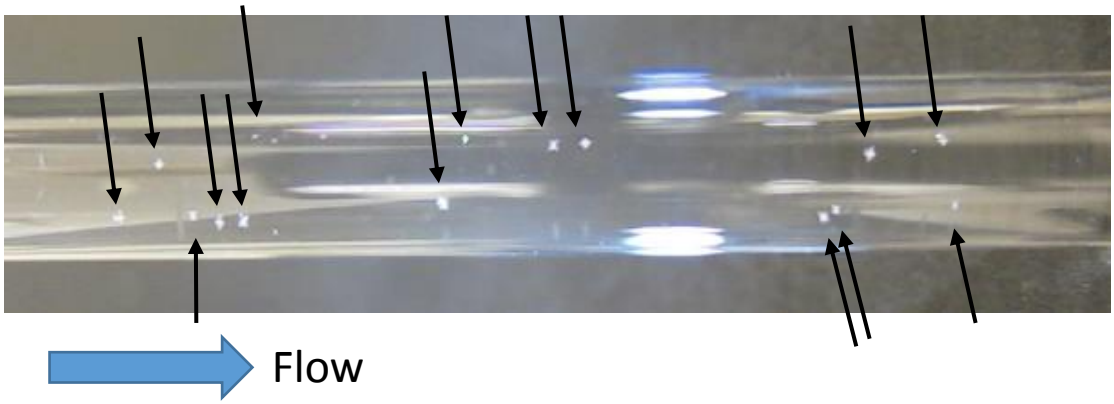

Figure 5-6 - Image showing the output of the nucleation pipe of section 5.1.1 during irradiation. Black arrows show initial crystals produced which were of similar size. Outer diameter of pipe is 8.0 mm.

However, in terms of a continuous process of nucleation and dissolving which can reach steady state, the setup faced problems. It was not cooling the solution effectively and reliably which is the most important factor for a fixed supersaturation experiment. The internal volume was large, using a lot of tubing (~2 m) between each water bath and the pipe. This helped get the solution to room temperature as the cold

bath could not fully do so. After nucleation the long return tube length resulted in the crystals growing quite large before they reached the water bath. This meant crystals were not dissolving fully before going back into the reservoir and therefore being passed through into the cooling section. Similarly, given that the cool water bath was not actively cooled, the solution running through it caused it to slowly heat up. For this experiment an ice bath was placed before the water bath to take some heat out of the pipes as a precooling stage. The sudden temperature drop at the tubing surface could trigger spontaneous nucleation which is unwanted, as well as requiring manual addition of ice. Finally because the warm water bath maintained temperature only through heating, it could not be cooled to different temperatures for a variable-temperature experiment. For these reasons an active cooling system was sought.

5.1.2 Heater-chiller loop flow

A system where both heating and cooling could be controlled was developed from the previous loop flow apparatus.

Figure 5-7 - Custom-manufactured cooling coil to fit 4.5 mm ID glass pipe. The internal coil with fused pipe (left to right) is surrounded by a water jacket with inlet/outlet top and bottom.

Design

In designing the active-cooling system many principles were kept the same. A reservoir of heated solution was pumped through a loop of tubing with a peristaltic pump, cooled to supersaturation and irradiated in a glass pipe. Lessons learned from

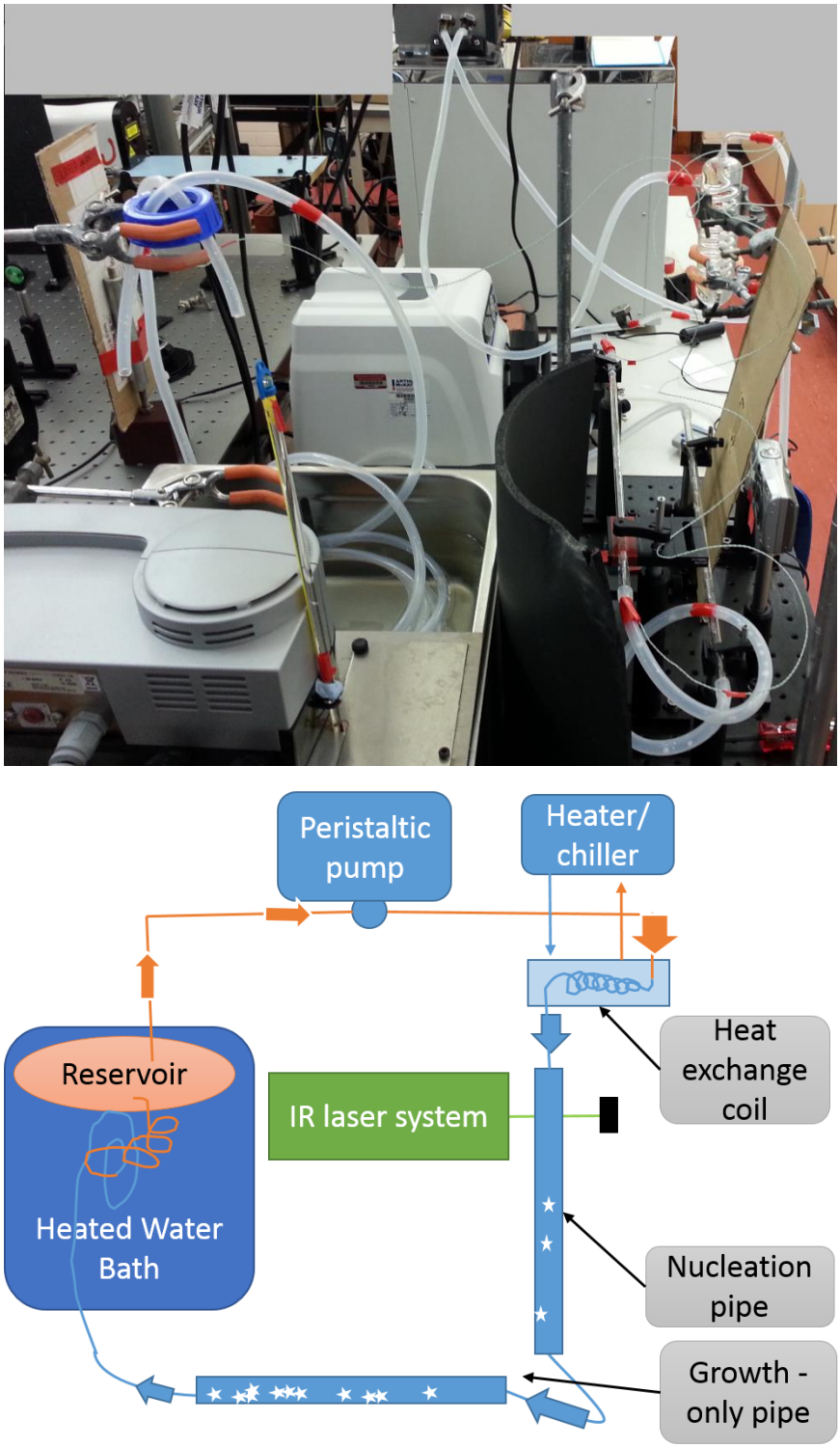

Figure 5-8 - (Top) Photograph of the looped flow apparatus showing the cooling coil at the top right of the picture (cropped for clarity). (Bottom) Diagram of looped flow setup as pictured in (A). A solution in a heated water bath was pumped through silicone tubing by a peristaltic pump. The solution was flowed through a heat exchange coil where it became

supersaturated before being irradiated by a nanosecond laser pulse in a square glass pipe. The solution was then flowed through a silicone tube into a round glass pipe where the crystals were visible. The solution was then flowed through silicone tube placed in a heated water bath, to dissolve crystals before it was returned into the resevoir.

the previous setup were then incorporated. The hot water bath was kept as it was high enough above saturation temperature that variations of a few °C could still bring the solution to a uniform state. The cooling bath was replaced by a glass coil with a water jacket (designed by Martin Ward, Figure 5-7) which acts as a heat exchanger, and linked to a circulating heater/chiller (HC) bath (TX150, Grant Instruments, Cambridge, UK). This not only enabled a continually renewed stream of water to cool the flowing solution but also enabled the temperature of the cooling water to be easily varied over an experiment. A second loop flow system was designed around this core cooling apparatus as described in Figure 5-8

The platinum resistance thermometer probe was replaced with a series of K-type thermocouples attached to a temperature logger (TC-08, Picolog). This enabled reading and logging of temperature at multiple points along the apparatus. Initially the three points measured were: inlet tube after the reservoir (A), 2 cm before the nucleation pipe (B) and 2 cm after the nucleation pipe (C). The air temperature 2 m above the apparatus and the internal cold junction temperature were also measured.

Later revisions included TCs 2 cm before the heat exchange coil (D) and after the growth pipe (E).

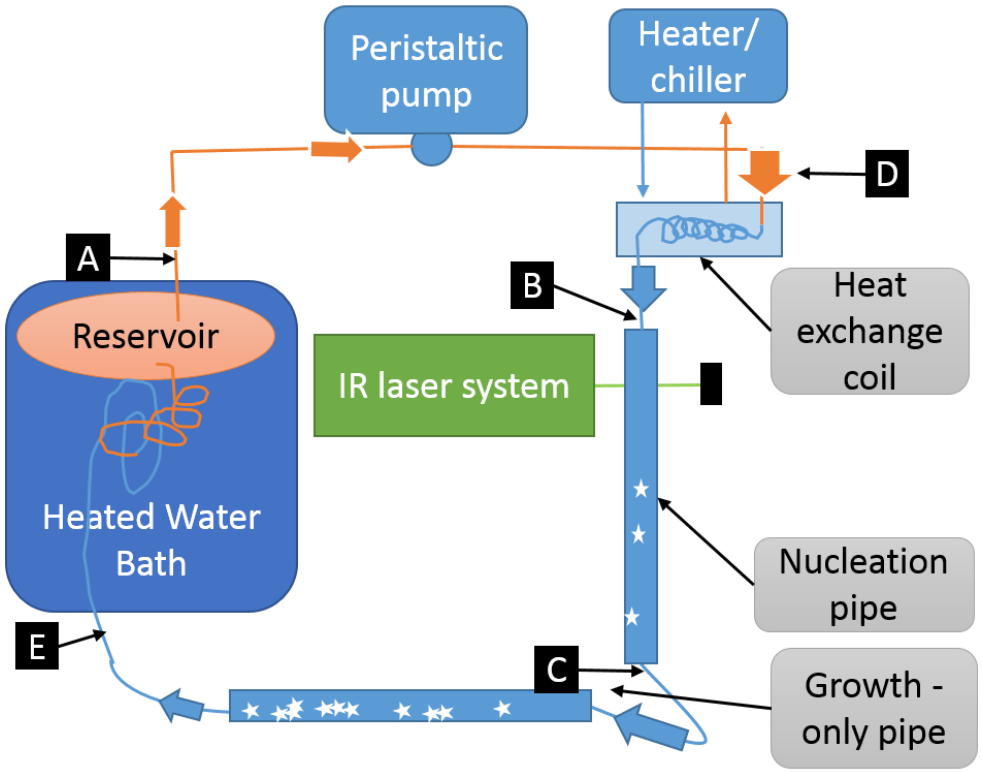

Figure 5-9 - Location of thermocouples in the loop flow apparatus as described Figure 5-8. Also measured were the air temperature 2 m above the apparatus and the thermocouple cold-junction temperature (not shown).

Initial tests

The system was run through with water to test the effect of flow rate on temperature from the 40 °C water bath to the nucleation pipe using only cooling from the air temperature of 21 °C.

It can be seen that at higher pump speed more heat was retained in the flowing solution than at lower speeds, as expected. At lower speeds the temperature drop before the cooling coil may leave the solution undersaturated sooner than desired giving rise to the possibility of unwanted nucleation here. This may be avoided by

using higher flow rates or a higher reservoir temperature if lower flow rates are desired.

Table 5-1 - Variation of nucleation pipe temperature with pump speed in loop flow apparatus (Figure 5-8)

Pump Speed / rpm (cm^3 min^{-1})	TC A (reservoir output) / °C	TC B (cool, pre-nucleation) / °C	TC C (post-nucleation) / °C
50 (80)	33.0	27.0	27.0
10 (16)	33.0	23.0	22.7
06 (10)	33.0	22.4	22.1

With this knowledge, the limits of stability of ammonium chloride in flow were to be tested. The questions asked were: "What is the maximum supersaturation in this system?" and "Is it the same as in batch vials?"

334.42 g of 0.418 g g_{H2O}^{-1} ammonium chloride was dissolved in 800.06 g of ultrapure water (T_{sat} = 31.1 °C, S_{21} = 1.11) in a 40 °C water bath. The apparatus contained around 400 ml working volume, therefore a 1 l stock solution was used so that the heated reservoir was at least half full, to dissolve crystals and facilitate continuous pumping. The solution was at first pumped through the system at high speed to maintain undersaturation, flush out air bubbles and prime the system for even hydrostatic pressure throughout. The flow rate was reduced to the chosen experimental speed of 10 rpm (16 ml min^{-1}), and the apparatus was allowed to cool gently to the target operating temperature of 21.0 °C. Unfortunately this lead to spontaneous nucleation before the desired temperature was reached as seen in Table 5-2. This is calculated to be around S = 1.05 (Table 5-3) which is when agitation nucleation is first seen. In order to prevent build-up of crystals inside the apparatus causing a blockage, the flow rate was increased to 40 rpm (64 ml min^{-1}) to allow undersaturated solution to flow through the system and redissolve crystals. On reducing back to 20 rpm (32 ml min^{-1}), a new higher experimental flow rate, spontaneous nucleation again occurred at a similar temperature as summarised in Table 5-2.

Table 5-2 - Results of initial supersaturation limit experiment in sequence.

Pump speed	TC B reading / °C	*S*	Notes and observations
100	35	0.96	35 °C all around system
10	26	1.05	Spontaneous nucleation in nucleation pipe
40	28	1.03	HC set to 25 °C, solution flows into hot water bath
20	25.6	1.06	Spontaneous nucleation observed in nucleation pipe

Table 5-3 - Expected temperatures of a 0.418 g/g_{H2O}^{-1} ammonium chloride solution for desired supersaturation ratio.

S_T	1.00	1.01	1.02	1.03	1.04	1.05	1.06	1.07	1.08	1.09	1.10	1.11	1.12	1.20
T/°C	31.1	30.1	29.1	28.2	27.2	26.3	25.4	24.5	23.6	22.8	21.9	21.0	20.2	13.9

It was unexpected that the new setup could not reach S = 1.11, given that it could more effectively cool the solution and redissolve the crystals faster than the first loop flow apparatus. The experiment was repeated, with a summary of the results shown in Table 5-4. This time the pump was kept constant at 10 rpm and the HC temperature dropped in stages. The solution spontaneously crystallised at 25.9 °C (S = 1.05) and on repeated attempt at 27.4 °C (S = 1.04).

In static vials the solution was metastable to just over S = 1.2 (at 13.9 °C) and only S = 1.06 (at 25.6 °C) was reached in the looped flow apparatus. The thermocouples were calibrated against a platinum resistance thermometer using the heater/chiller water bath. They deviated by up to 0.7 °C from the standard but no more than 0.2 °C from each other in the range 0 to 35 °C. To check that there was no discrepancy between external measurements and internal temperature, a calibration was performed with two thermocouples in a stream at 20 rpm at varying temperatures. The maximum difference when far from room temperature (difference at 10 °C) was:

silicone +3.3 °C compared to glass +1.5 °C. This is because these materials insulate against heat loss to differing degrees, and the thermocouple is measuring their temperature not that of the flowing liquid underneath.

Table 5-4 – Chronological summary of second supersaturation limit experiment showing observations and measured variables at certain experimental times and changed conditions with an arrow (→).

Timer	RPM	Chiller T / °C	A T / °C	B T / °C	C T / °C	Notes
<1:02	100	40	34.2	34.6	34.2	Many bubbles observed.
1:02	→ 10	40				
1:09	10	40	33.9	33.5	32.1	
1:10	10	→ 35.0				
1:17	10	35	33.9	31.3	30.5	
1:19	10	35	33.9	30.5	29.9	
1:23	10	35	33.9	30.4	29.9	
1:24	10	→ 30				
1:34	10	30	34.0	27.4	27.0	
1:36	10	→ 25.0				
1:40	10	26.7	33.9	25.9	25.5	Crystals nucleating in sq. pipe
1:40	10	→ 28.0				Not dissolving with increased temp
1:46	10	→ 30.0	33.9	27.6	26.4	Still crystals
	→ 100	30				
	→ 10	30				
1:54	10	30	34.3	27.6	27.0	No crystals
2:18		30		27.4	27.1	nucleation

To find out what may be the crucial factor preventing the apparatus reaching a metastable supersaturation suitable for NPLIN studies, the apparatus was slightly modified in different ways to try and isolate the critical points.

5.1.3 Problems with joins

Connecting different sized tubes

The initial constructions of the looped flow apparatus required different sizes of tubing for different connectors and this lead to some problems. Three alternative methods were explored to connect a larger diameter silicone tube (ID = 8.0 mm) to a smaller one (6.5 mm):

1) Simply pushing the smaller tube inside the larger one. This had an unfortunate effect on the shape of the inner tube: folding it to create a region of increased pressure which caused spontaneous nucleation. It would often allow the tubes to separate with pressure and contaminated the inside of the larger tube with the outside of the inner tube.

2) Use prefabricated Luer hose connectors to attach each sized tube. The smaller diameter of the Luer connector had similar bad effects on the flow, and acted as a focus point for nucleation and blockages.

3) Use a custom blown glass pipe connector, with or without a hose barb, made from fusing two differently sized pipes which snugly fit each sized tube. This worked much better but faced the same problems as the other glass to silicone joins described below.

Eventually it was decided that having variable sized tubes and pipes were not suited for this apparatus and a uniform sizing was found. This simplified volume and pressure calculations.

In undersaturated regions, a small length (60 mm) of glass pipe of similar ID was used to connect two identical tubing segments. In crystallised or supersaturated regions, crystal build-up could occur at these points (see next section) so their use was minimized or avoided.

Connecting pipes to tubes

The apparatus setup used glass pipes which were connected to the silicone tubing by pushing the silicone over the glass and using friction to hold it on. This was to keep the apparatus modular, allow easy cleaning of each part, and to use readily available parts to facilitate reproducibility. When the ID of the pipe and tube were not close the join resembled a sharp cliff creating an expansion zone that could easily slide off with a slight increase in internal pressure.

Figure 5-10 – (Left) Diagram showing how a larger ID grey tube slips completely over a black pipe leaving a sharply shaped red disturbance zone. (Right) Diagram of the connection of a glass pipe (black) inside a stretched silicone tube (grey) of similar ID and the red zone showing a typical region of flow disruption in red.

Smaller tubing was found which better matched the ID of the pipe and the elasticity of the silicone rubber allowed it to affix itself more strongly to the glass pipe when stretched (Figure 5-10). However this meant that the flow has a disturbance-zone: a volume of solution which does not directly fit into the laminar flow path of the system and disturbs the overall flow in this region. The dead volume has the potential to act as a site to initiate spontaneous nucleation, or to trap crystals.

Further join problems

Air bubbles at joins. The disturbance zones in the joins can allow air bubbles to accumulate and grow. These further change the flow pattern possibly contributing to spontaneous nucleation. They offer an interface for crystals to preferentially grow on as well as obscure observation of crystal growth.

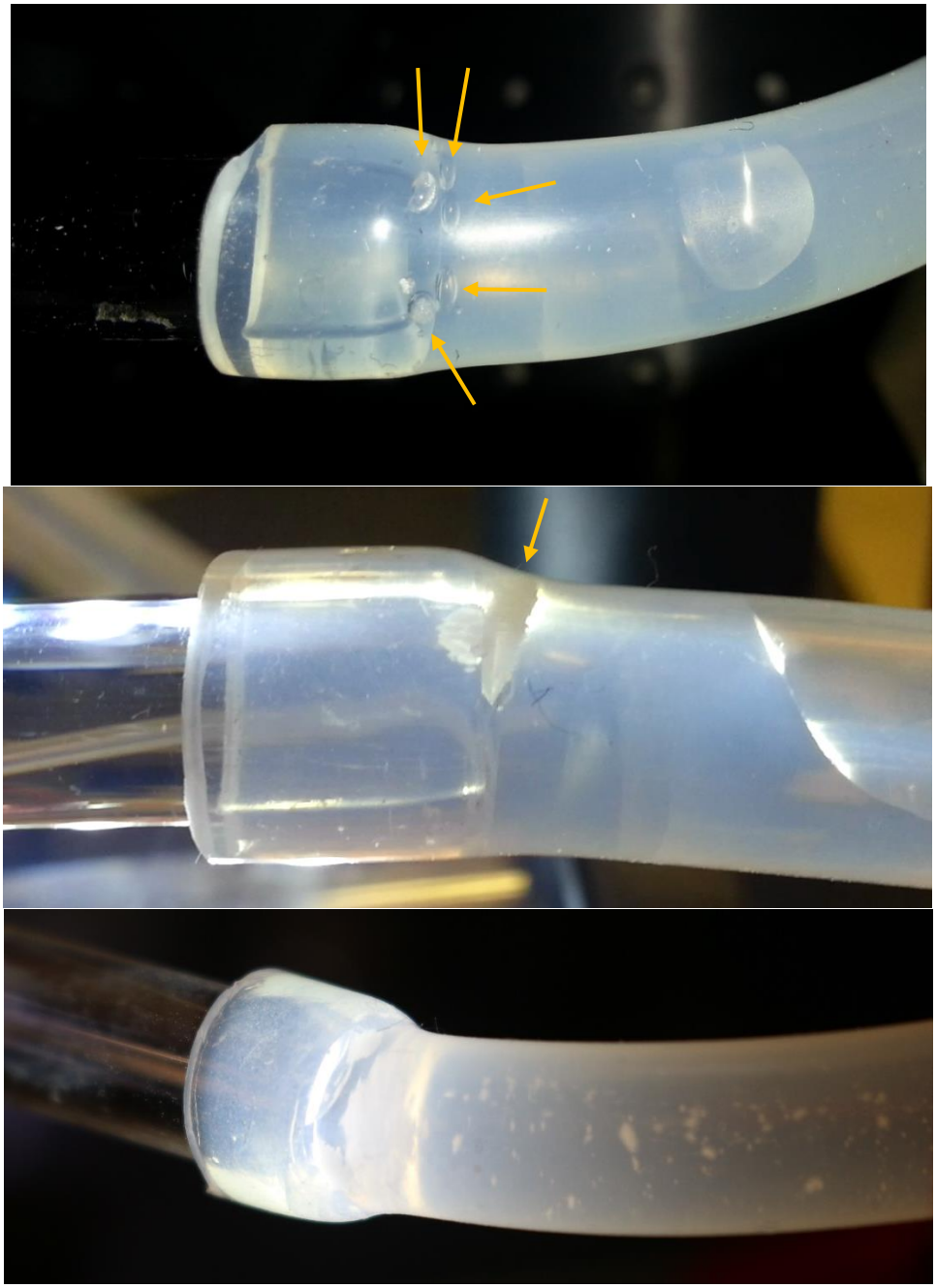

Figure 5-11 - Photographs showing crystals accumulating in the disturbance-zone of a silicone tube stretched over a glass pipe. (Top) Bubbles of air (yellow arrow) accumulating at the disturbance zone. (Mid) The crystal growing in the disturbance zone eventually grows large enough to spawn secondary crystals as seen in (Bottom).

Accumulation of already grown crystals at the join.

This is a threefold problem:

1) These crystals would have otherwise been flushed downstream to be dissolved and replaced with fresh solution but instead they reduce the concentration of incoming solution.
2) They grow quickly in the high supersaturated solution which is constantly refreshed which can cause dendrites to break off and form secondary nucleation downstream.
3) They can grow so quickly they block the flow until pressure builds up, causing joins to burst open.

Join Alternatives

Flexible tubing is needed at the peristaltic pump for it to work in the system, however all the tubing in the supersaturated region could be replaced by a monolithic glass section with cooling, laser irradiation and growth monitoring all occurring without changes in the flow profile of the apparatus. Such a piece was constructed but, due to time constraints, was not tested. Some differences in conditions are foreseeable:

1) A long piece of glassware can take up a lot of space, require custom glassblowing, and is fragile.
2) It is a lot harder to clean, especially if there is a blockage.
3) Due to a lack of a coil imparting radial mixing to the moving fluid, the cooling would be less efficient and may need a longer section to get the same temperature as the above setup.

Yet it may offer easily modelled laminar flow and more predictable distance of pipe to rate of cooling.

Despite these problems it was found that a very accurately aligned join, and coating the glass inside and at the lip with a hydrophobic coating, helped to minimize the

tube–glass join issues, but never completely eliminate them. This however offered enough leeway with stable, undersaturated solution to perform an NPLIN experiment for a reasonable length of time (~2 hours).

5.1.4 Problems with glass heat exchanger coil

The advantage of a heat exchanger containing a coil is that for a compact apparatus it offers a large surface area for cooling with a distinct temperature gradient. The cooling inlet pipe passes the solution output pipe, so that they should be of similar temperature and the solution inlet doesn't undergo an immediate temperature shock. The cooling coil can cause problems, however, as we discuss in this section.

Gravity effects

Due to the 3 dimensional nature of the coil geometry, different orientations in space offer different environments for the solution. Pumping the solution from top-to-bottom was observed to more pressure on the output pipe and bottom-to-top less due to gravity. Going from bottom-to-top allows air bubbles to easily clear the cooling coil, yet any pre-formed crystals will sink back into the apparatus to grow larger. In ammonium chloride this enables secondary crystals to spawn, absolutely detrimental to the experiment, as shown previously. Going from top-to-bottom traps air at the top of the coil which breaks good hydraulic flow conditions and can lead to solution stagnating, crystallising around the air bubbles and blockage as described in the previous section. Ideally solution would flow horizontally to eliminate gravity effects, however because the curves of the coil are tight, they have directly vertical turns which accentuates the problem: trapping both air and crystals at the top and bottom of each turn, which ruins the flow and concentration characteristics of the system.

Join from cooling coil to nucleation pipe

The design of how the coil attaches to the nucleation pipe is important because this is the critical supersaturated region before laser irradiation. Disturbances in the conditions of the experiment here are the most likely to cause spontaneous nucleation and doing so close to the laser irradiation zone could be confused with laser-induced

nucleation. What is desired is then a way of attaching these two pieces of glass piping to each other with as little change to flow or temperature as possible and, since it is highly likely to nucleate, a way to verify no nucleation has occurred or diagnose if it has. This is an extension of the join problems described in the previous section.

These designs for connections were tested:

Barbed hose attachment compared with a straight cut attachment. Barb advantages: Offered a tighter seal of the hose to the glass tube. Disadvantages: seal was too tight, hard to remove for cleaning, hard to align, caused turbulence. Using a straight cut pipe (with fire-polished edges) was preferred as the apparatus was easier to adjust and align once the two pieces were connected.

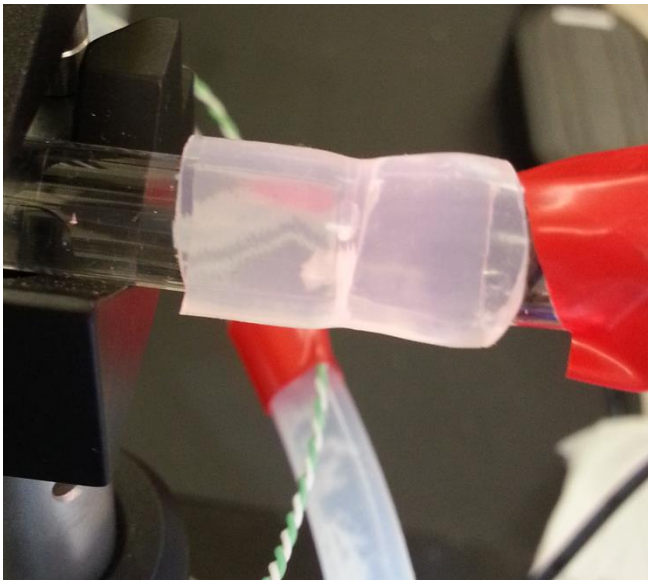

Figure 5-12 - Two glass pipes attached very closely together using a silicone tube section with crystals forming in-between. It was found that reducing the size of the glass/silicone/glass connection of cooling coil to nucleation pipe can leave a gap where nuclei gather if not aligned properly

Length of silicone tube connecting the two pieces of glass. Having a long piece of tubing between the heat exchange coil and the nucleation pipe was very

disadvantageous because it allowed for a large change in temperature to occur between these two points. Having the distance between glass tubing 35 mm was the minimum distance where it still behaved as a long tube with the flow at the two connections barely interacting with each other. Shorter than 35 mm and the flow started mixing, until it was < 1 mm and then it acted as if it were one continuous pipe with surface tension holding the solution together. This worked satisfactory but required very precise alignment and elastic tension in silicone to remove dead zones, very small disturbances ruined this. When the pipes were too close the join acted as one big dead-zone as seen in Figure 5-12.

Other solutions.

Plastic union: Having a plastic pipe union (Figure 5-13) worked better than the small-gap silicone tubing for keeping the two pipes attached in a preliminary test but was not tried here because the opacity of the joiners would mask any pre-nucleation issues.

Figure 5-13 - Black plastic union which connects two 3 mm ID glass pipes together while maintaining consistent ID. This showed good alignment, but it was not possible to monitor formation of crystals at the joint.

Monolithic glass. A monolithic cooling coil attached to a pipe was constructed but—due to time constraints—not tested. This would eliminate the gap, but would make it

harder to align the pipe after emptying the air bubbles out of the coil. A similar solution was tested in the segmented flow regime in Section 5.3.5.

5.1.5 Loop flow discussion

These first experiments with flow crystallising were important in understanding key areas where problems might show, as well as imaging lessons learned in Section 5.2 below. However the problem of group dispersion in laminar flow meant that this apparatus would not be used in the future and having a system approaching plug flow (for instance, in segmented slug flow below) is required. Although some basic understanding of the degree of allowable undercooling was observed, since MSZW is different for each apparatus, detailed investigations into it were held off until the apparatus design was better matured.

These experiments showed a few key features for looped flow crystallisation experiments. Active cooling is needed for reliability. The apparatus should have minimal variations in the geometry of the piping in the critical region: (during cooling – laser induced nucleation – measurement of crystals). For modular design the joins between parts which can disturb flow should be kept away from critical region and checked regularly for any build up which can damage the apparatus. Having flexible silicone tubing which matches the ID of the glass pipe enabled a good seal when stretched over the ends of it. Although laminar flow is a simpler regime to set up, it doesn't offer consistent crystal growth environments and so would give a wide CSD if developed further.

5.2 Imaging development on the flow system

The intention of making a laser-induced nucleation looped-flow system was to make it easier to perform tests on the process of nucleation. Altering the conditions of nucleation should affect the properties of the resultant crystals. Non-invasive in-situ techniques were required to preserve the supersaturation environment as a metal

probe may produce nucleation through heterogonous sites or through turbulent disturbance of flow.

Continuous monitoring was needed to differentiate between spontaneous and laser-induced nucleation. Digital video recordings gave more spatial resolution through magnification; lower light detection through modern imaging sensors; and clearer images through shorter acquisition times. It also allowed quantification, such as counting crystal number, habit and size measurements in an environment that is constantly changing.

Other non-invasive in-situ techniques, such as Raman spectroscopy; absorption spectroscopies and x-ray techniques could be used in line. Temperature measurements were used, but only on contact with the outside of the vessel walls to avoid the probe surface inducing heterogeneous nucleation.

5.2.1 Square pipe

In the early experiments a circular cross-section pipe was used for nucleation and imaging, however it could be seen that the crystals tended to gather together at the bottom as they moved through the pipe. The imaging was obscured by cylindrical distortion and the circular glass focuses the laser through the solution toward a point outside the pipe, which is undesirable. It was considered that a square cross-section glass pipe would improve both these issues. A 300 mm, 5.0 mm ID square pipe (borosilicate, CMScientific) was put onto the flow apparatus to replace the nucleation pipe.

At first the square pipe was connected to silicone tubes, but it was found to leak due to an imperfect seal. Two pieces of 4.7 mm ID round glass pipe were blown to the ends to facilitate attachment. However there were turbulent spots at the fused join, meaning lower speeds were necessary to avoid disturbed flow and possible nucleation.

5.2.2 Cameras

The cameras used initially were commercial digital cameras. The autofocus caused would not focus correctly on the same place when reset and had to be manually adjusted taking up time every recording. They were replaced with fixed lab cameras (Ace acA2040-90uc, Basler) which were used with removable C-Mount lenses which could be adjusted to maintain a fixed focus. The lab camera was operated using manufacturer supplied PC software which could adjust framerate and exposure time independently.

Since the crystals sink to the bottom of the pipe when growing larger, having the camera imaging from the side may mask crystals behind closer, larger ones as well as risk a stray laser beam damaging the imaging sensor. Imaging from the top allowed minimum chance of laser reflection (except by crystals forming) while getting the fullest picture of the pipe.

5.2.3 Lighting

A short exposure time is needed to get clear images of the moving crystals, and therefore a high intensity illumination was required. The crystals are ideally detected as soon as possible, when they are very small in size. Initially only room lighting was used, which resulted in low contrast so only relatively large crystals were spotted. It also resulted in large reflections of the strip lights in the curved tubes.

Orientation of the light is important to increase contrast and reduce glare. Different strategies were attempted.

Previous experiments in the group on bubbles used bright backlighting to see the bubbles as early as possible. This did not work well with crystals: whereas the smooth interface and focussing of bubbles offers good contrast the rough and opaque crystals block out light by creating a diffuse shadow. Crystals, on the other hand, are much better at scattering and reflecting light.

For the initial experiment in Section 4.3 a red laser pen was used with a cylindrical lens to form a line of illumination through a section of the pipe. This was great for

showing crystals that flow past the camera and illuminated more crystals than could be detected with room light alone. However it did not fully illuminate the volume under observation giving limited information.

The next simplest illumination scheme was to use cheap LED torches held by clamp stands. These provided some illumination.

- Advantage: light held from one place.
- Disadvantage: hard to move to find perfect lighting, could see the 5-LED pattern in reflections, diminished brightness over length of apparatus. Illumination changed as battery runs down.

A pair of commercial 3 W LEDs with spring clips and swan necks were bought to emulate a lab cold LED source.

- Advantages: Cheap, ran off ACDC adapter, could be easily moved, held themselves up, were reasonably powerful.
- Disadvantages: needed a lens to help focus, could be knocked out of alignment unless clamped, produced a lot of heat near lamp head.

Due to the versatility of these LEDs they were used for all experiments that required illumination.

The orientation of light which best illuminated crystals using reflection and scattering was also considered. We want light to illuminate the internal solution without highlighting texture of the outside glass. Due to dust in the laboratory the pipes needed wiped with lint free cloth before every recording, but scratches in the glass still showed on footage. The best solution found was using the silicone tubes on the end of the pipe as a diffuser into the pipe and using total internal reflection in the pipe to keep solution illuminated without losing much light to the outside.

If this was not available due to distance, tube material or other constraints, an acceptable compromise was orientating LEDs at 45 degrees relative to both the surface of the glass and camera. This minimised reflection off the surface of the glass.

5.2.4 Imaging conclusions

Designing of the apparatus with remote imaging in mind was useful. Having a square tube offered a much clearer picture and allowed a more even laser nucleation volume at the expense of reduced possible flow rates. For imaging, a good scientific camera and decent lighting offered much more useful images than a domestic digital camera. Having these considerations incorporated into the apparatus design means reliable and comparable data could be collected.

5.3 Segmented flow

One of the problems with the laminar-flow experiments (as detailed in Section 4.3) was dispersion of velocities and growth rates across the diameter of the flow. For this reason, it was also found that crystals had a tendency to adhere temporarily to the walls, where the flow was slowest.

To solve these issues, a segmented flow setup was designed and developed for continuous looped-flow laser-induced nucleation.

Segmented flow is a two-phase flow with two immiscible liquids of sufficient volume relative to the pipe diameter that they separate into discrete packets or "slugs". Laminar flow effects are limited to the length of the slug and actually create a radial mixing pattern within the slug. Thus using a simple pipe a system which more closely approaches plug flow can be achieved. Usually there is an experimental fluid and a carrier "counter-fluid". This should be able to create identical packets of fluid for repeatable crystallisation. The use of segmented flow has been demonstrated for cooling crystallisation and ultrasonic crystallisation.[21,26,59]

Segmented flow enables small packets of identical solution environments. This reduces variation and eliminated the laminar flow effects. It is possible to recombine the solution at the end of crystallisation to get the advantages of the small scale on a large volume. Initial work in the group indicated that an organic counter fluid would form a buffer segment with better affinity for the hydrophobic-coated glass pipe. The

segment of counter fluid would then push the aqueous segment, and crystals would get moved along with it. The movement of the segments mean there are currents within each that keep the segment evenly mixed, and so should enable full growth of crystals within to the saturation limit.

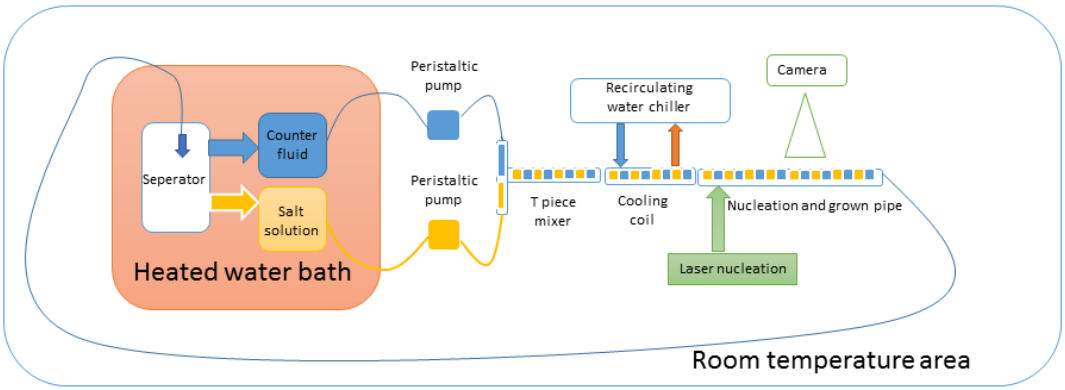

Figure 5-14 - Design of segmented flow apparatus showing undersaturated aqueous solution in yellow and counter fluid in blue being pumped via peristaltic pumps into a T-piece mixer, generating fluid slugs. The slugs then move into the cooling coil where the aqueous solution becomes supersaturated and susceptible to laser-induced nucleation. The laser hits a slug generating crystals which are imaged by the camera as they grow to macroscopic size. The slugs are then taken via an outlet tube into a gravity separator after getting heated to undersaturated temperature to dissolve the crystals and separated back into the feed bottles to start the process again.

Segmented flow NPLIN faces similar problems to loop flow NPLIN with the added complication of choosing a suitable counter fluid. Many of the design parameters of the loop flow system were chosen on the basis of a flowing aqueous salt solution. A counter fluid has to be completely immiscible with that solution and its components (e.g. water, NH_4Cl) as well as compatible with the materials used in the apparatus construction. There also needs to be a way of introducing both fluids and, for loop flow, a way of separating them at the end. The counter fluid should ideally be optically clear at the NPLIN laser wavelength: if it were to drastically absorb the energy, the sudden heating could break the apparatus.

5.3.1 Initial tests and tubing compatibility

Aqueous solution / air

The segmented flow system was first tested with air and water. This experiment demonstrated the ability to keep slugs separate most of the way through the system. However when there was a widening in a vertical section of pipe it allowed water to slip past the air and changed the uniform size of the slugs into random sized slugs.

On replacing the water with ammonium chloride solution a further problem was identified: crystals formed in one aqueous slug could transfer to another aqueous slug by sticking to the glass. This changes the experimental environment from discrete plug flow to a poorly mixed stream.

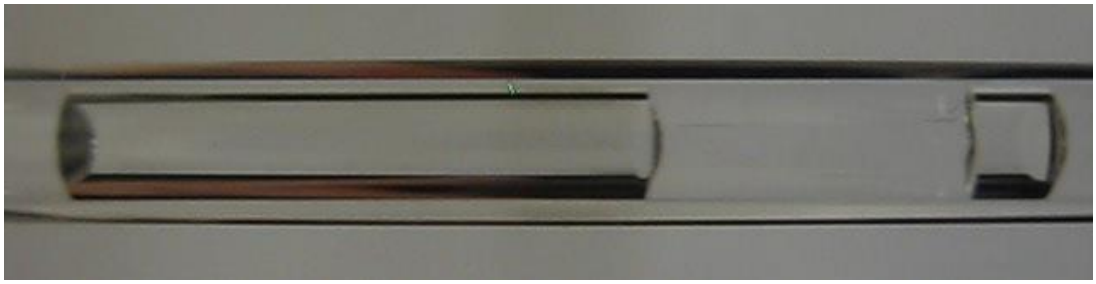

Figure 5-15 - Water/Air segmented flow showing air slugs of non-uniform size resulted from a widening of the glass pipe diameter. Image cropped to region of interest (ROI).

Hexane/aqueous

To prevent crystals transferring via the pipe inner walls, the air was replaced with hexane, a liquid that is insoluble with water. The glass was coated with hydrophobic Rain-X (following the procedure outlined in Chapter 2). The hypothesis was that a layer of hexane would surround the aqueous slug and any crystals formed would be kept in the aqueous layer due to surface tension. Because hexane is incompatible with silicone tubing, black Viton tubing (Masterflex Viton tubing 3.1 mm ID, Cole-Parmer, UK) was used instead. This meant unfortunately that the tube was opaque and crystal formation within could not be detected.

The aqueous/hexane segmented flow system successfully showed no transfer of crystals from one slug to another (no production of crystals observed in un-nucleated

slug following a nucleated slug). However, after around 30 minutes the slugs started breaking up like the aqueous/air system. It was considered that the hexane was degrading the hydrophobic coating. Furthermore, it was found that there were crystals forming before the laser target point. The cause was not proven at the time, but was suspected to be either the Viton tubing or the heat-exchange coil. As a result of the issues encountered the use of hexane was disfavoured.

5.3.2 Separation of fluids in loop flow.

To adapt previous linear segmented flow designs, which use two feedstock bottles, to a loop-flow crystallisation design, a fluid separation process was needed to complete the loop. A simple density-separation process using an inlet tube, sidearm flask and collection bottle was designed. Both containers were immersed in the hot water bath to ensure undersaturation.

For air/aqueous separation was facile: one container was exposed to the atmosphere. For hexane/aqueous the less-dense hexane lay on top of the aqueous layer, and was easily poured into a collection pot. Although some hexane evaporated into the atmosphere due to insufficient sealing (the hexane attacked the sealant) it kept the aqueous layer protected from atmospheric loss and therefore the supersaturation consistent.

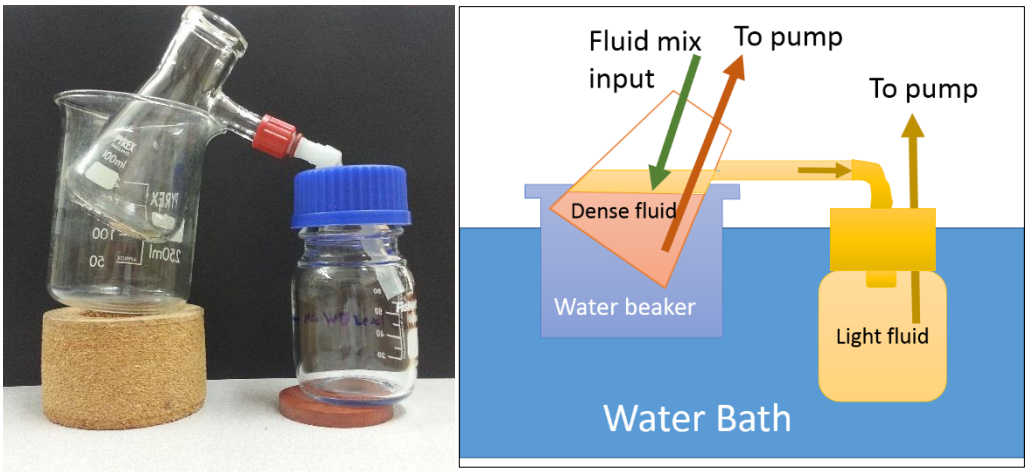

Figure 5-16 - (left) 3 components to separation apparatus. 1) conical flask with sidearm filled with 2 liquids from experiment, the denser liquid was pulled from this vessel, the less-dense liquid drained off into 2) the light-fluid reservoir. 3) the beaker, when filled with water, allowed efficient heat transfer from the water bath to the conical flask while allowing the lid of the bottle to be above the water level. (right) Schematic for separating two immiscible fluids of different densities from the output of the slug flow system

Dimethyl phthalate (DMP) was tested as an alternative to hexane due to the problems with hexane highlighted in the previous section. DMP was much denser than water and much more viscous as well. This lead to problems where some DMP would stay at the bottom of a pipe or piece of tubing and the aqueous layer would flow over it instead of pushing it. This lead to artificial constrictions along the pipe. Further, it was very hard to completely flush the DMP out of the system, as shown in Figure 5-17, and trace amounts had to be extracted from the pipes by mixing with ethanol and some sections of silicone tubing replaced with fresh tubing. This did not meet the reusability and modularity requirements.

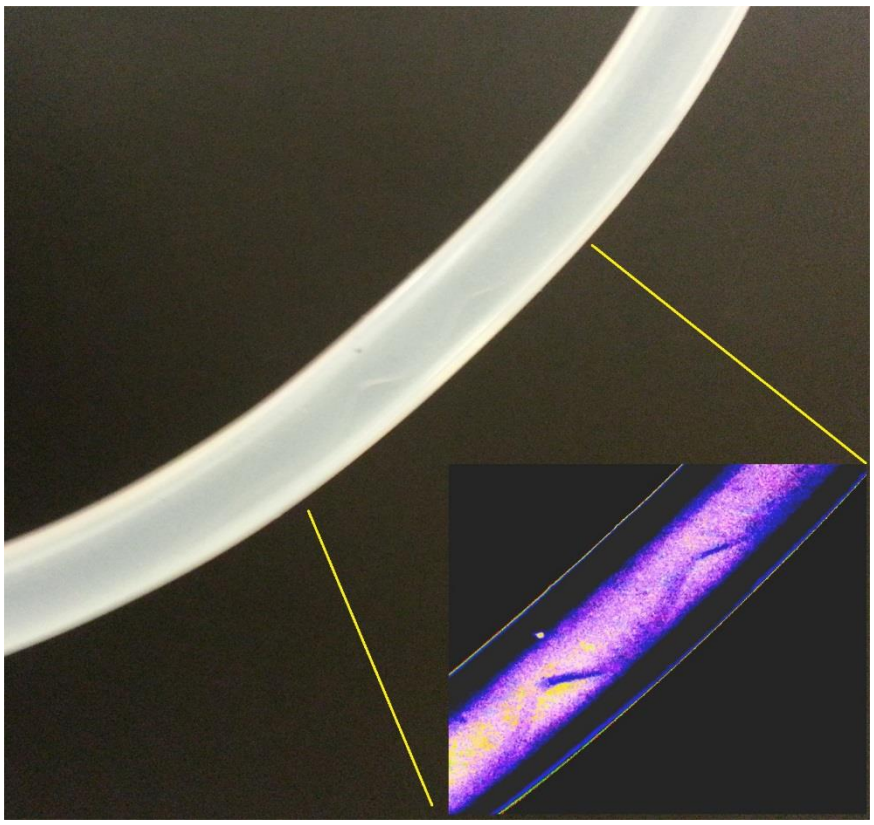

Figure 5-17 - Image showing silicone tube of flowing water with dimethyl phthalate staying in the tube 4.5 mm OD. Inset shows contrast enhanced view of the two colourless fluids.

Perfluoropolyether (PFPE) fluid (Galden SV110, Solvay, Italy) was sought as a replacement for hexane. Because it is perfluorinated it is non-reactive with most other solutions and has a very low miscibility with water (14 ppm). PFPE is hydrophobic and its similar viscosity to water means it acts as a good counter fluid. However, because it is denser than water, the aqueous layer sits atop it in the separator and has to be funnelled off. This can lead to crystals floating at the PFPE–water interface, and not dissolving properly, as well as forming crystals in the sidearm.

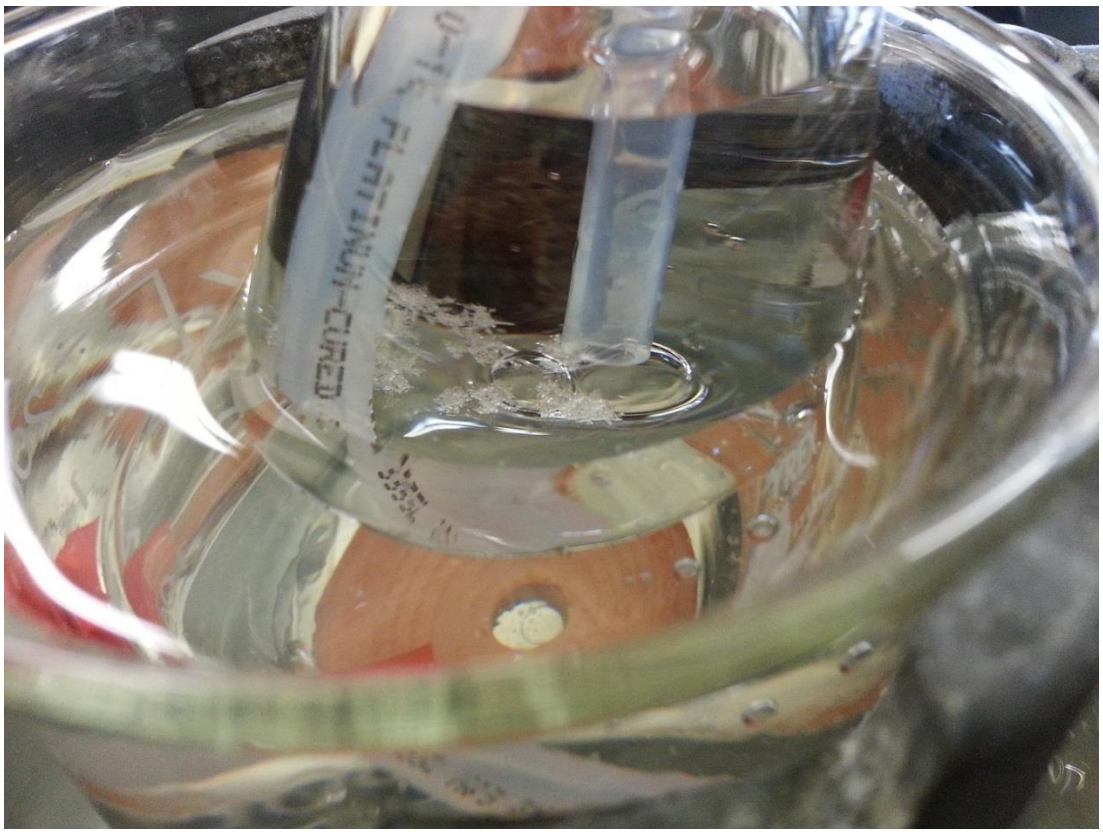

Figure 5-18 - Image of separator in beaker of water showing the two fluids (PFPE and aqueous ammonium chloride) forming an interface in the middle of the conical flask. At this interface sits crystals which had not dissolved in the tubing loop before entering the separator. This is undesired as it will lead to a concentration gradient in the aqueous layer.

To solve this the C_{sat} temperature was reduced to below room temperature by preparing a new solution. Except for this issue, the PFPE fluid worked well as a counter fluid, showing uniform slugs at all but high flow rates, and was easily recoverable due to its low interaction, which offsets the downside of it being reasonably high cost per litre.

5.3.3 Choice of chemical system

As before, ammonium chloride in water was chosen as test system, as it was well studied in laminar flow and batch by the group. It is useful in these initial experiments because it grows quickly and forms secondary nuclei if it is disturbed in flow. This makes it a good nucleation and flow indicator for these initial experiments while developing the apparatus. It also has little tolerance for resistance to agitation

nucleation, so acts as a good sign if the flow characteristics of the experimental apparatus are poor.

This setup would also work well for potassium chloride, which has been extensively studied in batch by our group, or any other ionic crystal which has high aqueous solubility and little solubility in the counter fluid. To use other crystal systems the appropriate fluid, counter-fluid and compatible tubing and coatings would need to be selected but otherwise should operate under similar principles.

5.3.4 Temperature of experiments.

Preliminary experiments used high reservoir temperatures (~40 °C), which became supersaturated at room temperature (20 °C). However for fears microcrystals were persisting in the apparatus, the target saturation temperature was changed to 20 °C and the solution was cooled below room temperature to generate supersaturation. Therefore if there was a crystal build-up during an experiment, the flow could be stopped and the apparatus could be passively allowed to warm and dissolve the blockage.

Advantages and Disadvantages are highlighted in Table 5-5.

5.3.5 Gravity affecting cooling coil

The problem between the coil and the nucleation pipe, as discussed earlier (Section 5.1.3) was solved by fusing the target (round) pipe to the heat exchange coil. However this did not completely prevent pre- nucleation. Crystals were observed inside the coil itself (Figure 5-19). The orientation of the coil made it difficult to see exactly where they were being produced. As an alternative, a straight piece of pipe with a condenser was used (Figure 5-20). This also acted to stop the gravity separation of slugs at the top and bottom of coil. The slugs were seen to maintain their segment uniformity easily until after the target nucleation zone.

Table 5-5 - Advantages and disadvantages of high and low T crystallisation experiments (relative to room T)

	Advantages	Disadvantage
High T	• larger supersaturation possible • can be used from a hot reaction • lower viscosity means more fluid-like properties. • Cheaper to have heating-only apparatus • More solute dissolved means larger crystals	• More likely to cause pressure buildups • Hot fluid is a hazard itself. • Larger energy needed to cool. • More solution dissolved means more mess when spilled.
Low T	• Any formed crystals will dissolve spontaneously if solution is left stagnant. • Less time to set up water bath. • Easier to use adhesives and adhesive tape on apparatus. • Closer to room temperature allows better external thermocouple calibration	• Limited supersaturation • Condensation forms if cooled too low obscuring optical measurement. • Limited by solute freezing point

The straight cooling section was made by fusing a condenser-type setup to a T-piece glass pipe to form a continuous system of segment-generation to cooling to nucleating and grown area in a monolithic piece of glass (Figure 5-20). This apparatus was tested for spontaneous nucleation meta-stability. A 0.3726 g g_{H2O}^{-1} solution of unfiltered aqueous ammonium chloride was prepared (C_{sat} = 20 °C) and flowed from the water bath at 35 °C to the cooling section which was gradually lowered from 20 °C to 18 °C (S = 1.02).

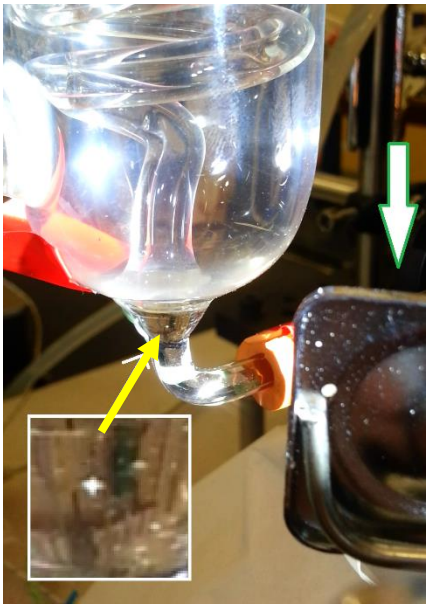

Figure 5-19 - Crystal of ammonium chloride observed in the cooling coil (enlargement in white inset box) before reaching the laser target area (large green and white arrow).

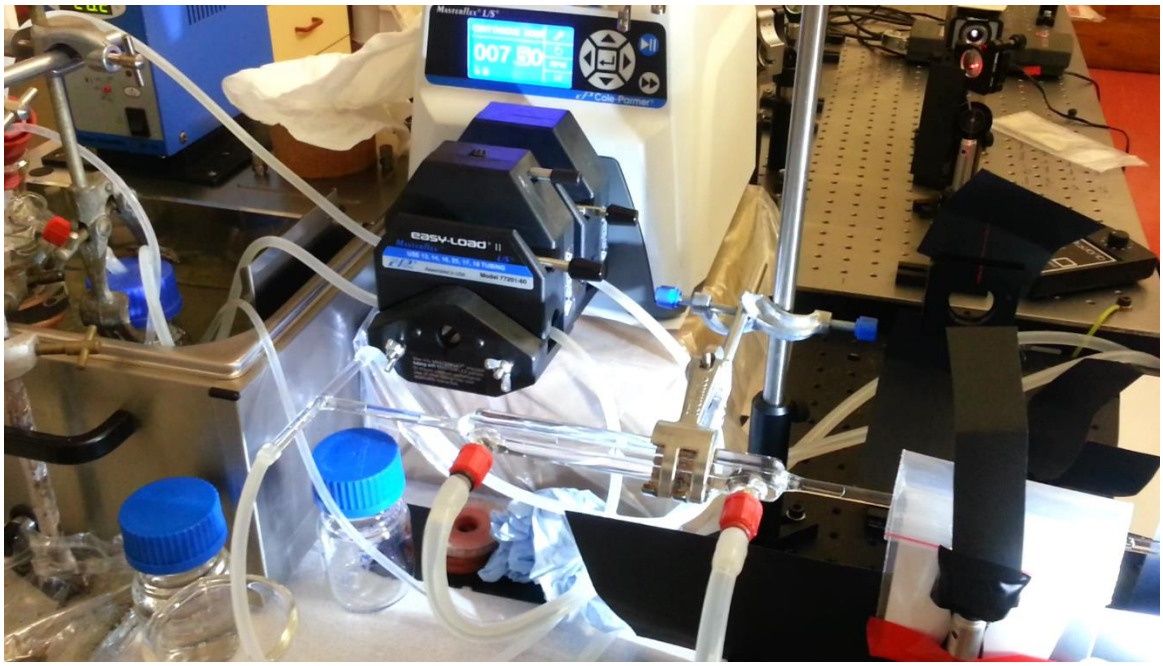

Figure 5-20 - Image of cooling apparatus with condenser replacing coil in centre, with PFPE / aqueous fluids passing through. Background left is water bath with separator components inside, back mid is peristaltic pump and back right is final mirror of NPLIN setup with a guide HeNe laser coaxially aligned.

Upon flowing aqueous ammonium chloride solution through the heat exchange pipe at this temperature, crystals were formed at the input join between the pipe and the cooling jacket (Figure 5-21). The supersaturation of 1.02 was much lower than spontaneous nucleation seen in batch or other flow regimes. Due to the location, likely explanations were: 1) the widening of the pipe where the cooling jacket was fused to the pipe was causing nucleation due to disturbances in the flow or 2) the sudden change in temperature was inducing nucleation.

To test hypothesis 2) would need several cooling sections to bring down to the desired temperature. Situation 1) was tested first by eliminating the fused section and submerging an internally smooth straight pipe into a removable external cooling jacket, thus avoiding the glass–glass join.

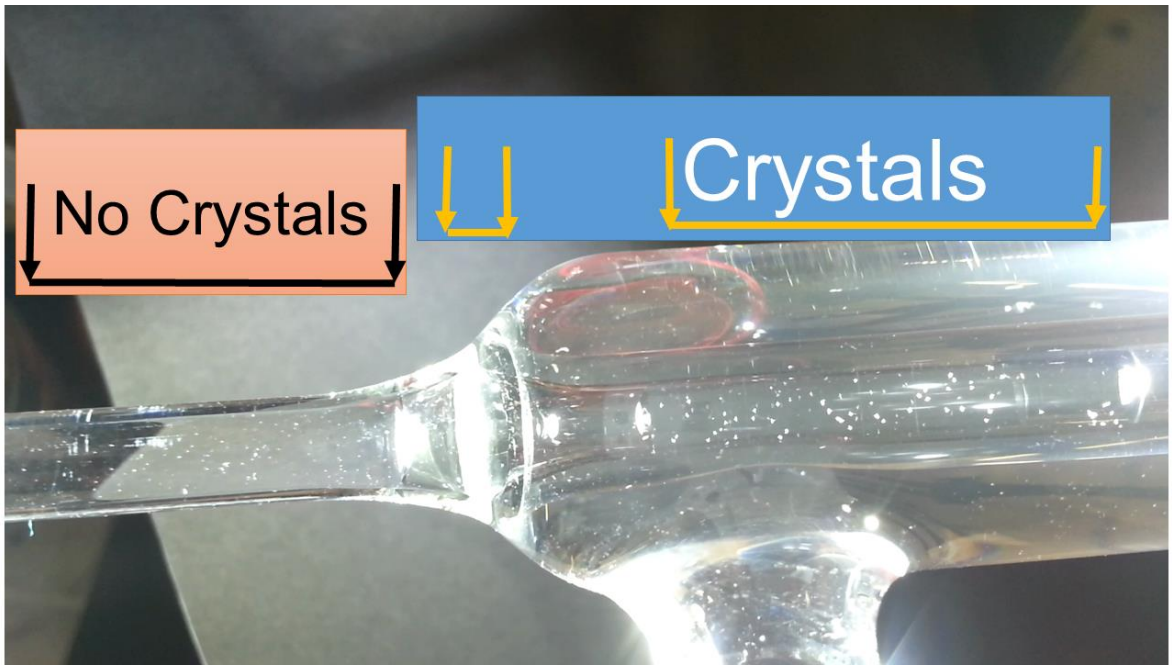

Figure 5-21 - Image of PFPE / aqueous ammonium chloride slugs in condenser-style cooling jacket showing crystals nucleated inside cooling jacket but not before. The middle slug is in the widened area where the glass pipe is fused ot the cooling jacket and may be the cause of agitation nucleation or simply the boundary between supersaturated temperature and undersaturated temperature. (Note that scratches on the glass show up white, but with less intensity than light off reflected crystals).

Figure 5-20

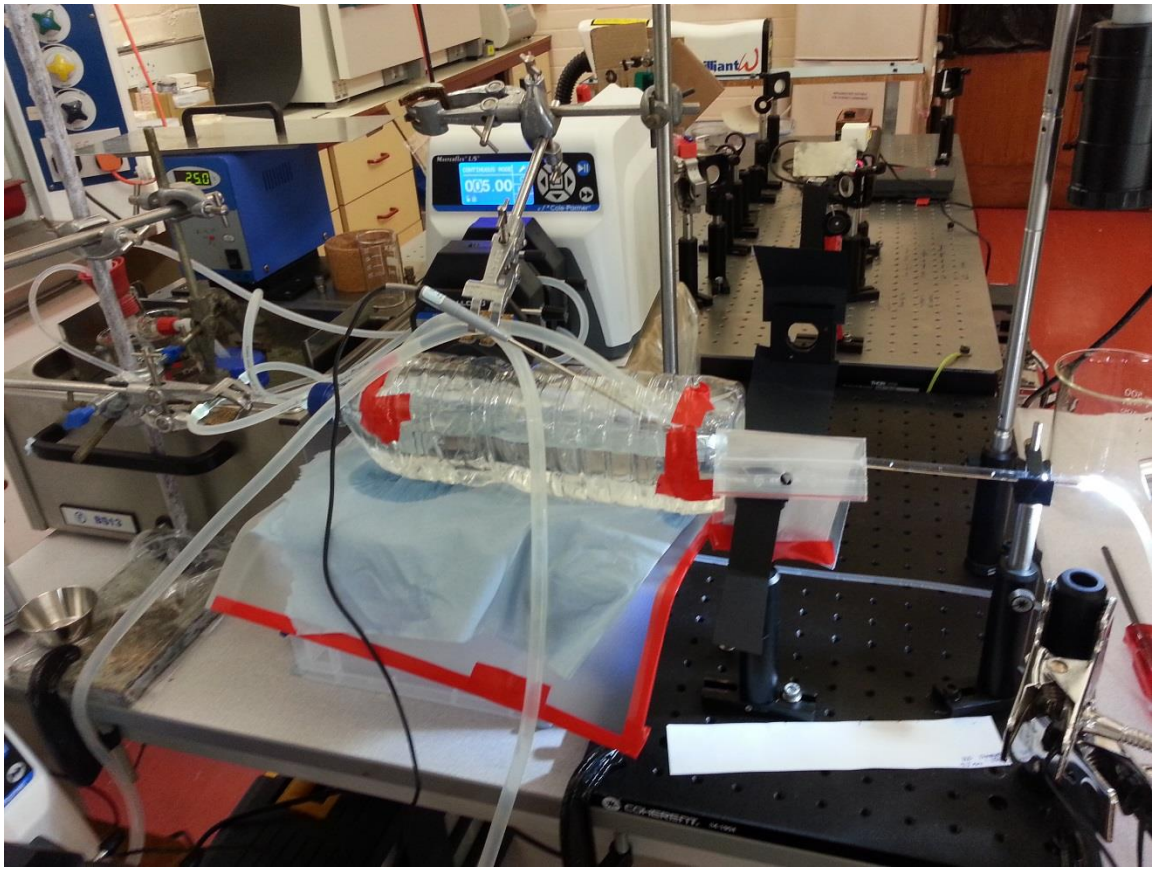

Figure 5-22 – Horizontal-only segmented cooling apparatus setup. The bottle in the middle of the picture acts as a cooling jacket for the continuous straight pipe piece from the T piece on the left, through the bottle cooling to laser target area and finally growth observation area. In the background from left to right can be seen waterbath with stock solutions and separator, peristaltic pump and laser table setup.

A 3 mm ID pipe with a T-piece was pushed through holes drilled into the ends of a 300 mm plastic container and sealed with PVC tape. The container was filled with water above the height of the pipe and connected to a heater-chiller. A calibrated thermometer measured the water temperature at the end closest to the nucleation area. The internal pipe temperature was calibrated against the water container temperature using flowing water and a pre-calibrated thermocouple. The two speeds selected for flow were 5.0 and 2.5 rpm (2.88 and 1.44 ml min^{-1} respectively).

On cooling to 8.8 °C (S = 1.13) at 5.0 rpm, spontaneous nucleation was limited to an occasional crystal in a slug every so often. On lowering the flow rate to 2.5 rpm (temperature drops to 8.6 °C, S = 1.136) the solution was still metastable.

The system was left primed with solution and left overnight at room temperature. Upon cooling back down to 15 °C crystals had spontaneously formed in every segment. The system was then left flowing with the heat exchange bath set to 25 °C for 30 minutes to allow any microscopic crystals to dissolve and the solution to mix and equilibrate. The solution was then cooled back down to 8.6 °C where spontaneous nucleation was reduced to roughly 1 crystal every 10 segments, acceptable for a NPLIN experiment. A laser pulse was introduced to the flowing solution (0.44 W, 174 MW cm^{-2}). With a single pulse, nucleation occurred in nearly every segment and with 10 pulses per second many crystals formed in each segment.

After some time, it was noted that the flow pipe had damage at the exit of the laser beam. This was determined to be caused by focusing occurring at the boundary of two segments, the differing refraction indices of the liquids acting as a lens to focus much higher intensity light on the exit of the pipe. Continuously running laser pulses were then disfavoured.

This apparatus allowed for the cooling to supersaturation needed for the NPLIN experiments. However the fact that there was still occasional spontaneous nucleation means that the solution is on the edge of its metastable region. Having 1 in 10 slugs spontaneously nucleate is similar to the spontaneous nucleation in the batch experiments at this supersaturation.

This showed a successful operation of a continuous looped flow NPLIN apparatus for future testing of NPLIN experiments. So long as spontaneously nucleated slugs are identified and ruled out of tests it can produce several segments of supersaturated solution per minute ready to be fired upon. It can only do this for one concentration per run, but it can change temperature (and therefore supersaturation) per run increasing the number of experiments able to be performed.

The apparatus as-is is not ready for industrial applications such as production of seed crystals since that would require reducing the spontaneously nucleated segments to 0 and introducing an automatic nucleation process that does not damage the equipment.

Eliminating the disturbances to flow in the critical areas caused by fused glassware and changing height enabled a simpler and more effective apparatus.

5.3.6 Filtration

Based on earlier results described in Chapter 4, detailed work was carried out by Ward *et al.* on effects of filtration of ammonium chloride on NPLIN.[60] Because of this the effect of using otherwise identical experimental conditions but with filtered solution in looped segmented flow was performed.

The equipment was set up as Section 5.3.5 with some additions. Conditions had to be observed to verify clean filtered solutions. Glass pipes were acid cleaned and Rain-X coated as described in Chapter 2. Silicone tubes were washed out with hot water then rinsed with 18.2 MΩ cm water, dried in oven and sealed with kitchen film until use. Fresh aqueous solution was syringe filtered through 0.22 um PES filters into a clean duran flask and fresh Galden liquid which had not been in contact with salt solution was filtered through a paper filter into a clean Duran flask.

What was found was that spontaneous nucleation did not occur at any temperature down to 8.8 °C (S = 1.13), and laser-induced nucleation did not occur for every slug but rather 3 out of 10 for similar intensities (0.444 W, 174 MW cm^{-2}). For a higher intensity (0.650 W, 257 MW cm^{-2}) every slug nucleated, but the number of crystals was not observed to change.

One of the key reasons for setting up this apparatus was to control the number of crystals produced using variable power. This could not be achieved with filtered solution. Since the aim of this experimental technique was to enable laser induced nucleation without spontaneous nucleation it seems filtration has a massive effect. Further work on filtration and contaminants on the ppm level is needed to best tune

the reliability of this experiment to find the balance between spontaneous and laser-induced nucleation. If there is an additive that could be added in fixed concentrations which could change the nucleation number but otherwise leave the solution unaffected this could be a major boon to this work.

Since filtration seems to eliminate spontaneous nucleation this could be a good way of obtaining industrial reliability mentioned in the previous section. However since the number of nuclei produced is not affected by the laser intensity as much this would only be more beneficial if it happens to make the crystals with desired properties, whereas the unfiltered has a chance to adjust the number of crystals produced to get better results.

6 Conclusions and future work.

The practical application of NPLIN to continuous flow was investigated. Supersaturated aqueous solutions were screened with a nanosecond pulsed laser (44 MW cm^{-2}) for NPLIN activity.

It can be seen that not all organic compounds tested could be nucleated under these easy-to-obtain conditions, including compounds previously reported to be NPLIN active. Succinic acid showed the most promise as a future system, however at 300 g kg_{H2O}^{-1}, low numbers of large crystals were produced so may not be ideal for further studies on the NPLIN process. Adipic acid produced only 1 or 2 crystals per pulse. It may be good for developing studies on that particular system, but this is too few crystals for studying the NPLIN mechanism or developing NPLIN flow systems. This is also the first time NPLIN activity has been found in nicotinic acid. One of the most important questions for the future is what determines whether chemical systems will undergo NPLIN or not. There is still not a definitive answer but an easy way to tell if there are is using reasonably high solubility solutes when can grow quickly in the laser path to rule them in.

When trying to nucleate a new compound making sure the entire experimental space of metastability has been tested is needed. The MSZW for laser induced nucleation is not necessarily the same as the spontaneous nucleation MSZW. Any system of choice should be screened for activity in this manner.

Aqueous inorganic chemical systems tested showed overall much easier lability to NPLIN compared with the organic compounds. They also typically have significantly higher solubility, leading to cases like ammonium nitrate (1920 g per kg of water) where the crystals grow rapidly to a significant volume of the solution. Ammonium chloride was chosen as a model compound for NPLIN as it is fast growing, easily to handle and relatively cheap. KCl and $NaNO_3$ could also be used as they had useful sizes and number of crystals formed by NPLIN in solution. In the future salts like

CsCl could be used as the higher cost is offset by being a heavier nuclei (will show up easier on X-Ray sources) and this system was seen to produce more crystals per pulse.

Ammonium chloride was further characterised as showing an exponential increase of crystals produced per NPLIN pulse with higher supersaturation and higher laser power. In the future more detailed work to quantify and model this behaviour could lead to the control of crystal number needed to significantly influence growth parameters like CSD. This would make it useful for industrial applications like seed production or even in situ seeding. A surprising result was the diminishing of NPLIN effects upon filtration, reducing the number of crystals from 350 to 10 per 70 mJ pulse. This gives interesting hints as to the mechanism of NPLIN in this system: impurities. By tailoring the levels of impurities this could lead to a reliable way of generating crystal number control in the future. KCl also showed the possibility of similar behaviour and comparing these models could help validate the method. A further effect to investigate is the variance of crystal number per pulse at different temperatures but the same supersaturation. For better results for all of these experiments having a temperature controlled target environment to ensure supersaturation control would be a big help.

The first reported demonstration on NPLIN in continuous flow was shown, with a S_{23} = 1.1 solution of aqueous ammonium chloride producing crystals only when irradiated by an NPLIN laser.

The development of a continuous NPLIN environment which involves a re-dissolution step and loop flow was constructed for both laminar and slug-flow regimes. This enabled extended run times for more in depth experiments. NPLIN was hindered by spontaneous nucleation caused by both design elements and flow regimes. Investigating the allowed subcooling for different flow regimes on the apparatus would be a very useful step in the future and be the first steps towards understanding the metastable zone width in that regime. This would then allow a better understanding of where the system does not produce spontaneous nucleation but does allow laser induced nucleation and therefore could be further developed for

industrial applications. Using a solution filtered through a 0.2 μm PES filter was observed to both hinder NPLIN and spontaneous nucleation and unless understanding of the impurities is obtained (as described above) this is not a useful way of achieving stable solution.

7 References

1 J. W. Mullin, *Crystallization*, Butterworth-Heinemann, Oxford; Boston, 2001.

2 P. Ayazi Shamlou, A. G. Jones and K. Djamarani, *Chem. Eng. Sci.*, 1990, **45**, 1405–1416.

3 D. Erdemir, A. Y. Lee and A. S. Myerson, *Acc. Chem. Res.*, 2009, **42**, 621–629.

4 R. J. Davey, S. L. M. Schroeder and J. H. ter Horst, *Angew. Chemie Int. Ed.*, 2013, **52**, 2166–2179.

5 D. Gebauer, A. Völkel and H. Cölfen, *Science (80-.).*, 2008, **322**, 1819–1822.

6 A. Jawor-Baczynska, J. Sefcik and B. D. Moore, *Cryst. Growth Des.*, 2013, **13**, 470–478.

7 W. Pan, A. B. Kolomeisky and P. G. Vekilov, *J. Chem. Phys.*, 2005, **122**, 174905-174905–7.

8 W. Pan, P. G. Vekilov and V. Lubchenko, *J. Phys. Chem. B*, 2010, **114**, 7620–7630.

9 D.-K. Bučar, R. W. Lancaster and J. Bernstein, *Angew. Chemie Int. Ed.*, 2015, **54**, 6972–6993.

10 S. L. Morissette, S. Soukasene, D. Levinson, M. J. Cima and Ö. Almarsson, *Proc. Natl. Acad. Sci.*, 2003, **100**, 2180–2184.

11 Y. Yang, L. Song and Z. K. Nagy, *Cryst. Growth Des.*, 2015, **15**, 5839–5848.

12 J. B. Rawlings, C. W. Sink and S. M. Miller, in *Handbook of Industrial Crystallization*, 2002, pp. 201–230.

13 G. Ruecroft, D. Hipkiss, T. Ly, N. Maxted and P. W. Cains, *Org. Process Res. Dev.*, 2005, **9**, 923–932.

14 C. Virone, H. J. M. Kramer, G. M. van Rosmalen, A. H. Stoop and T. W. Bakker, *J. Cryst. Growth*, 2006, **294**, 9–15.

15 J. A. Jacob, S. Sorgues, A. Dazzi, M. Mostafavi and J. Belloni, *Cryst. Growth Des.*,

2012, **12**, 5980–5985.

16 T. Rungsimanon, K. Yuyama, T. Sugiyama, H. Masuhara, N. Tohnai and M. Miyata, *J. Phys. Chem. Lett.*, 2010, **1**, 599–603.

17 F. C. Wen, T. McLaughlin and J. L. Katz, *Phys. Rev. A*, 1982, **26**, 2235–2242.

18 N. E. B. Briggs, U. Schacht, V. Raval, T. McGlone, J. Sefcik and A. J. Florence, *Org. Process Res. Dev.*, 2015, **19**, 1903–1911.

19 H. Yang, X. Yu, V. Raval, Y. Makkawi and A. Florence, *Cryst. Growth Des.*, 2016, **16**, 875–886.

20 S. Lawton, G. Steele, P. Shering, L. Zhao, I. Laird and X.-W. Ni, *Org. Process Res. Dev.*, 2009, **13**, 1357–1363.

21 M. Jiang, Z. Zhu, E. Jimenez, C. D. Papageorgiou, J. Waetzig, A. Hardy, M. Langston and R. D. Braatz, *Cryst. Growth Des.*, 2014, **14**, 851–860.

22 C. J. Callahan and X.-W. Ni, *Cryst. Growth Des.*, 2012, **12**, 2525–2532.

23 Y. Yang, L. Song, Y. Zhang and Z. K. Nagy, *Ind. Eng. Chem. Res.*, 2016, **55**, 4987–4996.

24 H. N. Kim, J. R. G. Sander, B. W. Zeiger and K. S. Suslick, *Cryst. Growth Des.*, 2015, **15**, 1564–1567.

25 R. Jamshidi, D. Rossi, N. Saffari, A. Gavriilidis and L. Mazzei, *Cryst. Growth Des.*, 2016, **16**, 4607–4619.

26 M. Jiang, C. D. Papageorgiou, J. Waetzig, A. Hardy, M. Langston and R. D. Braatz, *Cryst. Growth Des.*, 2015, **15**, 2486–2492.

27 B. A. Garetz, J. E. Aber, N. L. Goddard, R. G. Young and A. S. Myerson, *Phys. Rev. Lett.*, 1996, **77**, 3475–3476.

28 A. J. Alexander and P. J. Camp, *Cryst. Growth Des.*, 2009, **9**, 958–963.

29 M. R. Ward and A. J. Alexander, *Cryst. Growth Des.*, 2012, **12**, 4554–4561.

30 J. Zaccaro, J. Matic, A. S. Myerson and B. A. Garetz, *Cryst. Growth Des.*, 2001, **1**, 5–8.

31 C. Duffus, P. J. Camp and A. J. Alexander, *J. Am. Chem. Soc.*, 2009, **131**, 11676–11677.

32 M. R. Ward, I. Ballingall, M. L. Costen, K. G. McKendrick and A. J. Alexander, *Chem. Phys. Lett.*, 2009, **481**, 25–28.

33 A. Ikni, B. Clair, P. Scouflaire, S. Veesler, J.-M. Gillet, N. El Hassan, F. Dumas and A. Spasojević-de Biré, *Cryst. Growth Des.*, 2014, **14**, 3286–3299.

34 I. S. Lee, J. M. B. Evans, D. Erdemir, A. Y. Lee, B. A. Garetz and A. S. Myerson, *Cryst. Growth Des.*, 2008, **8**, 4255–4261.

35 B. A. Garetz, J. Matic and A. S. Myerson, *Phys. Rev. Lett.*, 2002, **89**, 175501.

36 J. Matic, X. Sun, B. A. Garetz and A. S. Myerson, *Cryst. Growth Des.*, 2005, **5**, 1565–1567.

37 X. Sun, B. A. Garetz and A. S. Myerson, *Cryst. Growth Des.*, 2006, **6**, 684–689.

38 B. Clair, A. Ikni, W. Li, P. Scouflaire, V. Quemener and A. Spasojević-De Biré, *J. Appl. Crystallogr.*, 2014, **47**, 1252–1260.

39 X. Sun, B. A. Garetz and A. S. Myerson, *Cryst. Growth Des.*, 2008, **8**, 1720–1722.

40 M. R. Ward, S. McHugh and A. J. Alexander, *Phys. Chem. Chem. Phys.*, 2011, **14**, 90–93.

41 W. Li, A. Ikni, P. Scouflaire, X. Shi, N. El Hassan, P. Gémeiner, J.-M. Gillet and A. Spasojević-de Biré, *Cryst. Growth Des.*, 2016, **16**, 2514–2526.

42 M. R. Ward, A. Rae and A. J. Alexander, *Cryst. Growth Des.*, 2015, **15**, 4600–4605.

43 M. R. Ward, G. W. Copeland and A. J. Alexander, *J. Chem. Phys.*, 2011, **135**, 114508-114508–8.

44 I. S. Lee, J. M. B. Evans, D. Erdemir, A. Y. Lee, B. A. Garetz and A. S. Myerson,

Cryst. Growth Des., 2008, **8**, 4255–4261.

45 X. Sun, B. A. Garetz, M. F. Moreira and P. Palffy-Muhoray, *Phys. Rev. E*, 2009, **79**, 21701.

46 B. C. Knott, M. F. Doherty and B. Peters, *J. Chem. Phys.*, 2011, **134**, 154501-154501–6.

47 G. Di Profio, M. T. Reijonen, R. Caliandro, A. Guagliardi, E. Curcio and E. Drioli, *Phys. Chem. Chem. Phys.*, 2013, **15**, 9271–9280.

48 Y. Yani, P. S. Chow and R. B. H. Tan, *Cryst. Growth Des.*, 2012, **12**, 4771–4778.

49 T. Rungsimanon, K. Yuyama, T. Sugiyama and H. Masuhara, *Cryst. Growth Des.*, 2010, **10**, 4686–4688.

50 A. Soare, R. Dijkink, M. R. Pascual, C. Sun, P. W. Cains, D. Lohse, A. I. Stankiewicz and H. J. M. Kramer, 2011, 2311–2316.

51 S. L. Eldridge, V. K. Almeida, A. K. Korir and C. K. Larive, 2007, **79**, 8446–8453.

52 R. A. Granberg and Å. C. Rasmuson, *J. Chem. Eng. Data*, 1999, **44**, 1391–1395.

53 A. Apelblat and E. Manzurola, *J. Chem. Thermodyn.*, 1987, **19**, 317–320.

54 E. M. Gonçalves and M. E. Minas da Piedade, *J. Chem. Thermodyn.*, 2012, **47**, 362–371.

55 Y. Corvis, N. Guiblin and P. Espeau, *J. Phys. Chem. B*, 2014, **118**, 1925–1931.

56 A. Seidell, *Solubilities . Vol. 1. 3rd Ed.*, D.Van Nostrand Company; New York, 3rd edn., 1940.

57 D. R. Lide and David, *CRC handbook of chemistry and physics : a ready-reference book of chemical and physical data*, CRC Press, 2004.

58 C. Sudha and K. Srinivasan, *CrystEngComm*, 2013, **15**, 1914–1921.

59 K. Robertson, P.-B. Flandrin, A. R. Klapwijk and C. C. Wilson, *Cryst. Growth Des.*, 2016, **16**, 4759–4764.

60 M. R. Ward, A. M. Mackenzie and A. J. Alexander, *Cryst. Growth Des.*, 2016, **16**, 6790–6796.

61 P. G. Vekilov, *Cryst. Growth Des.*, 2010, **10**, 5007–5019.